J Mol Evol (2005) 61:456–469
DOI: 10.1007/s00239-004-0317-z

JOURNAL OF MOLECULAR EVOLUTION

Insights on the Evolution of Metabolic Networks of Unicellular Translationally Biased Organisms from Transcriptomic Data and Sequence Analysis

Alessandra Carbone,[1] Richard Madden[2]

[1] Génomique Analytique, Université Pierre et Marie Curie, INSERM U511, 91 Bd de l'Hôpital, 75013 Paris, France
[2] Institut des Hautes Études Scientifiques, 35 route de Chartres, 91440 Bures-sur-Yvette, France

Received: 9 November 2004 / Accepted: 20 April 2005 [*Reviewing Editor:* Dr. Richard Kliman]

Abstract. Codon bias is related to metabolic functions in translationally biased organisms, and two facts are argued about. First, genes with high codon bias describe in meaningful ways the metabolic characteristics of the organism; important metabolic pathways corresponding to crucial characteristics of the lifestyle of an organism, such as photosynthesis, nitrification, anaerobic versus aerobic respiration, sulfate reduction, methanogenesis, and others, happen to involve especially biased genes. Second, gene transcriptional levels of sets of experiments representing a significant variation of biological conditions strikingly confirm, in the case of *Saccharomyces cerevisiae*, that metabolic preferences are detectable by purely statistical analysis: the high metabolic activity of yeast during fermentation is encoded in the high bias of enzymes involved in the associated pathways, suggesting that this genome was affected by a strong evolutionary pressure that favored a predominantly fermentative metabolism of yeast in the wild. The ensemble of metabolic pathways involving enzymes with high codon bias is rather well defined and remains consistent across many species, even those that have not been considered as translationally biased, such as *Helicobacter pylori*, for instance, reveal some weak form of translational bias for this genome. We provide numerical evidence, supported by experimental data, of these facts and conclude that the metabolic networks of translationally biased genomes, observable today as projections of eons of evolutionary pressure, can be analyzed numerically and predictions of the role of specific pathways during evolution can be derived. The new concepts of *Comparative Pathway Index*, used to compare organisms with respect to their metabolic networks, and *Evolutionary Pathway Index*, used to detect evolutionarily meaningful bias in the genetic code from transcriptional data, are introduced.

Key words: Codon bias — Metabolic networks — Unicellular organisms — Codon Adaptation Index — Transcriptomic data

Introduction

In silico methods capable of indicating the metabolism and lifestyle of an organism and explaining its evolution in the wild would be an invaluable tool, especially for organisms for which these characteristics are still unknown. High expression rates of certain genes during exponential growth, or of enzymes involved in fundamental metabolic activities like glycolysis, have been very often reported in the literature for fast growers and studied, since the 1980s, through the notion of the *Codon Adaptation Index* (CAI) (Sharp and Li 1987). For fast-growing organisms like *Escherichia coli* and *Saccharomyces cerevisiae*, but also *Caenorhabditis elegans* and *Dro-*

This article contains online-only suppplementary material. This material can also be found at http://www.ihes.fr/~carbone/data.htm.

Correspondence to: Alessandra Carbone; *email:* carbone@ihes.fr

sophila melanogaster, genes have been ranked by CAI values and correlated with gene expression levels and functional activity (Sharp and Li 1987; Sharp et al. 1986, 1988; Shields and Sharp 1987; Stenico et al. 1994). Carbone et al. (2003) showed that the CAI can be defined purely by sequence analysis, that it can be calculated for genomes of organisms whose biological activities are not known, and that the resulting ranking of genes correlates well with the dominant codon bias of the organism. This bias need not be related to translational efficiency as for fast growers, but can have any other nature (such as compositional, as for AT- and GC-skew bias, or physical, e.g., strand bias). Exploiting the fact that CAI is a *universal* measure for analyzing dominant codon bias of any origin in organisms which are not necessarily translationally biased, one can numerically evaluate the strength of different codon biases for an organism and classify genes accordingly to dominant biases (Carbone et al. 2004). For translationally biased organisms, where gene ranking based on CAI has immediate biological interpretation, one can shift the paradigm of the 1980s, which is applied to genes, to groups of enzymes and their *metabolic activity*, instead, and approach, in a systematic way, the classification of metabolic pathways distinguishing those which are essential for the life cycle of the organism from those which are rarely activated but employed to survive under specific environmental conditions. Namely, through the new notion of the *Relative Pathway Index*, we rank metabolic pathways and correlate them with the importance of their metabolic function for the life of the organism through evolution. Metabolic pathways that are constitutive in the everyday life of the organism and metabolic pathways that need to be activated rapidly under specific conditions are well characterized by the analysis. Strong evolutionary pressures which favored a given metabolism of an organism in the wild are also characterized in the analysis.

Several energy metabolism pathways turn out to be constituted by enzymes with *high* codon bias in translationally biased organisms known to be driven by very different physiologies: for instance, the highly biased codon composition of glycolytic enzymes is strikingly evident in fast-growing aerobic bacteria and in *S. cerevisiae*, and the key role of photosynthetic pathways for *Synechocystis* (Mrázek et al. 2001) or of methane metabolism for *Methanosarcina acetivorans* can be identified by the high codon bias of their enzymes. Important metabolic pathways can be detected for organisms which are not necessarily fast growing and whose genomes might have a homogeneous codon composition even though the signal is weaker. For instance, a highly biased codon composition of glycolytic enzymes is present in *Mycobacterium tuberculosis H37Rv* (*mtbRv*) whose genome displays only a weak form of translation bias (Carbone et al. 2004), and more surprisingly in *Helicobacter pylori* (*hpy*), a genome of rather homogeneous codon composition (Lafay et al. 2000), where glycolytic enzymes are biased above average. This finding suggests that translational selection affected *hpy*.

In general, given an organism or groups of organisms whose genomes have been affected by some (weak or strong) form of translational selection and have a similar lifestyle, we show that genetic coding is tuned, favoring specific pathways and disfavoring others. These coding features hold across organisms and detecting them allows us to predict or confirm the lifestyle of an organism. This is done with the help of the new concept of the *Comparative Pathway Index*, which enables organism comparisons based on their metabolic activities. Several examples, supported by experimental evidence, have been chosen to illustrate how well the method works in view of its application to subsequent analysis of poorly studied organisms.

To validate our statistical analysis, we consider the metabolic activities of *S. cerevisiae* reported by transcriptomic data under sufficiently different biological conditions and compare them with the classification of metabolic pathways obtained by sequence analysis. Because changes in gene expression over sufficiently long periods of time and variations of biological conditions might be complex and might involve the integration of many kinds of information on the nutritional and metabolic state of the cell, we consider mRNA abundance collected during the *S. cerevisiae* cell cycle under diauxic shift (deRisi et al. 1997) (here glucose quantities decrease in the medium during the cell cycle and induce the yeast to move from fermentation to aerobic respiration), and we analyze the yeast metabolic network through these data. A classification of metabolic pathways based on transcriptomic data and on the new concept of the *Evolutionary Pathway Index* is proposed. The comparison between this metabolic classification and the one obtained through sequence analysis suggests that the coding sequence of enzymes involved in specific metabolic functions contains information on the physiological responses of an organism during evolutionarily favored conditions. Namely, we argue in favor of the fact that in *S. cerevisiae* the biasing of genes involved in the fermentative state corresponds to a strong evolutionary pressure favoring this fermentative metabolic state of yeast in the wild (Wagner 2000). The high transcription of enzymes involved in highly active pathways during fermentation (and possibly not during aerobic respiration) correlates particularly well with the high CAI value of these enzymes. This observation is supported also by the available transcriptomic data

Table 1. List of organisms considered for metabolic pathway comparison analysis

Organism	Sign			DT	P	ER	CP	CER	μM	σM	Min	Max
Agrobacterium tumefaciens (agro)	+	+	×	2 h	156	917	30	72	0.53	0.06	0.30	0.77
Bacillus subtilis (bsub)	+	−	−	60 m	104	754	27	63	0.41	0.06	0.32	0.58
Escherichia coli (ecoli)	+	−	−	30 m	148	2908	34	96	0.40	0.07	0.25	0.64
Haemophilus influenzae (hin)	+	−	+	30 m	88	565	29	62	0.43	0.06	0.31	0.63
Vibrio cholera (vcho)	+	−	−	30 m	170	852	32	90	0.36	0.07	0.22	0.63
Saccharomyces cerevisiae (yeast)	+	−	−	90 m	86	599	20	39	0.31	0.12	0.15	0.73

Note. On the right of each organism, three symbols (+, −, ×) are used to represent in short the codon bias signature of the organism. Columns are interpreted as follows: (1) +, translational bias; (2) +, GC3 content; (3) +, strand bias; ×, no replication origin is known. (−) No bias is present. No GC-skew bias or AT-skew bias is detected for these six organisms. Doubling time (DT) given in minutes (m) or hours (h); number of metabolic pathways (P) included in BioCyc and of enzymatic reactions (ER) involved in these pathways; number of metabolic pathways constituted by enzymes whose corresponding genes are clustered along the genome sequence (CP); and number of enzymatic reactions involved in such pathways (CER). Mean (μM), standard deviation (σM), minimum and maximum PI(P), for pathways P in the metabolic network M.

on seripauperine proteins (Holstege et al. 1998; James et al. 2003; Viswanathan et al. 1994) and on Hem13 proteins (Amillet et al. 1995).

Our results open a way of exploring evolutionary pressure and natural selection for organisms grown in the wild, understanding the need for different levels of gene regulation in unicellular organisms, and, hopefully, predicting the metabolic activities of translationally biased organisms, as well as suggesting the best conditions for growth in the laboratory. Similar questions have been addressed by Akashi and Gojobori (2002), who report that metabolic efficiency is related to amino acid composition for the genomes of *E. coli* and *B. subtilis*.

Materials and Methods

Organisms and Genomes

An analysis of metabolic pathways has been done for the *translationally* biased organisms listed in Table 1 plus *Pyrococcus abissi, Synechocystis, Methanobacterium thermoautotrophicum, Methanosarcina acetivorans, Thermosynecoccus elongatus*, and *Chlorobium tepidum*. The metabolic pathways of the last six translationally biased organisms are much less known than for those listed in Table 1. The analysis was also done for *Helicobacter pylori* (*hpy*) and *Mycobacterium tuberculosis H37Rv* (mtbRv), the second genome displaying some weak form of translational bias. All genomes have been completely sequenced. Genomes along with gene annotation were retrieved from the genomes directory of GenBank via FTP. All coding sequences (CDS) were considered, including those annotated as hypothetical and those predicted by computational methods only. An *enzyme* refers to a protein participating in a metabolic reaction, not a complex.

Fast and Slow Growth

An organism is fast growing if it has a doubling time of at most a couple of hours. Translational bias is usually detected in genomes of fast growers. Weak forms of translational bias can be detected for organisms that are not growing fast, for instance, *M. tuberculosis H37Rv*, which has a doubling time of 20 h, or *M. thermoautotrophicum* (Carbone et al. 2004).

Metabolic Networks

For all organisms in Table 1, *H. pylori*, and *M. tuberculosisH37Rv*, we used *BioCyc software distribution*, which includes EcoCyc and MetaCyc databases (Karp et al. 2000, 2002), version 7. The pathway/genome databases for *B.subtilis*, *S. cerevisiae*, *M. tuberculosis*, and *H. influenzae* were created by DoubleTwist Inc. The numbers of pathways and enzymatic reactions in Table 1 come from the BioCyc database. In BioCyc, pathways are organized into several functional classes, used in Figs. 1 and 3. We disregard from our analysis fragmentary pathways with no assigned function in the BioCyc network. The methane metabolism networks for organisms in Table 1 and *Methanosarcina acetivorans* and the photosynthetic networks (Calvin cycle, photosystems I and II) for *Synechocistis* are taken from the KEGG database at http://www.genome.ad.jp/kegg/pathway.html.

Translational Bias

Translational selection refers to the benefit of an increased translational output for a fixed investment in the translational machinery (ribosomes, tRNA, elongation factors, etc.) if only a subset of codons (and their corresponding tRNAs) is used preferentially. Since the benefit of using a particular codon depends on how often it is translated, the strength of translational selection, and hence the degree of codon bias, is expected to vary with the expression level of a gene within an organism. This pattern has been confirmed for the organisms in Table 1 and others. Mutational bias (i.e., an excess or deficit of G + C content compared to A + T content, for instance) might obscure translational selection, which can appear in strong or weak forms (see below).

Codon Bias, Codon Weights, and Codon Adaptation Index

Sharp (Sharp and Li 1987) formulated the hypothesis that for each genome sequence G, there is a set S of coding sequences, constituting roughly 1% of the genes in G, which are representative of the dominating codon bias in G. This bias can be described by listing a set of codon weights calculated on genes in S as follows: given an amino acid j, its synonymous codons might have different frequencies in S; if x_{ij} is the number of times that the codon i for the amino acid j occurs in S, then one associates to i a *weight* w_{ij} relative to its sibling of maximal frequency y_j in S,

$$w_{i,j} = x_{i,j}/y_j \tag{1}$$

Such weights describe codon preferences in G and they are successfully used by Sharp to correlate gene expression levels with translational codon bias in fast-growing organisms. This is done by computing the CAI (Sharp and Li 1987) for all genes, $\mathrm{CAI}(g) = \left(\prod_{k=1}^{L} w_k\right)^{1/L}$, where g is a gene, w_k is the weight of the kth codon in g, L is the number of codons in g, and S consists of genes coding for proteins known to be highly expressed, such as ribosomal and glycolytic proteins are for fast growers. Genes are then ranked by CAI values. Genes ranking the highest are the most biased and those ranking the lowest are the least affected by selective bias. For fast growers, genes with high CAI value turn out to be most expressed and translationally biased (Sharp and Li 1987).

More generally, CAI correlates with *any* kind of dominating bias in genomes (like GC content, preference for codons with G or C at the third nucleotide position, a leading strand richer in G + T than a lagging strand), not just with translational bias (Carbone et al. 2004). This is shown by observing that the set of most biased genes S (consisting of 1% of the genes in G and where the size of S is suggested by Sharp's original work) can be automatically computed by a pure statistical analysis of the collection of all genes which is not based on biological knowledge of the organism. In the case of fast growers, S indeed is found to consist of highly expressed genes. The lack of reliance on biological knowledge allows computation of weights for organisms of unknown lifestyle. Codon weights, reference set S, and CAI values are calculated with the program *CAIJava* written by the authors, which uses parsers of GenBank flat files from the *Biojava* (http://www.biojava.org) programming package. A description of the algorithm and a validation of the approach are reported by Carbone et al. (2004). The program *CAIJava* is available at http://www.ihes.fr/∼carbone/data.htm.

Detection of Weak and Strong Forms of Translational Bias

In Carbone et al. (2004), two numerical criteria were introduced to detect translational bias. The *ribosomal criterion* defines the z-score$(CAI(r) - \mu)/\sigma$, for each gene of a ribosomal protein r, where mean μ and standard deviation σ are calculated for the CAI distribution over all CDS; this allows us to define the average $\bar{z}_{\mathrm{Rib}}$ of z-scores for ribosomal proteins and say that an organism characterized by translational bias is expected to have high $\bar{z}_{\mathrm{Rib}}$ i.e., >1. The *strength criterion* computes codon weights, as in (1), based on all genes in the genome G ($w_k(G)$) and on the genes in the set S (w_k) and expects the difference between w_k (G) and w_k to be large for translationally biased genomes (i.e.,$\sum_{k=1}^{64} (w_k(G) - w_k)/2 > 8$; this sum is an indicator of the number of amino acids having different preferred codons in the entire genome and in the set of most biased genes; the threshold 8 has been empirically calculated on known translationally biased organisms [Carbone et al. 2004]). The combination of the two criteria allows determination of which genomes are *strongly* translationally biased, that is, those satisfying both criteria, from those that are *weakly* so, that is, those that only satisfy the ribosomal criterion. Notice that our numerical criteria provide quantitative values ranging within a continuous interval and that, based on these values, one can identify strong, weak, and absent forms of bias as well as finer classifications.

Codon Bias Signatures

Given a genome sequence, weak and strong tendencies toward content bias, translational bias, and strand bias can be identified (Carbone et al. 2004). The collection of strong codon biases affecting CDS coding is referred to as the *codon bias signature* of the genome. Signatures for the genomes in Table 1 have been analyzed by Carbone et al. (2004). Codon signatures are indicators of the evolutionary pressure organisms undergo.

Ranking of Pathways in the Metabolic Network of an Organism

For each pathway P of the metabolic network M of an organism, we compute the mean of the CAI values of the enzymes involved in P. If an enzyme is involved in more than one reaction in P, its CAI value is counted with multiplicity. Some enzymes in a pathway might contribute no CAI value due to the fact that they have not been identified in the genome. This numerical index of pathways is called the *Pathway Index* (PI), and we denote PI(P) the mean value for a pathway P. This index allows us to define a ranking of pathways involved in metabolism.

There is a significant difference in PI values between pathways (see Table 1). *S. cerevisiae* is the organism in Table 1 that displays the most variation of PI values among pathways, with $\mu_M = 0.31$ and $\sigma_M = 0.12$, where μ_M and σ_M are the mean and the standard deviation of the distribution of PI(P) values for P in M, with a minimum and a maximum PI value of 0.15 and 0.73 for the methionine biosynthesis from homoserine pathway and the glycolysis pathway. This large spread among PI values justifies the use of the average CAI of genes involved in a pathway as a biological relevant measure. In the sequel, we consider the interval$[\mu_M - \sigma_M, \mu_M + \sigma_M]$, and intuitively, we say that PI(P) values $\geq \mu_M + \sigma_M$ are "high" and those $\leq \mu_M - \sigma_M$ are "low."

Clustering of Genes Along the Genome and Pathway Index

The pathway index is independent of the localization of genes along the genome. To see this, we consider the enzyme positions along the genomic sequence, and we allow up to three genes coding for proteins that do not belong to the pathway to intercalate between two genes coding for enzymes in the pathway.

We say that two enzymes are *clustered* if they are located in this pattern along the genomic sequence. The results are displayed in Table 1. Most pathways consist of enzymes which are not clustered in the same genomic region. On average, only 7–8% of enzymatic reactions are involved in "clustered" pathways. In particular, in *E .coli* this value drops to 3%.

Ranking of Metabolic Networks and Network Comparison Across Organisms

To compare the distribution of codon bias in metabolic pathways across organisms, we define the *Relative Pathway Index* as $RPI(P) = (PI(P) - \mu_M)/\sigma_M$, where the mean and the standard deviation are taken over all Ps in the metabolic network M of an organism. This measure is used to compare organisms with respect to common metabolic pathways. After this normalization of PI values we can define the *Comparative Pathway Index* CPI(P) to be the average of the RPI(P) for all organisms sharing a pathway P, for comparison of the ranking of pathways over multiple organisms.

For visual representation and comparison (see Fig. 1), we recall that an RPI(P) value of $+1$ corresponds to a pathway with a bias one σ above the mean for the organism, and a value of -1, one σ below. So the interval $[-1,1]$ is mapped into a continuous range of colors, going gradually from violet, blue, and green (lower values) to yellow, orange, and red (higher values) and pathways are as-

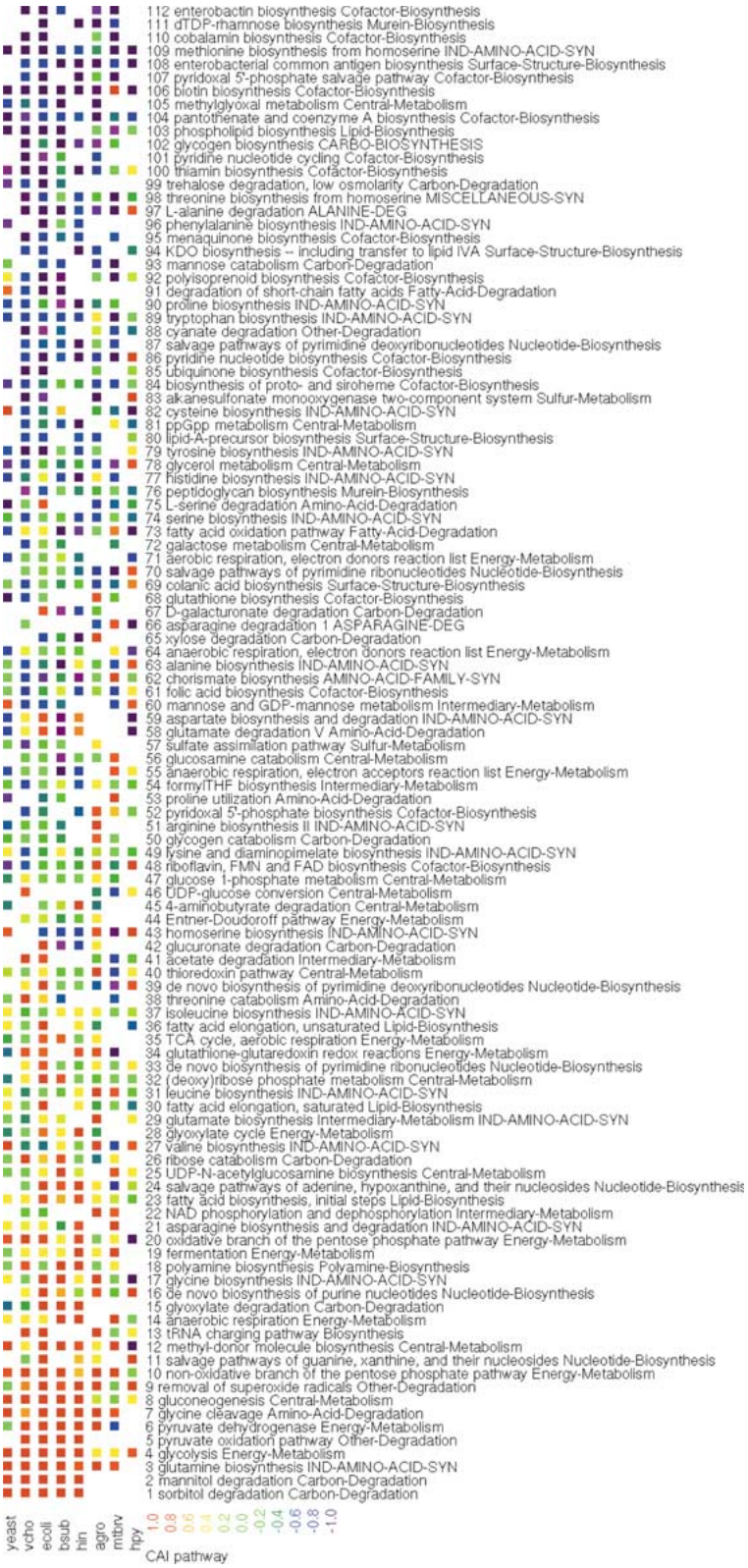

Fig. 1. Metabolic pathways occurring in four or more organisms among those listed in Table 1, *Mycobacterium tuberculosis H37Rv* (mtbrv), and *Helicobacter pylori* (hpy). For each organism, the RPI value associated with a pathway, if it exists, is indicated by the corresponding ranking color. Each row corresponds to a pathway denoted by (Biocyc) name and functional classification. Pathways are increasingly ordered from top to bottom by CPI.

signed the corresponding color. Pathways with RPI(P) values falling outside the interval take the values of the closer extremes, −1 (violet), +1 (red). The mapping provides a good spread of colors for a suitable reading of metabolic differences, especially for CAI homogeneous organisms, independent of the width of the underlying statistical distribution.

Transcriptomic Data and Expression Levels

Transcriptomic data for *S. cerevisiae* are taken from the study reported by Holstege et al. (1998) and based on Affymetrix GeneChip high-density oligonucleotide array (HDA) technology (downloaded from http://www.wi.mit.edu/young/expression.html in 1999, and

Table 2. PI of methane metabolism pathway (PI[Met]) in some translationally biased organisms

Organism	μ	σ	$\mu + \sigma$	PI(Met)	μ_R
Agrobacterium tumefaciens	0.44	0.11	0.55	0.51	0.64
Bacillus subtilis	0.37	0.07	0.44	0.48	0.64
Escherichia coli	0.30	0.10	0.40	0.41	0.60
Haemophilus influenzae	0.38	0.09	0.47	0.48	0.58
Vibrio cholerae	0.28	0.08	0.36	0.36	0.64
Saccharomyces cerevisiae	0.16	0.12	0.28	0.18	0.78
Methanosarcina acetivorans	0.50	0.06	0.56	0.57	0.63

Note. Only *M. acetivorans* is known to use methane metabolism in an essential way.

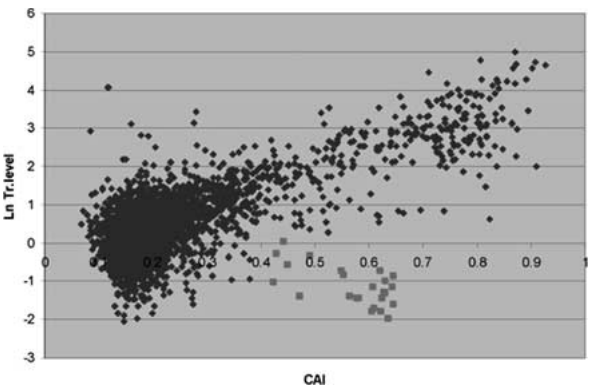

Fig. 2. Transcriptional level of *S. cerevisiae* genes are plotted (in log scale) with CAI values; a group of outliers displaying high CAI values and low transcriptional levels is illustrated as light gray squares.

available at http://www.ihes.fr/∼carbone/data.htm). It concerns a set of 4849 genes whose expression profiles are determined by growing yeast cultures to midlog phase. Expression levels are defined as the numbers of copies of a given mRNA per yeast cell. The arrays can detect as few as 0.1 mRNA molecule/cell; the dynamic range over which detection is accurate is approximately 0.1–100 mRNA molecule/cell. The yeast genome is covered by four HDAs and each gene is represented on the HDA by 20- to 25-mer oligos that match the sequence of the message (perfect match oligos) and 20 oligos that are identical but differ by one base (mismatch oligos). Expression levels are calculated by subtracting the signal of a mismatch from its perfect match partner and averaging the difference for each oligo pair for a given gene. The average difference value is a measure of the expression level of that gene used in Fig. 2.

Transcriptomic data on the *S. cerevisiae* cell cycle under diauxic shift are taken from deRisi et al. (1997). Expression levels are computed as absolute fluorescence intensity minus background. Because of the considerable variation across microarray experiments, expression levels shown do not translate into absolute mRNA concentrations and are informative only when taken in relation to other genes. Despite the differences in technology and definitions of expression levels, transcriptomic data collected at different time points by deRisi et al. (1997), when plotted with CAI values (not shown), display shapes similar to Fig. 2, constructed from Holstege et al. (1998). Compare with the slope of the distributions of pathways in Fig. 3.

Transcriptomic Data as Indices of Metabolic Networks

A transcriptional pathway index for a metabolic network can be calculated from mRNA abundance levels obtained through microarray analysis. We define the $PI_T(P)$ of a pathway P as the average of the expression levels of the enzymes involved in P at a given environmental condition (analogous to our definition of an index based on CAI values). Again, enzymes are counted with multiplicity and omitted where data are lacking.

Normalization of PI_T values is done as for PIs above, by defining $RPI_T(P) = (PI_T(P) - \mu_T)/\sigma_T$, where μ_T, σ_T are the mean and standard deviation of the distribution of $PI_T(P)$ values for P in M at a given time point. The visual representation (in Fig. 3) of the interval $[-1, +1]$ is mapped into a continuous range of colors, going gradually from violet to red, as above. Pathways P with $RPI_T(P)$ value falling outside the interval take the values of the closer extremes (violet or red).

For a given organism and a set of microarray data experiments obtained under different biological conditions, we define the *Evolutionary Pathway Index* (EPI) to be a numerical ranking of pathways P, ordering them by the *maximum* among the $PI_T(P)$ values within all conditions in the set. Intuitively, the maximum value obtained over a sufficiently large set of transcriptomic data corresponding to different biological states should provide information on those pathways and enzymes that are rarely highly translated but that on certain occasions need to be expressed in large quantities and/or rapidly.

An evolutionarily meaningful set of experiments is a set of transcriptomic data which presents a sufficiently large variation of gene expression levels under sufficiently large changes in biological conditions. The transcriptomic data on the diauxic shift of deRisi et al. (1997) present such variation.

Metabolic Activities Derived from CAI Values

Genes with *high* CAI values in fast-growing organisms are commonly interpreted as those which are involved in maintaining this growth rate or in enzymatic activities with a rapid response (Gouy and Gautier 1982; Sharp and Li 1987; Sharp et al. 1988; Médigue et al. 1991; Shields and Sharp 1987; Carbone et al. 2004). Genes with such properties are coding for ribosomal proteins, heat shock proteins, antioxidant proteins, proteins involved in the respiratory chain, structural genes (for eukaryotes), and enzymes involved in the metabolic pathways of amino acids biosynthesis. Functional groups of genes which have *low* CAI values are transcription factors, genes involved in pattern formation (for eukaryotes), cell cycle progression, clock genes, genes involved in the metabolic pathways of nucleotide biosynthesis, carbohydrates, lipids, and secondary metabolites, but also degradation as the

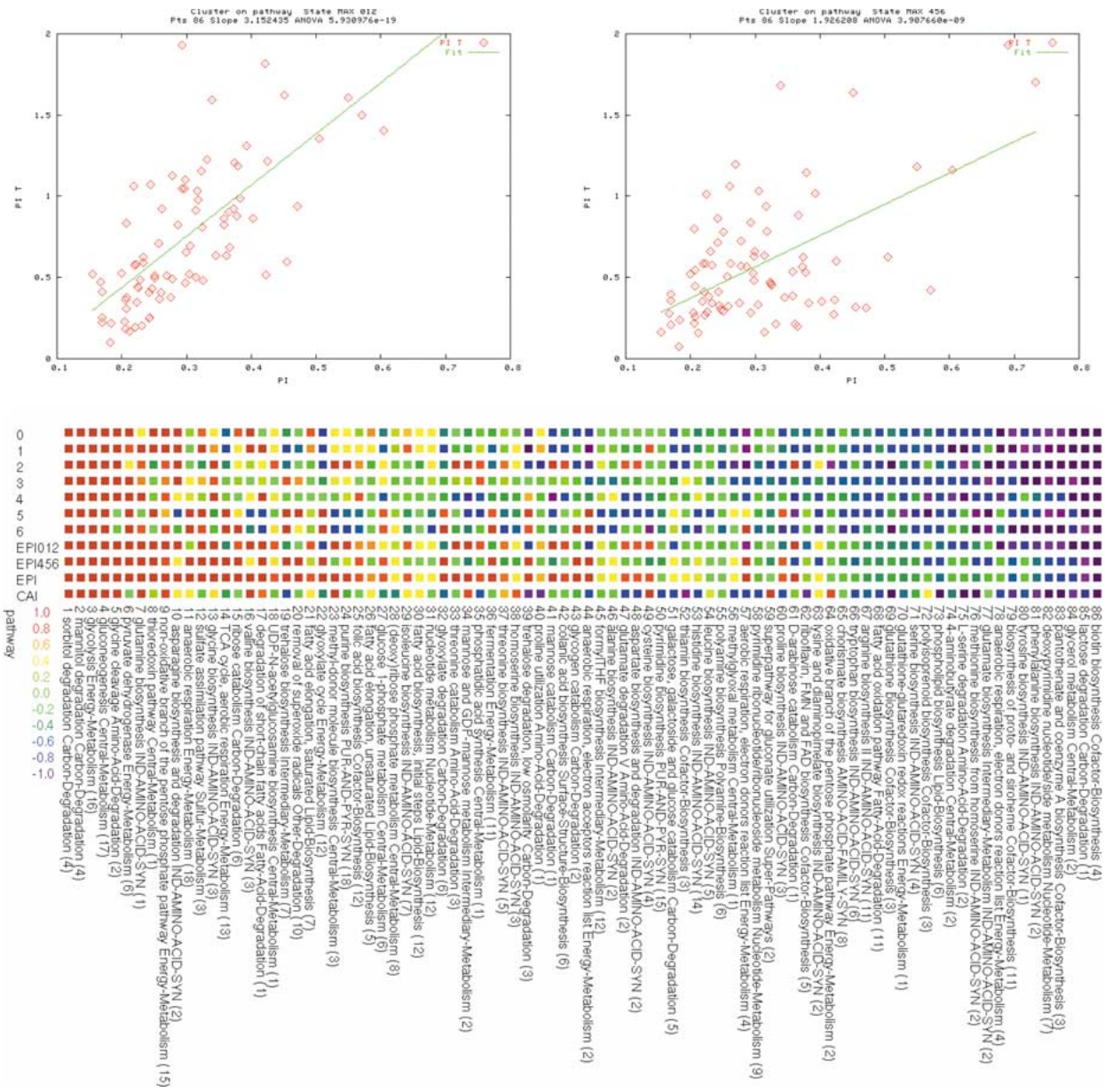

Fig. 3. *S. cerevisiae* cell cycle during diauxic shift. **Top**: Plots corresponding to the activity of 86 metabolic pathways during time points 0, 1, 2 (left) and 4, 5, 6 (right). Each point in a plot is a metabolic pathway P represented by its maximum $PI_T(P)$ (y-axis) value calculated over three time points and PI(P) (x-axis) value; slopes of the distribution of metabolic pathways go down from the anaerobic state (fermentation), left to the aerobic state (respiration), right. (Also, the r^2 values of the fits are 0.782 and 0.583, respectively, based on the least-squares fit model). **Bottom**: RPI_T value of metabolic pathways during time points 0...6 of the diauxic cycle; EPI value for time points 0, 1, 2 (EPI012), 4, 5, 6 (EPI456), and all (EPI); and RPI(P) values (CAI). Pathways (cited by name, functional classification, and number of distinct enzymes involved) are ordered by EPI.

ubiquitin–proteosome pathway, or apoptosis. When the organism is not growing fast, then high-CAI-value genes are often correlated with a dominant bias of other origins, like GC3 content or strand bias (Carbone et al. 2003).

A more careful analysis reveals that for fast growers, there exists a large gap between the mean (μ) of the CAI distribution over all CDSs and the average CAI value for ribosomal proteins (μ_R); for *E. coli*, for instance, $\mu_R = 0.60$ and $\mu = 0.30$, with a standard deviation $\sigma = 0.10$. For many species that do not grow fast, the gap between μ and μ_R is less important, but ribosomal proteins still display a relatively high CAI, that is $\mu_R > \mu + \sigma$. *Mycoplasma pulmonis*, for instance, has $\mu_R = 0.7$, $\mu = 0.57$, and $\sigma = 0.05$. This organism has a dominant codon bias with no apparent translational origin but, rather, a dominant AT3 bias (Carbone et al. 2004); nevertheless, the codon composition of its ribosomal proteins is largely affected by AT3 bias.

For those translationally biased organisms for which not much is known of the metabolic activity of their enzymes, CAI analysis of specific genes and comparison with the coding of ribosomal proteins suggest a criterion to infer lifestyle: genes whose CAI value is close to μ_R, that is, $\geq \mu_R - \sigma$, can be treated as indicators of important metabolic activities for the organism. (Notice that this bound implicitly considers the "strength" of the translational bias of the genome, indicated by how large the interval $\mu_R - \mu$ is.) We discuss this hypothesis for ferrodoxin metabolism, photosynthesis, and methanogenesis.

Ferrodoxin in P. abissi

The archaea *P. abissi* has been computationally classified as a translationally biased organism (Carbone et al. 2004), with $\mu = 0.45$, $\sigma = 0.07$, and $\mu_R = 0.59$. Among its most biased genes, besides ribosomal proteins and elongation factors, we find ferrodoxin (CAI(fdxA) = 0.71), ferredoxin oxidoreductase (CAI(for) = 0.63), and keto-valine–ferredoxin oxidoreductase γ-chain (CAI(PAB1470) = 0.62). Ferredoxin appears to be the major metabolic electron carrier in pyrococci (Cohen et al. 2003). After reduction during peptide or sugar degradation, it is mainly reoxidized by a membrane-bound hydrogenase (Silva et al. 2000), potentially generating membrane potential. In addition, ferredoxin has been suggested to be reoxidized by ferredoxin–NADP oxidoreductase (Silva et al. 2000; Schut et al. 2001). Moreover, NADPH can also be oxidized via the conversion of pyruvate to alanine, via glutamate dehydrogenase (CAI(PAB0391) = 0.74) and alanine aminotransferase (CAI(PAB1810) = 0.55) (Ward et al. 2000). The high bias of all genes involved in ferrodoxin metabolism hints at the importance of this pathway for the organism.

Photosynthesis Pathways: Synechocystis

The cyanobacterium *Synechocystis* is classified to be *translationally biased* (Mrázek et al. 2001) and its most biased genes are ribosomal proteins, phycocyanin (CAI(cpcB) = 0.79, CAI(cpcA) = 0.78), allophycocyanin (CAI(apcB) = 0.78, CAI(apcA) = 0.72), photosystem II proteins (CAI(psbA2) = CAI(psbA3) = 0.77, CAI(psbI) = 0.70)), fructose-1,6-bisphosphatealdolase (CAI(cbbA) = 0.71), and ferredoxin (CAI(petF) = 0.76) (Carbone et al. 2004). The presence of proteins involved in *photosynthesis* within the most biased genes is a good indicator of the known photosynthetic activity and lifestyle of *Synechocystis*. In fact, the metabolic networks of photosystem I, photosystem II, and the Calvin cycle have PI = 0.62, 0.58, and 0.62, respectively, and from $\mu_R = 0.60$, $\mu = 0.50$, and $\sigma = 0.07$, a photosynthetic preference of *Synechocystis* is confirmed with $\text{PI(P)} \geq \mu_R - \sigma$, for all three pathways P above.

Methane Metabolism: Methanosarcina acetivorans

The archaeon *M. acetivorans* has been computationally classified as a translationally biased organism (Carbone et al. 2004), with $\mu_R = 0.63$, $\mu = 0.50$, and $\sigma = 0.06$. Besides ribosomal proteins, methanol-5 hydroxybenzimidazolylcobamide comethyltransferase (CAI(mtaB1) = 0.83, CAI(mtaB2) = 0.75, CAI(mtaC1) = 0.71, CAI(mtaB3) = 0.68), methyl coenzyme M reductase (CAI(MA4546) = 0.79, CAI(MA4547) = 0.76, CAI(MA4550) = 0.73), and methylcobamide methyltransferase isozyme M (CAI(mtaA) = 0.72) are among the most biased genes. In particular, $\text{PI(Met)} = 0.57 \geq \mu_R - \sigma$, where Met is the methane metabolism network. As shown in Table 2, no organism in Table 1 has PI(Met) within 1 SD σ from μ_R, while *M. acetivorans* does. From this and the high CAI value of proteins involved in methane metabolism, one can infer the unusual living environmental conditions of these bacteria.

Metabolic Activities and RPI Values: Analysis of Metabolic Networks Across Species

For translationally biased organisms whose metabolic network has been partially reconstructed, CAI values of enzymes might be profitably used as indicators of preferential metabolic pathways and of lifestyle. Using the notion of *Relative Pathway Index* (RPI; defined in Materials and Methods), we observe that pathways can be grouped into classes with low, medium, and high RPI. As shown in Fig. 1 (and the same conclusions hold for pathways shared by fewer than four organisms), there are pathways that display the same bias across organisms: shared high RPI values (red and orange squares) suggest that a metabolic activity is favored and that it has a possibly constitutive regime; shared low RPI values (violet and blue squares) suggest that a metabolic activity is likely not involved in chains of rapid enzymatic responses. Pathways with low RPI values are essentially cofactors–coenzymes involved in vitamin biosynthesis which are known not to be usually produced with a high efficiency, and pathways with high RPI values are mainly involved in energy metabolism. There is a third group of pathways that display mixed RPI values across species, and from this set of pathways one might expect to infer *differences* in lifestyle. These pathways are mainly involved in central metabolism and amino acid synthesis and degradation. A thorough organism comparison can be realized by fol-

lowing the ranking described by the metabolic maps in Fig. 1. Here we consider a few specific pathways which are highly biased in one organism, but not in others, and argue, based on experimental evidence, in favor of their importance for the life of the organism. Below, a pathway is associated with the numbering listed in Fig. 1.

Glycolytic Pathway

For all translationally biased organisms in Table 1, the glycolytic pathway is expected to be especially favored because of fast growth. It has been observed that most genes with the highest CAI values are involved in this pathway (Sharp and Li 1987), and accordingly, we find that the RPI value of the pathway (4) is one of the highest as displayed in Fig. 1.

Glutamate Biosynthesis for A. tumefaciens

The genome of *A. tumefaciens* contains seven glutamine synthetase genes encoded in three distinguished types (with CAI(glnA I) = 0.77, CAI(glnA II) = 0.74, CAI(glnA III) = 0.57), and the presence of multiple copies of these genes seems to be related to the observation that this bacterium requires high concentrations of glutamate for optimal growth (Wood et al. 2001). The RPI value of the glutamate biosynthesis pathway (29) in *A. tumefaciens* is high; note that for all other organisms in Table 1 this pathway has a much lower RPI.

Metabolic Differences Between S. cerevisiae *and Aerobic Bacteria*

A number of pathways involved in amino acid biosynthesis (homoserine [43], valine [27], and cysteine [82]) and intermediate metabolism (mannose and GDP-mannose [60]) are highly biased in *S. cerevisiae* but not in most translationally biased aerobic bacteria in Table 1. The highly biased mannose and GDP-mannose metabolic pathway confirms the experimental evidence that *S. cerevisiae* can produce ethanol from glucose and mannose if the concentrations of sugars are high or when the yeast is grown under anaerobic conditions (Ratledge 1991), and this finding agrees with the statistical evidence reported in the next section, that the genome of *S. cerevisiae* has undergone strong selective pressure favoring a predominantly fermentative metabolism.

Also, the pyruvate dehydrogenase pathway (6) and the removal of superoxide radicals pathway (9) are highly biased in aerobic bacteria in Table 1 but not in the *S. cerevisiae* genome. In this respect, note that aerobic conditions lead to the generation of acetyl-CoA and pyruvate dehydrogenase, and its coenzymes play a decisive part in this reaction. Also, since oxygen and its derivatives are toxic and can lethally damage certain cellular components, protective enzyme systems have been evolved by aerobic organisms (that use oxygen as terminal electron acceptor in respiration in a crucial way), and this agrees with the removal of superoxide radical pathway being highly biased. On the other hand, again, the absence of bias for these two pathways found in *S. cerevisiae* sustains the hypothesis of selective pressure favoring fermentation in this organism (see below).

L-Serine Degradation in E. coli

L-serine is a preferred growth factor for *E. coli* and experimental evidence is reported in several studies (Pizer and Potochny 1964). The high RPI value of the L-serine degradation pathway (75) justifies the sensitivity of *E. coli* to L-serine and its potential toxicity to the cell (Newman and Walker 1982).

Ammonia Assimilation Pathway in E. coli

The enteric bacterium *E. coli* (and many other organisms) have two primary pathways of glutamate synthesis, the glutamate dehydrogenase (GDH) and the glutamine synthetase–glutamate synthase (GOGAT) pathway. GDH plays a role in glutamate synthesis when *E. coli* is under energy (and carbon) restriction but not under ammonium or phosphate restriction, and the GOGAT pathway is responsible for glutamate synthesis when energy is plentiful or when the ammonium or phosphate concentration becomes low. In an energy-rich (glucose-containing), nitrogen-poor environment, glutamine synthetase and glutamate synthase form the ammonia assimilatory cycle GOGAT, which is ATP-dependent and *essential* for nitrogen-limited growth and for steady-state growth with some sources of nitrogen. We found that the RPI value of GOGAT is high (with CAI(glnA) = 0.60, CAI(gltD) = 0.49, and CAI(gltB) = 0.42), and this is in agreement with the essential role of the pathway. In particular, RPI(GOGAT) is higher than RPI(GDH) (with CAI(gdhA) = 0.41), and this sustains the experimental evidence that GOGAT plays at least two roles for which GDH cannot substitute. GOGAT can fix ammonium into organic molecules (glutamine, thence glutamate and other compounds) when the external concentration of ammonium is low, and it reduces the concentration of glutamine when that concentration becomes high (Reitzer 1986). Note also that a strain deficient in glutamate dehydrogenase has no observable growth phenotype under usual growth conditions (Reitzer 1986) but that GDH appears to be important during energy-limited growth because,

through its use, the cost of biosynthesis is scaled down (Helling 1994).

Evolution of Metabolic Networks and Transcriptomic Data in *S. cerevisiae*

The high CAI value of genes is a good indicator not only of the high level at which a protein might be constitutively translated but also of the "possibility" for a protein to be highly expressed under very specific biological conditions. The next two examples suggest that codon bias is more informative than expression data for those enzymes involved in the wild that may not be highly expressed in laboratory experiments.

Seripauperine Proteins in Yeast

We consider the set of outlier ORFs (see Fig. 2 and also Carbone et al. [2003]) in the correlation plot between *S. cerevisiae* transcriptomic data (Holstege et al. 1998) and CAI values (Carbone et al. 2003). These outliers correspond to the gene family of seripauperines (the majority of unknown ORFs within the set are homologous to PAU1), which are small proteins (100 aa) presenting a strong sequence identity to proteins that are serine rich but deprived of the serine-rich domains. These genes are highly induced during fermentation conditions or long-lasting anaerobism (experimental evidence is reported on brewery yeast by James et al. [2003]), while their expression is difficult to detect under normal conditions. (Viswanathau et al. 1994)

Hem13 Proteins in Yeast

Hem13 is an enzyme involved in the heme biosynthetic pathway of *S. cerevisiae*. It is an oxidase with oxygen as a substrate (Zitomer and Lowry 1992). It displays a quite high CAI value (0.47), compared to $\mu = 0.16$ and $\sigma = 0.12$ for all *S. cerevisiae* genes, and it is highly translated under anaerobic conditions (Amillet et al. 1995) but not otherwise. Several facultative aerobic organisms contain a second enzyme catalyzing the same reaction as Hem13 but where the role of oxygen is replaced by molybdenum cofactor and S-adenosylmethionine. Since *S. cerevisiae* does not contain such an alternative enzyme, it is plausible that during anaerobism (or micro-aerobism) *S. cerevisiae* produces a large quantity of Hem13 to efficiently use the little oxygen present in the medium and to induce the heme necessary for its metabolism.

These examples suggest that we look at the drastic changes in the expression of genes involved in fundamental cellular processes which are detectable along the switch from anaerobic growth (fermentation) to aerobic respiration upon depletion of glucose in the cell cycle of *S. cerevisiae*. This cycle is known as the diauxic shift; it has been documented by Johnston and Carlson (1992) and studied through DNA microarrays by deRisi et al. (1997). Through this global view of the way the cell adapts to a changing environment, and by comparing transcriptomic levels to PI values of metabolic networks, we aim to detect those pathways that might be important for cell viability but whose relevance might be difficult to observe in laboratory experiments. For this, we analyze thoroughly the transcriptomic data of deRisi et al. (1997) collected along seven time points (0...6) at successive 2-h intervals during diauxic shift. We look at slopes of the regression lines for PI_T values in terms of PI values of metabolic pathways and notice that the change in transcriptomic values taking place from fermentation (corresponding to time points 0, 1, 2) to aerobic respiration (corresponding to time points 4, 5, 6) *globally* affects the entire set of metabolic pathways involved in the cell cycle. The regression lines associated with the successive time points 0...6, corresponding to the progressive depletion of glucose in the medium, display gradually decreasing slopes (not shown). In particular, pathways with a low PI value (that is, $PI(P) < 0.25$) on time points 0, 1, 2 suddenly augment their PI_T on time points 4, 5, 6, and accordingly, pathways with a medium–high PI value ($0.25 < PI(P) < 0.45$) decrease in PI_T. (Figure 3 summarizes this observation; it shows average PI(P) and $PI_T(P)$ values computed over time points 0, 1, 2 and 4, 5, 6 and decreasing slopes for the corresponding regression lines.) The list of affected pathways is given in Fig. 3. Below, we refer to pathways with the numbering listed in Fig. 3.

It has been suggested that the high slope associated with the fermentative state (i.e., a strong correlation between CAI values and expression levels) might indicate a strong evolutionary pressure that favored a predominantly fermentative metabolism of yeast in the wild (Wagner 2000). Moving the organism to an unfavored state is then reflected by the drop in slope as less often used genes (with correspondingly lower CAI values) are moved to higher expression levels. Our analysis confirms that pathways which are highly active during fermentation are also highly biased and leads us to conclude that the coding sequences of enzymes involved in specific metabolic functions (indexed by PI values) describe the physiological responses of yeast precisely during fermentation (indexed by PI_T). The examples of seripauperine and Hem13 proteins discussed above, presenting strong codon bias (i.e., large CAI values) and large RNA abundance during fermentation, sustain this hypothesis. Other metabolic pathways playing a crucial role in fermentation are detectable from the

analysis of the diauxic cycle. We see that pathways with a high RPI value (red and orange squares in the CAI line in Fig. 3, bottom) and at least two enzymes participating in the metabolic reaction have a high EPI value during fermentation (i.e., at time points 0, 1, 2; see red and orange squares in the EPI012 line in Fig. 3). They are glycolysis (3), gluconeogenesis (4), glycine cleavage (5), glutamine biosynthesis (7), sorbitol (1) and mannitol (2) degradation, and the non-oxidative branch of the pentose phosphate pathway (9). These are also highly expressed during aerobic respiration, while mannose, GDP-mannose (34), and valine biosynthesis (16), methyl-donor molecule biosynthesis (23), and cysteine biosynthesis (49) are highly expressed only during fermentation. There are three pathways where this claim is not verified by the diauxic cycle dataset (i.e., RPI is high but EPI012 is low): homoserine biosynthesis (38), gluconate utilization (59), and the oxidative branch of the pentose phosphate pathway (64). There is experimental evidence, however, of the involvement of the oxidative pentose phosphate pathway and of the gluconate utilization pathway during fermentation. It has been reported (Middelhoven et al. 2000) that under anaerobic conditions, the yeast *Saccharomyces bulderi* rapidly ferments (δ-gluconolactone to ethanol and carbon dioxide. In particular, levels of the pentose phosphate pathway enzymes were 10-fold higher in δ-gluconolactone-grown anaerobic cultures than in glucose-grown cultures (van Dijken et al. 2002). Also, growth of *S. cerevisiae* on δ-gluconolactone was found to be associated with a specific coordinate induction of the synthesis of two enzymes of the oxidative pentose phosphate pathway, 6-phosphogluconate dehydrogenase and 6-phosphogluconolactonase, together with that of gluconokinase (Sinha and Maitra 1992). For the homoserine biosynthesis pathway we could not find experimental evidence of its involvement in fermentation, and we claim that there is some time point during fermentation when genes belonging to this pathway are highly expressed.

Discussion

New measures aiming to numerically study biological and evolutionary questions and to index metabolic pathways across translationally biased organisms with respect to genetic coding are introduced. The approach seems to apply profitably also to genomes displaying *weak* forms of translational bias. Even though the interval between μ and μ_R is much less pronounced in genomes that present weak forms of translational bias, CAI analysis and RPI analysis help to determine metabolic preferences and to reveal interesting information on lifestyle. We discuss two examples.

The Case of M. thermoautotrophicum

The archaeon *M. thermoautotrophicum* has been computationally classified to have a weak form of translational bias (Carbone et al. 2004), with $\mu = 0.51$, $\sigma = 0.07$, and $\mu_R = 0.59$. Besides ribosomal proteins, tungsten formylmethanofuran dehydrogenase and methyl reductase dehydrogenase, that is, genes involved in methane metabolism, are among the most biased genes in *Methanobacterium*.

The Case of M. tuberculosis H37Rv

The virulent strain *M. tuberculosis H37Rv* has a doubling time of about 20 h and its genome presents a weak form of translational bias (Carbone et al. 2004), with $\mu_R = 0.57$, $\mu = 0.50$, and $\sigma = 0.07$. The metabolic map of *M. tuberculosis H37Rv* is displayed in Fig. 1. Among networks with a high RPI value, a key example is provided by the biotin biosynthesis pathway (106 in Fig. 1), which turns out to have a very high RPI for *Mycobacteria* (note that also the clinical isolate *M. tuberculosis* CDC displays a very high RPI value for biotin biosynthesis; not shown) but a very low RPI for all other organisms we studied: *M. tuberculosis* has a lipid-rich cell envelope which contributes to virulence and antibiotic resistance. Acyl-coenzyme A carboxylase, which catalyzes the first committed step of lipid biosynthesis, consists in mycobacteria of two subunits, one of which is indeed biotinylated. Genes encoding a biotinylated protein have been cloned and sequenced and the presence of biotin-binding sites has been experimentally demonstrated (Norman et al. 1994). Several other metabolic pathways have been ranked high in RPI for *M. tuberculosis H37Rv* despite their low RPI values for other species. Experiments demonstrated that the chorismate biosynthesis pathway (62) is essential for the viability of *M. tuberculosis H37Rv* (Parish and Stoker 2002) and that the aspargine degradation pathway (66), pyridoxal 5-phosphate biosynthesis (52), valine degradation (not shown in Fig. 1), and leucine biosynthesis (31) are also essential pathways (Sassetti et al. 2003). Finally, the ppGpp metabolic pathway (81) is essential for long-term survival of mycobacteria under starvation conditions (Primm et al. 2000). All these pathways of *M. tuberculosis* have high RPI values. Note that the serine biosynthesis pathway, which has been detected to be essential by Sassetti et al. (2003), has been found to be very highly ranked in the *M. tuberculosis* CDC strain (not shown).

In genomes where codon usage has a *strictly* mutational origin (i.e., strand bias or compositional

bias), one expects highly ranked pathways to have a different base composition with no associated biological meaning. However, there are genomes that might present weak tendencies toward translational bias which can be identified by our approach but cannot be detected with classical statistical methods such as hidden Markov chains and multivariance statistical methods (Perrière and Thioulouse 2002; Nicolas et al. 2002; Lafay et al. 2000) or with numerical criteria based on ribosomal analysis (Carbone et al. 2004).

The Case of H. Pylori

H. pylori is a microaerophilic, Gram-negative bacterium, whose infection is associated with type B gastritis and peptic ulcer disease and is a risk factor for gastric carcinomas in humans. *H. pylori* is a slow grower. It has been cultured on diverse agar-based media, resulting in 2 to 4 days of growth at 37°C. Its genome is known to display no sharp dominant codon bias but, rather, a homogeneous codon composition (Lafay et al. 2000), with $\mu = 0.55$, $\sigma = 0.12$, and $\mu_R = 0.59$. Despite this fact, we observe that the pathway for glycolysis (4) has a high RPI in *H. pylori*, and this indicates that some translational bias in this organism is nevertheless present. In this respect, note that glucose appears to be the only carbohydrate utilized by this bacterium (Tomb et al. 1997) and that rapid growth with a doubling time of about 50 min has been reported (Andersen et al. 1997). Our analysis also indicates the thioredoxin pathway (40) to have a rather high RPI value (see Fig. 1), and this is experimentally confirmed by the finding that *H. pylori* has a thioredoxin-dependent peroxiredoxin system playing a critical role in the defense against oxygen toxicity that is essential for survival and growth, even in microaerophilic environments (Baker et al. 2001). Another highly RPI ranked pathway is riboflavin biosynthesis (48), which turns out to play a crucial role in ferric iron reduction and iron acquisition by *H. pylori* (Worst et al. 1998). In fact, as other pathogenic bacteria, *H. pylori* encounters an iron-limiting environment when it attempts to colonize or invade a mammalian host.

To summarize, we proposed that the lifestyle of an organism can be deduced for translationally biased organisms by analyzing the set of most biased genes in the genome, and we observed that weakly translationally biased genomes also carry information on lifestyle. The case of *H. pylori* suggests that this rule might be extended to a much broader class of organisms. In support of this hypothesis, we found that the most biased genes of the cyanobacterium *Thermosynechococcus elongatus* have photosynthetic functions. Over the first 24 top CAI ranked genes there are 6 photosystem I and II proteins, 1 phycobilisome small core linker polypeptide, 2 phycocyanin subunits, 2 allophycocyanin subunits, 2 cytochrome b6 proteins, and 2 ribosomal proteins. There is no evidence that *Thermosynechococcus elongatus* is translationally biased, neither experimental nor computational (Carbone et al. 2004) (in particular, no compositional bias has been detected), but its most biased genes highly reflect the lifestyle of this organism. Again, *Chlorobium tepidum*, a Gram-negative bacterium of the green sulfur phylum, is an obligate anaerobic photolithoautotroph and lives in high-sulfide hot springs where anoxic layers containing reduced sulfur compounds are exposed to light. It is a thermophile, growing optimally at 48°C. There is no evidence that *C. tepidum* is translationally biased, neither experimental nor computational (Carbone et al. 2004), but we note that its first 20 top CAI ranked genes contain 2 hydrogenase/sulfur reductases, 3 sulfite reductase subunits, 2 iron–sulfur cluster binding proteins, 1 ferrodoxin protein, and 1 ribosomal protein. These are proteins that characterize well the living conditions of these bacteria. Note that the strong GC3 bias of this genome does not prevent the genomic coding from revealing the crucial role of certain enzymes.

These observations lead us to conclude that there is still much to understand about the role of codon bias in genomes and that refined quantitative measures of codon bias which are able to differentiate bias *strengths* are needed to investigate in silico a new range of biological possibilities for larger classes of organisms.

Dominant Codon Bias and tRNA Charging Pathways

Charging of tRNA pathways has been described for *E. coli*, *A. tumefaciens*, and *V. cholerae* among the organisms listed in Table 1. For these organisms most amino acids have a tRNA charging pathway P with $\mathrm{PI(P)} \geq \mu + \sigma$. Namely, *E. coli*, *A. tumefaciens*, and *V. cholerae* have 20, 16, and 18 pathways P with PI(P), $\geq \mu + \sigma$ respectively. This finding leads to the hypothesis that all translationally biased genomes present high bias on tRNA charging pathways. We also verified that in *H. pylori*, 19 tRNA charging pathways P display $\mathrm{RPI(P)} \geq \mu$ and 12 of them have $\mathrm{RPI(P)} \geq \mu_R$. This last observation suggests a need for efficiency of this process which is *independent* of the strength of translational bias. Note also that, for *E. coli*, *A. tumefaciens*, and *V. cholerae*, we separated two sets of genes, one containing the 2% of most biased genes and the other containing all other genes. We then applied linear discriminant analysis and observed that the amino acid separation coefficients do not display a significant correlation between the organism-preferred codons and the specific codons of the tRNA charging complexes displaying a high RPI. The availability of

further metabolic information on genomes will allow us to verify the hypothesis for a class of organisms displaying strong and weak forms of translational bias.

PI, PI_T, and "Logically" Differentiated Regulation for Unicellular Organisms

Constitutive high expression of rarely used but genomically favored (i.e., with high PI) pathways is expected to be avoided by specific patterns of regulation, and the existence of such patterns can be detected by combining sequence analysis and transcriptomic data: the four logical combinations coming from "high" and "low" PI_T and PI values lead us to envisage at least four different kinds of enzyme regulation. Given a set of experiments, it is reasonable to distinguish the regulation of enzymes in a pathway P which has "high" PI(P) and "low" PI_T(P) for all (or most) time point experiments from the regulation of a pathway P′ where PI_T(P′) and PI(P′) are always "high." Enzymes participating in P′ are likely to be constitutively regulated, while it is plausible that enzymes participating in P are regulated under specific biological conditions (as in the case of seripauperine or Hem13 proteins discussed above). The number of "logically" foreseeable regulation modes becomes larger if we consider the frequency at which high and low PI_T(P) values, for a pathway P, occur in experiments. This logic-based diversity characterizing metabolic pathways challenges the understanding of the underlying regulatory mechanisms. The interplaying role of statistical analysis and transcriptomic data turns out to be essential here.

Caveats to the Analysis Based on Transcriptomic Data

A major concern with our analysis based on microarray data is the noisiness of transcriptomic data and the limited correlation between mRNA and protein expression levels. However, the amount of noise is smaller and the correlation higher for highly expressed genes (Gygi et al. 1999), those of most interest in our analysis.

Acknowledgments. Part of this work was done while the authors were visiting the Institut des Hautes Études Scientifiques. The authors are grateful to David Fell for his encouragement of this work and to Jean-Michel Camadro, Nadya Morozova, Eric Stewart, and Catherine Vaquero for stimulating conversations and insights. A.C. is supported by a grant from the Fondation pour la Recherche Médicale.

References

Akashi H (2001) Gene expression and molecular evolution. Curr Opin Genet Dev 11:660–666

Akashi H (2003) Translational selection and yeast proteome evolution. Genetics 164:291–1303

Akashi H, Gojobori T (2002) Metabolic efficiency and amino acid composition in the proteomes of *Escherichia coli* and *Bacillus subtilis*. Proc Natl Acad Sci USA 99:3695–3700

Amillet JM, Buisson N, Labbe Bois R (1995) Positive and negative elements involved in the differential regulation by heme and oxygen of the HEM13 gene (coproporphyrinogen oxidase) in *Saccharomyces cerevisiae*. Curr Genet 28:503–511

Andersen AP, Elliott DA, Lawson M, Barland P, Hatcher VB, Puszkin EG (1997) Growth and morphological transformations of *Helicobacter pylori* in broth media. J Clin Microbiol 35:2918–2922

Baker LMS, Raudonikiene A, Hoffman PS, Poole LB (2001) Essential thioredoxin–dependent peroxiredoxin system from *Helicobacter pylori*: Genetic and kinetic characterization. J Bacteriol 183:1961–1973

Carbone A, Zinovyev A, Képès F (2003) Codon Adaptation Index as a measure of dominating codon bias. Bioinformatics 19:2005–2015

Carbone A, Képès F, Zinovyev A (2004) Codon bias signatures, organisation of microorganisms in codon space and lifestyle. Mol Biol Evol 22:547–561

Cohen NG, et al. (2003) An integrated analysis of the genome of the hyperthermophilic archaeon *Pyrococcus abyssi*. Mol Microbiol 47:1495–1512

deRisi JL, Iyer VR, Brown PO (1997) Exploring the metabolic and genetic control of gene expression on a genomic scale. Science 278:680–686

Gombert AK, Moreira dos Santos M, Christensen B, Nielsen J (2001) Network identification and flux quantification in the central metabolism of *Saccharomyces cerevisiae* under different conditions of glucose repression. J Bacteriol 183:1441–1451

Gouy M, Gautier Ch (1982) Codon usage in bacteria: correlation with gene expressivity. Nucleic Acids Res 10:7055–7070

Gygi SP, Rochon Y, Franza BR, Aebersold R (1999) Correlation between protein and mRNA abundance in yeast. Mol Cell Biol 19:1720–1730

Helling BR (1994) Why does *Escherichia coli* have two primary pathways for synthesis of glutamate? J Bacteriol 176:4664–4668

Holstege FCP, Jennings EG, Wyrick JJ, Lee TI, Hengartner CJ, Green MR, Golub TR, Lander ES, Young RA (1998) Dissecting the regulatory circuitry of a eukaryotic genome. Cell 95:717–728

Karp PD, Riley M, Paulsen IT, Paley S, Pellegrini-Toole A (2000) The EcoCyc and MetaCyc Databases. Nucleic Acids Res 28:56–59

Karp PD, Riley M, Saier M, Paulsen IT, Collado-Vides J, Paley S, Pellegrini-Toole A, Bonavides C, Gama-Castro S (2002) The EcoCyc Database. Nucleic Acids Res 30:56–58

James TC, Campbell S, Donnelly D, Bond U (2003) Transcription profile of brewery yeast under fermentation conditions. J Appl Microbiol 94:432–448

Jeppsson M, Johansson B, Hahn-Hägerdal B, Gorwa-Grauslund MF (2002) Reduced oxidative pentose phosphate pathway flux in recombinant xylose-utilizing *Saccharomyces cerevisiae* strains improves the ethanol yield from xylose. Appl Environ Microbiol 68:1604–1609

Johnston M, Carlson M (1992) Regulation of carbon and phosphate utilization. In: Jones EW, Pringle JR, Broach JR (eds). The molecular biology of the yeast *Saccharomyces:* Gene expression. Cold Spring Harbor Laboratory Press, Cold Spring Harbor, NY, 1992, pp 193–281

Lafay B, Atherton JC, Sharp PM (2000) Absence of translationally selected synonymous codon usage bias in *Helicobacter pylori*. Microbiology 146:851–860

Médigue C, Rouxel T, Vigier P, Hénaut A, Danchin A (1991) Evidence for horizontal gene transfer in *Escherichia coli* speciation. J Mol Biol 222:851–856

Middelhoven WJ, Kurtzman CP, Vaughan-Martini A (2000) *Saccharomyces bulderi* sp. nov., a yeast that ferments gluconolactone. Antonie van Leeuwenhoek 77:223–228

Mrázek J, Bhaya D, Grossman AR, Karlin S (2001) Highly expressed and alien genes of the *Synechocystis* genome. Nucleic Acids Res 29:1590–1601

Newman EB, Walker C (1982) L-Serine degradation in *Escherichia coli* K-12: A combination of L–serine, glycine, and leucine used as a source of carbon. J Bacteriol 151:777–782

Nicolas P, Bize L, Muri F, Hoebeke M, Rodolphe F, Dusko Ehrlich S, Prum B, Bessières Ph (2002) Mining *Bacillus subtilis* chromosome heterogeneities using hidden Markov models. Nucleic Acids Res 30:1418–1426

Norman E, De Smet KA , Stoker NG, Ratledge C, Wheeler PR, Dale JW (1994) Lipid synthesis in mycobacteria: characterization of the biotin carboxyl carrier protein genes from *Mycobacterium leprae* and *M. tuberculosis*. J Bacteriol 176:2525–2531

Parish T, Stoker NG (2002) The common aromatic amino acid biosynthesis pathway is essential in *Mycobacterium tuberculosis*. Microbiology 148:3069–3077

Perrière G, Thioulouse J (2002) Use and misuse of correspondence analysis in codon usage studies. Nucleic Acids Res 30:4548–4555

Pizer IL, Potochny LM (1964) Nutritional and regulatory aspects of serine metabolism in *Escherichia coli*. J Bacteriol 88:611–619

Primm TP, Andersen SJ, Mizrahi V, Avarbock D, Rubin H, Barry CE 3rd (2000) The stringent response of *Mycobacterium tuberculosis* is required for long-term survival. J Bacteriol 182:4889–4898

Ratledge C (1991) Yeast physiology—A micro-synopsis. Bioprocess Eng 6:195–203

Reitzer LJ (1986) Ammonia assimilation and the biosynthesis of glutamine, glutamate, aspartate, asparagine, L-alanine, and D-alanine. In: Neidhardtf C, Ingraham JL, Low KB, Magasanik B, Schaechter M, Umbarger HE (eds). *Escherichia coli* and *Salmonella typhimurium*: Cellular and molecular biology. American Society for Microbiology, Washington, DC, pp 302–320

Sassetti CM, Boyd DH, Rubin EJ (2003) Genes required for mycobacterial growth defined by high density mutagenesis. Mol Microbiol 48:77–84

Schut GJ, Zhou J, Adams MW (2001) DNA microarray analysis of the hyperthermophilic archaeon *Pyrococcus furiosus*: Evidence for a new type of sulfur-reducing enzyme complex. J Bacteriol 183:7027–7036

Sharp PM, Li W-H (1987) The codon adaptation index—A measure of directional synonymous codon usage bias, and its potential applications. Nucleic Acids Res 15:1281–1295

Sharp PM, Tuohy TMF, Mosurski KR (1986) Codon usage in yeast: cluster analysis clearly differentiate highly and lowly expressed genes. Nucleic Acids Res 14:8207–8211

Sharp PM, Cowe E, Higgins DG, Shields DC, Wolfe KH, Wright F (1988) Codon usage patterns in *Escherichia coli*, *Bacillus subtilis*, *Saccharomyces pombe*, *Drosophila melanogaster* and *Homo sapiens*; A review of the considerable within species diversity. Nucleic Acids Res 16:8207–8211

Shields DC, Sharp PM (1987) Synonymous codon usage in *Bacillus subtilis* reflects both traditional selection and mutational biases. Nucleic Acids Res 15:8023–8040

Silva PJ, van den Ban EC , Wassink H, de Haaker HCB , Robb FT, Hagen WR (2000) Enzymes of hydrogen metabolism in *Pyrococcus furiosus*. Eur J Biochem 267:6541–6551

Sinha A, Maitra PK (1992) Induction of specific enzymes of the oxidative pentose phosphate pathway by glucono-delta-lactone in *Saccharomyces cerevisiae*. J Gen Microbiol 138:1865–1873

Stenico M, Loyd AT, Sharp PM (1994) Codon usage in *Caenorhabditis elegans*: delineation of translational selection and mutational biases. Nucleic Acids Res 22:2437–2446

Tomb JF, et al. (1997) The complete genome sequence of the gastric pathogen *Helicobacter pylori*. Nature 388:539–547

van Dijken JP, van Tuijl A, Luttik MAH, Middelhoven WJ, Pronk JT (2002) Novel pathway for alcoholic fermentation of δ-gluconolactone in the yeast *Saccharomyces bulderi*. J Bacteriol 184:672–678

Viswanathan M, Muthukumar G, Cong YS, Lenard J (1994) Seripauperins of *Saccharomyces cerevisiae*: A new multigene family encoding serine-poor relatives of serine-rich proteins. Gene 148:149–153

Wagner A (2000) Inferring lifestyle from gene expression patterns. Mol Biol Evol 17:1985–1987

Ward DE, Kengen SW, Van der Oost J, De Vos WM (2000) Purification and characterization of the alanine aminotransferase from the hyperthermophilic Archaeon *Pyrococcus furiosus* and its role in alanine production. J Bacteriol 182:2559–2566

Wood WD, et al. (2001) The genome of the natural genetic engineer *Agrobacterium tumefaciens* C58. Science 294:2317–2323

Worst DJ, Gerrits MM, Vandenbroucke-Grauls CMJE, Kusters JG (1998) *Helicobacter pylori* ribBA-mediated riboflavin production is involved in iron acquisition. J Bacteriol 180:1473–1479

Zitomer RS, Lowry CV (1992) Regulation of gene expression by oxygen in *Saccharomyces cerevisiae*. Microbiol Rev 56:1–11

org	path	meancai	rpi
yeast	sorbitol degradation	0.69044563032330708	3.1451292784085374
vcho	sorbitol degradation	0.63109074155285627	3.578888393457214
ecoli	sorbitol degradation	0.4894085406638351	1.317831207122744
bsub	sorbitol degradation	0.47965328767636478	1.2266294175420331
hin	sorbitol degradation	0.56443870613843428	1.8989217688086322
yeast	mannitol degradation	0.69044563032330708	3.1451292784085374
vcho	mannitol degradation	0.54298863825891541	2.4497559076166686
ecoli	mannitol degradation	0.50543549900454399	1.5226028272752743
bsub	mannitol degradation	0.47341733051635027	1.122067623342019
hin	mannitol degradation	0.56443870613843428	1.8989217688086322
yeast	glutamine biosynthesis	0.54953273363146293	1.975009338925634
vcho	glutamine biosynthesis	0.56175943565034414	2.6903258409936259
ecoli	glutamine biosynthesis	0.61006042249898129	2.8593639666533188
bsub	glutamine biosynthesis	0.57962263262381308	2.9028715411619093
hin	glutamine biosynthesis	0.4817244296967782	0.70927983480501855
agro	glutamine biosynthesis	0.57474706764068884	1.0251677023690902
mtbrv	glutamine biosynthesis	0.6011138177829275	0.89304810118975986
yeast	glycolysis	0.732164339311203 28	3.4915552932180631
vcho	glycolysis	0.5252588756316553	2.2225280640101492
ecoli	glycolysis	0.58033799837857247	2.4796095046642725
bsub	glycolysis	0.5522090743825977	2.4432130217789139
hin	glycolysis	0.58227085264997058	2.1553934466861917
agro	glycolysis	0.53998385824063877	0.47227132192543075
mtbrv	glycolysis	0.57396182601928081	0.33152671892207203
hpy	glycolysis	0.6041000193544 71	0.73544798381950471
vcho	pyruvate oxidation pathway	0.5177096300617462	2.1257755677827586
ecoli	pyruvate oxidation pathway	0.4744920557295616	1.1272477712618323
bsub	pyruvate oxidation pathway	0.54632510027935666	2.3445531250743201
hin	pyruvate oxidation pathway	0.5369083224580935	1.502964743077484
yeast	pyruvate dehydrogenase	0.31644122380609985	0.039451772698847358
vcho	pyruvate dehydrogenase	0.58686666039492019	3.0121045730383815
ecoli	pyruvate dehydrogenase	0.62632640151318886	3.0671894819693475
bsub	pyruvate dehydrogenase	0.56832726449748128	2.7134757632351483
hin	pyruvate dehydrogenase	0.55237535592802833	1.7254200724600823
agro	pyruvate dehydrogenase	0.651486147383322	2.2456752492993837
mtbrv	pyruvate dehydrogenase	0.52902570372410684	-0.59778239860349425
yeast	glycine cleavage	0.4507795480917719	1.1549774312703336
vcho	glycine cleavage	0.40054405108973751	0.6241603225913378
ecoli	glycine cleavage	0.5223900335743511	1.7392258095646216
bsub	glycine cleavage	0.55329059715944495	2.4613475212813234
hin	glycine cleavage	0.53517520542301689	1.4780381065866544
agro	glycine cleavage	0.59809850530902309	1.3965639453454115
mtbrv	glycine cleavage	0.59239689026003384	0.71277619943056814
yeast	gluconeogenesis	0.60472923305046022	2.4333529403709049
vcho	gluconeogenesis	0.48868662556786563	1.7538114944461523
ecoli	gluconeogenesis	0.5399459603886162	1.9635325994503254
bsub	gluconeogenesis	0.49517271643050836	1.4868523911534755
hin	gluconeogenesis	0.56938321443868811	1.9700363897767204
agro	gluconeogenesis	0.52620417529151542	0.25311040560852305
mtbrv	gluconeogenesis	0.56609656310424228	0.16886781189248137
hpy	gluconeogenesis	0.59994075377956 38	0.56099742347238268
yeast	removal of superoxide radicals	0.30551868706056601	-0.051247363687748376
vcho	removal of superoxide radicals	0.40168824448967289	0.6388245120902078 5
ecoli	removal of superoxide radicals	0.57548685862371951	2.4176279529518441
bsub	removal of superoxide radicals	0.45616726021840859	0.83282601148576407
hin	removal of superoxide radicals	0.63454775641789052	2.9072684503447972
agro	removal of superoxide radicals	0.60642866344502322	1.5290521235488643
mtbrv	removal of superoxide radicals	0.55055498545905479	-0.15254242710260413
hpy	removal of superoxide radicals	0.61786088698048958	1.3126150401152723
yeast	non-oxidative branch of the pentose phosphate pathway	0.42565117193895424	0.9463150967816424
vcho	non-oxidative branch of the pentose phosphate pathway	0.50992185234807696	2.0259660004711724
ecoli	non-oxidative branch of the pentose phosphate pathway	0.47212972203039177	1.097064945011438
bsub	non-oxidative branch of the pentose phosphate pathway	0.486060679769848 29	1.3340657575049684
hin	non-oxidative branch of the pentose phosphate pathway	0.47367316711595275	0.59348217568410244
agro	non-oxidative branch of the pentose phosphate pathway	0.61748955122212912	1.7049715775347944
mtbrv	non-oxidative branch of the pentose phosphate pathway	0.62038471562123321	1.2915831805275817
hpy	non-oxidative branch of the pentose phosphate pathway	0.5908850414811937	0.1811769824974791
vcho	salvage pathways of guanine, xanthine, and their nucleosides	0.3438703161385897	-0.10218051190334468
ecoli	salvage pathways of guanine, xanthine, and their nucleosides	0.47406932053935164	1.12184661110444936
hin	salvage pathways of guanine, xanthine, and their nucleosides	0.47379167726318799	0.59518665339727495
agro	salvage pathways of guanine, xanthine, and their nucleosides	0.53711742145249397	0.42668167262988771
hpy	salvage pathways of guanine, xanthine, and their nucleosides	0.65263465016903366	2.7711183177654353
yeast	methyl-donor molecule biosynthesis	0.5710148939327877	2.1533940340236168
vcho	methyl-donor molecule biosynthesis	0.38924553505629483	0.47935649818561815
ecoli	methyl-donor molecule biosynthesis	0.46972962013835867	1.0663995659348344
bsub	methyl-donor molecule biosynthesis	0.5045792745587363	1.6445774315756501
hin	methyl-donor molecule biosynthesis	0.49122551696991446	0.845929665100319 75
agro	methyl-donor molecule biosynthesis	0.53180814389594944	0.34223951684377663
mtbrv	methyl-donor molecule biosynthesis	0.65111414308271043	1.9270883300085879
hpy	methyl-donor molecule biosynthesis	0.55965961480232451	-1.128499709962401
vcho	tRNA charging pathway	0.43337358268482462	1.0449095355274471
ecoli	tRNA charging pathway	0.50847866401814411	1.5614742392924861
agro	tRNA charging pathway	0.58714362075660409	1.2223304346384889
mtbrv	tRNA charging pathway	0.55948368824943506	0.032109129083575452
hpy	tRNA charging pathway	0.59801405257734541	0.48018649704915 95
yeast	anaerobic respiration	0.36642374387224902	0.4544992575497534 5
vcho	anaerobic respiration	0.382010094015603 32	0.38662577754468902
ecoli	anaerobic respiration	0.42689286011385896	0.51908718352091898
bsub	anaerobic respiration	0.47729604581955909	1.1871042201126136
hin	anaerobic respiration	0.55495490809177217	1.76252060161848
mtbrv	anaerobic respiration	0.61892825039720156	1.2614625038220868
hpy	anaerobic respiration	0.5888977445764797	0.097824512605918207
yeast	glyoxylate degradation	0.25011367135211532	-0.51132245368888907
vcho	glyoxylate degradation	0.32390922896561897	-0.3580054143406779
ecoli	glyoxylate degradation	0.48884582830802648	1.3106416008150956
bsub	glyoxylate degradation	0.53333063737455599	2.1266676712255128
hin	glyoxylate degradation	0.52068124470453003	1.2695780413804323
vcho	de novo biosynthesis of purine nucleotides	0.39600375714038699	0.56597109439127147
ecoli	de novo biosynthesis of purine nucleotides	0.49196676819673507	1.3505169098926912
bsub	de novo biosynthesis of purine nucleotides	0.4430307164498391	0.61255820803833916
hin	de novo biosynthesis of purine nucleotides	0.44733175637109479	0.21462560858349594
agro	de novo biosynthesis of purine nucleotides	0.56605481414307302	0.88692052727588366
mtbrv	de novo biosynthesis of purine nucleotides	0.54577124345870087	-0.251473416911138
hpy	de novo biosynthesis of purine nucleotides	0.61164842324424928	1.0520479374850262
yeast	glycine biosynthesis	0.37859998542652501	0.5556089740136495
vcho	glycine biosynthesis	0.35264274610091118	0.010248536665117212
ecoli	glycine biosynthesis	0.51838956200240904	1.6881129890439637
bsub	glycine biosynthesis	0.55329059715944495	2.4613475212813234
hin	glycine biosynthesis	0.45500685509478628	0.32501307350633118
agro	glycine biosynthesis	0.58628697363693916	1.208705769368672
mtbrv	glycine biosynthesis	0.56150270568372473	0.073863762422954116
hpy	glycine biosynthesis	0.55420679659247141	-1.357205277098755
yeast	polyamine biosynthesis	0.32485013582911743	0.10927813961406 16
vcho	polyamine biosynthesis	0.41455752776845517	0.80375957352769078
ecoli	polyamine biosynthesis	0.39675840919019989	0.13406837914985 52
bsub	polyamine biosynthesis	0.48686343179199321	1.3475259512778464
hin	polyamine biosynthesis	0.53405154585792525	1.4618770205482583
agro	polyamine biosynthesis	0.51376554486094683	0.055278448737250289
mtbrv	polyamine biosynthesis	0.574400293879196	0.34059452805087337
yeast	fermentation	0.29791630966303417	-0.11437636858650422
vcho	fermentation	0.38713943383895161	0.45236432417319472
ecoli	fermentation	0.41973868390008845	0.42768042853925686
bsub	fermentation	0.43233421401719 53	0.43320394736547591
hin	fermentation	0.52507059584417959	1.3327080886157112
agro	fermentation	0.53481791965047 82	0.39010892100252043
mtbrv	fermentation	0.61618432697328285	1.2047163289098493
yeast	oxidative branch of the pentose phosphate pathway	0.42205103830715995	0.91642011735664008
vcho	oxidative branch of the pentose phosphate pathway	0.47308113642192584	1.5538087238729725
ecoli	oxidative branch of the pentose phosphate pathway	0.4637124755694263	0.98952032185876948
bsub	oxidative branch of the pentose phosphate pathway	0.43969025003959061	0.55654673259714982
hin	oxidative branch of the pentose phosphate pathway	0.5008470497662727	0.98431180874407853
agro	oxidative branch of the pentose phosphate pathway	0.51915033201268423	0.14092155755938465
mtbrv	oxidative branch of the pentose phosphate pathway	0.58485255057498142	0.556754199824648 91
hpy	oxidative branch of the pentose phosphate pathway	0.55884769936292389	-1.1625535833703473
yeast	asparagine biosynthesis and degradation	0.37372077889859756	0.51509276164972118
vcho	asparagine biosynthesis and degradation	0.37363317629875137	0.279265685428009
ecoli	asparagine biosynthesis and degradation	0.42815851467034749	0.53525807063349662
bsub	asparagine biosynthesis and degradation	0.38453528853519647	-0.36826746768493374
hin	asparagine biosynthesis and degradation	0.49084934257679275	0.84051931936790436
mtbrv	asparagine biosynthesis and degradation	0.61440138062089444	1.1678438037184302
vcho	NAD phosphorylation and dephosphorylation	0.33505385382186631	-0.21517388708745364
ecoli	NAD phosphorylation and dephosphorylation	0.3644797756951258	-0.27834600020914807
agro	NAD phosphorylation and dephosphorylation	0.61323163400441949	1.6372509309509669
mtbrv	NAD phosphorylation and dephosphorylation	0.59151470966061781	0.69453211354891808
yeast	fatty acid biosynthesis, initial steps	0.35722304482209549	0.37809800778118513
vcho	fatty acid biosynthesis, initial steps	0.39270796668882413	0.52373164804154237
ecoli	fatty acid biosynthesis, initial steps	0.45746884653728531	0.90974735400276552
bsub	fatty acid biosynthesis, initial steps	0.44252997714690773	0.60416203106061805
hin	fatty acid biosynthesis, initial steps	0.48600588747184137	0.7708581006981341
agro	fatty acid biosynthesis, initial steps	0.53880592543679784	0.45353672305238873
mtbrv	fatty acid biosynthesis, initial steps	0.57036061828943907	0.25705133015883436
hpy	fatty acid biosynthesis, initial steps	0.5810854796613516	-0.22984246789331716
vcho	salvage pathways of adenine, hypoxanthine, and their nucleosides	0.34946463907479403	-0.030482657625380005
ecoli	salvage pathways of adenine, hypoxanthine, and their nucleosides	0.49393334642652303	1.37564328769374 34
bsub	salvage pathways of adenine, hypoxanthine, and their nucleosides	0.44996880506880 91	0.72889303454579257
hin	salvage pathways of adenine, hypoxanthine, and their nucleosides	0.52627571969080433	1.350040838478 11
agro	salvage pathways of adenine, hypoxanthine, and their nucleosides	0.52927022275641455	0.30187479114332783
mtbrv	salvage pathways of adenine, hypoxanthine, and their nucleosides	0.51763163548488589	-0.8334193641356471
hpy	salvage pathways of adenine, hypoxanthine, and their nucleosides	0.59208400732515 11	0.23131349997960449
yeast	UDP-N-acetylglucosamine biosynthesis	0.29647433209423935	-0.12635035521167878
vcho	UDP-N-acetylglucosamine biosynthesis	0.34095044677184716	-0.13960208565851304
ecoli	UDP-N-acetylglucosamine biosynthesis	0.41386178847746868	0.3525931055691 76

bsub UDP-N-acetylglucosamine biosynthesis 0.4657531374247172 0.9935577955498359 2
hin UDP-N-acetylglucosamine biosynthesis 0.45042759512944497 0.25915165373901244 2
mtbrv UDP-N-acetylglucosamine biosynthesis 0.5993780525328718 0.857151312807241 88 2
hpy UDP-N-acetylglucosamine biosynthesis 0.59981483910929567 0.5557162303413844 2
yeast ribose catabolism 0.31473803493381353 0.025308743161062169 2
vcho ribose catabolism 0.44365858584289114 1.1767239956658149 2
ecoli ribose catabolism 0.4319815628466 0.58410400585901845 2
bsub ribose catabolism 0.45350098544363288 0.78811908564791278 2
hin ribose catabolism 0.44067659642927526 0.1189074607027714 2
agro ribose catabolism 0.4797672607604726 -0.48545206909636335 2
mtbrv ribose catabolism 0.58138964790905501 0.4851390524514492 3
yeast valine biosynthesis 0.50448644104551632 1.6009515600279003 2
vcho valine biosynthesis 0.31792573616579217 -0.43469093995788616 2
ecoli valine biosynthesis 0.34802134240582783 -0.48863044583982268 2
bsub valine biosynthesis 0.43284551207667993 0.4417771689413878 2
hin valine biosynthesis 0.44446519132987783 0.17339710334491204 2
agro valine biosynthesis 0.60646295512018256 1.5295975203462877 2
mtbrv valine biosynthesis 0.52216452084061316 -0.73967625781897506 2
hpy valine biosynthesis 0.60308543472228626 0.69289363031247853 2
yeast glyoxylate cycle 0.26073471732764425 -0.42312685225072522 2
vcho glyoxylate cycle 0.34845774964737658 -0.0433871345860862 71 2
ecoli glyoxylate cycle 0.43796077907270708 0.6604986509210391 2
bsub glyoxylate cycle 0.43036853675115161 0.40024433323059821 2
hin glyoxylate cycle 0.55053841083207833 1.6990001240471158 2
agro glyoxylate cycle 0.48663943384655772 -0.37615262032126484 2
yeast glutamate biosynthesis 0.31416589667552036 0.020557791332757303 2
vcho glutamate biosynthesis 0.31898867234470479 -0.42106815769602385 2
ecoli glutamate biosynthesis 0.41883196273060364 0.41609552521855664 2
bsub glutamate biosynthesis 0.42263844748239066 0.27062958724571107 2
agro glutamate biosynthesis 0.58230009677589012 1.1452959224704333 2
hpy glutamate biosynthesis 0.59476339996505623 0.34384555908913594 2
yeast fatty acid elongation, saturated 0.3728481881237119 0.50784689637639979 2
vcho fatty acid elongation, saturated 0.36354395391379196 0.14996038707753512 2
ecoli fatty acid elongation, saturated 0.50641817831242253 1.5351582248552094 2
hin fatty acid elongation, saturated 0.46385039379960047 0.45220568088713664 2
agro fatty acid elongation, saturated 0.48785963243432423 -0.35674579931015316 2
mtbrv fatty acid elongation, saturated 0.56561949285402868 0.15900167946762564 2
hpy fatty acid elongation, saturated 0.57510064304084518 -0.48086228935701764 2
yeast leucine biosynthesis 0.34530137221660412 0.27910219437328465 2
vcho leucine biosynthesis 0.31855675452121884 -0.4266036946182743 2
ecoli leucine biosynthesis 0.39522294179403228 0.11445017463964607 2
bsub leucine biosynthesis 0.39412636201714307 -0.20744855475093629 2
hin leucine biosynthesis 0.4532652644139244 0.29996456441026687 2
agro leucine biosynthesis 0.61122132057956535 1.6052776167679113 2
mtbrv leucine biosynthesis 0.59316567193010306 0.72867511947286523 2
hpy leucine biosynthesis 0.58093612898263824 -0.23610662898631235 2
yeast (deoxy)ribose phosphate metabolism 0.25736013770239113 -0.45114886442691771 2
vcho (deoxy)ribose phosphate metabolism 0.38588791039007553 0.43632457336040831 2
ecoli (deoxy)ribose phosphate metabolism 0.49907739676052854 1.4413672696651023 2
bsub (deoxy)ribose phosphate metabolism 0.45602491057068417 0.83043915503568377 2
hin (deoxy)ribose phosphate metabolism 0.43853330131961965 0.088081418946972509 2
agro (deoxy)ribose phosphate metabolism 0.49416840123583644 -0.25640709366098596 2
mtbrv (deoxy)ribose phosphate metabolism 0.55372171926198122 -0.08705225025768322 2
hpy (deoxy)ribose phosphate metabolism 0.58976752768378149 0.13430550852131942 2
vcho de novo biosynthesis of pyrimidine ribonucleotides 0.38412029630634176 0.4136705116552738 2
ecoli de novo biosynthesis of pyrimidine ribonucleotides 0.44245027745143478 0.71785961968010348 2
bsub de novo biosynthesis of pyrimidine ribonucleotides 0.40641392394406622 -0.001416106410660031 2
hin de novo biosynthesis of pyrimidine ribonucleotides 0.4143255384811122 -0.26008785774876664 2
agro de novo biosynthesis of pyrimidine ribonucleotides 0.54175725117254547 0.50047650062087579 2
mtbrv de novo biosynthesis of pyrimidine ribonucleotides 0.56422670843578981 0.13019796449384985 2
hpy de novo biosynthesis of pyrimidine ribonucleotides 0.59423268583878475 0.32158600988632774 2
yeast glutathione-glutaredoxin redox reactions 0.25068135335338898 -0.50660850596252516 2
vcho glutathione-glutaredoxin redox reactions 0.41788225625020065 0.84636989490461889 2
ecoli glutathione-glutaredoxin redox reactions 0.43941024755278241 0.67901807317916929 2
hin glutathione-glutaredoxin redox reactions 0.48886427284993605 0.81196896155082832 2
agro glutathione-glutaredoxin redox reactions 0.55644567196981165 0.73409056656583838 2
mtbrv glutathione-glutaredoxin redox reactions 0.50429919768860465 -1.1091431108697367 2
yeast TCA cycle, aerobic respiration 0.26888666616141943 -0.3554342698116273 5 2
vcho TCA cycle, aerobic respiration 0.35408222865337474 0.028697205334972491 2
ecoli TCA cycle, aerobic respiration 0.43984744445760643 0.68460400636894303 2
bsub TCA cycle, aerobic respiration 0.44774340239714649 0.69157845874039925 2
hin TCA cycle, aerobic respiration 0.43144018915138438 -0.013935597231311743 2
agro TCA cycle, aerobic respiration 0.53230335323475386 0.35011564380996146 2
yeast fatty acid elongation, unsaturated 0.35722866423138122 0.37814467052822753 2
vcho fatty acid elongation, unsaturated 0.35563069051462626 0.04854257253115437 2
ecoli fatty acid elongation, unsaturated 0.504119055676303 1.5057830273212069 2
hin fatty acid elongation, unsaturated 0.4585225944179524 0.37557835809555296 2
agro fatty acid elongation, unsaturated 0.4848217494222603 -0.40506278771413962 2
hpy fatty acid elongation, unsaturated 0.57367621909882516 -0.54060638368857383 2
yeast isoleucine biosynthesis 0.37733907991205851 0.5451386003365849 2
vcho isoleucine biosynthesis 0.32753856947839194 -0.31149113009621782 2
ecoli isoleucine biosynthesis 0.3762642232962547 -0.12777966213136216 2
bsub isoleucine biosynthesis 0.42578589838960007 0.32340466339994051 2
hin isoleucine biosynthesis 0.46021654904842485 0.39994173947785977 2
agro isoleucine biosynthesis 0.53431943619262268 0.38218072034683059 2
mtbrv isoleucine biosynthesis 0.56536369916698259 0.15371169463057299 2
hpy isoleucine biosynthesis 0.59201078185246225 0.22839350066308309 2
yeast threonine catabolism 0.32242686499780132 0.089155655547247289 2
vcho threonine catabolism 0.46062004433943093 1.3941051146134751 2
ecoli threonine catabolism 0.43164637098139563 0.57982136034134057 2
bsub threonine catabolism 0.3743406454310827 -0.539206771282147 2
mtbrv threonine catabolism 0.53155052262286651 -0.54556745207771884 2
vcho de novo biosynthesis of pyrimidine deoxyribonucleotides 0.38607517298004029 0.4387245645729495 2
ecoli de novo biosynthesis of pyrimidine deoxyribonucleotides 0.48549678830404147 1.267851925257649 2
bsub de novo biosynthesis of pyrimidine deoxyribonucleotides 0.40900502540821015 0.042030346329971373 2
hin de novo biosynthesis of pyrimidine deoxyribonucleotides 0.43488605101778843 0.035624671580920336 2
agro de novo biosynthesis of pyrimidine deoxyribonucleotides 0.4765807067718314 -0.53613306768119173 2
mtbrv de novo biosynthesis of pyrimidine deoxyribonucleotides 0.51422725605447339 -0.90382421178621086 2
hpy de novo biosynthesis of pyrimidine deoxyribonucleotides 0.60932632077137083 0.95465283965309178 2
yeast thioredoxin pathway 0.33934484224977524 0.22964004684852005 2
vcho thioredoxin pathway 0.35834099637918632 0.083278342550499374 2
ecoli thioredoxin pathway 0.42759142531822947 0.52801254076214865 2
bsub thioredoxin pathway 0.39264704978923365 -0.23225301327480938 2
hin thioredoxin pathway 0.41856517198010973 -0.19911113145446663 2
agro thioredoxin pathway 0.59721631049680568 1.3825329531861987 2
mtbrv thioredoxin pathway 0.51983978740691728 -0.78775330286436207 2
hpy thioredoxin pathway 0.59758403187323356 0.46237558242824645 2
vcho acetate degradation 0.42952981459232503 0.99564710864986872 2
ecoli acetate degradation 0.45544921170733954 0.88394308799965171 2
agro acetate degradation 0.49406848416310567 -0.2579962388754462 2
mtbrv acetate degradation 0.52437536614752811 -0.6939544955436544 2
hpy acetate degradation 0.58149882070176007 -0.21250585525940807 2
ecoli glucuronate degradation 0.5145493006010603 1.6390471256252017 2
bsub glucuronate degradation 0.35273208101954279 -0.90152970054228387 2
hin glucuronate degradation 0.37909946094651581 -0.76672855882747226 2
agro glucuronate degradation 0.53612223877715453 0.41085364893262966 2
yeast homoserine biosynthesis 0.40274729569188206 0.75612468187085558 2
ecoli homoserine biosynthesis 0.34304340156805291 -0.55223209680221785 2
bsub homoserine biosynthesis 0.36298763804499512 -0.72956901903250926 2
hin homoserine biosynthesis 0.38592090372149479 -0.6686188403528 74 2
agro homoserine biosynthesis 0.55944119268476 5 0.78173324943157296 2
mtbrv homoserine biosynthesis 0.51094043940603351 -0.97179778233522218 2
hpy homoserine biosynthesis 0.63281076408847448 1.9396522878309985 2
vcho Entner-Doudoroff pathway 0.37232552968334254 0.26250664996512812 2
ecoli Entner-Doudoroff pathway 0.40606903888128609 0.25302749078872944 2
bsub Entner-Doudoroff pathway 0.38401724397221204 -0.37695381167211539 2
hin Entner-Doudoroff pathway 0.41870176613304222 -0.19714655968694578 2
agro Entner-Doudoroff pathway 0.53293236045425696 0.36011977809267504 2
yeast 4-aminobutyrate degradation 0.25791611381479673 -0.44653212067758824 2
ecoli 4-aminobutyrate degradation 0.38240450642190027 -0.049327117399719491 2
bsub 4-aminobutyrate degradation 0.42081822188984358 0.2401088429683301 2
hin 4-aminobutyrate degradation 0.50157469984151726 0.99477726984742754 2
agro 4-aminobutyrate degradation 0.48094020144326982 -0.46679686811849386 2
vcho UDP-glucose conversion 0.4226556429586027 0.90754648205094302 2
agro UDP-glucose conversion 0.4837365749433436 -0.42232155029708657 2
mtbrv UDP-glucose conversion 0.52582387551690402 -0.6639983512430857 2
hpy UDP-glucose conversion 0.59405418263216181 0.31409911493857617 2
yeast glucose 1-phosphate metabolism 0.26216081556492526 -0.41128474253415931 2
vcho glucose 1-phosphate metabolism 0.39221900946428007 0.51746508384185319 2
ecoli glucose 1-phosphate metabolism 0.3998485140660108 0.17354971855371398 2
bsub glucose 1-phosphate metabolism 0.39640192259630913 -0.16929295315474568 2
hin glucose 1-phosphate metabolism 0.43766143715825007 0.07554179202032001398 2
agro glucose 1-phosphate metabolism 0.53247198626369918 0.35279769166849384 2
mtbrv glucose 1-phosphate metabolism 0.54239852198906524 -0.32122355672111524 2
yeast riboflavin, FMN and FAD biosynthesis 0.20650060389073052 -0.87347894224777534 2
vcho riboflavin, FMN and FAD biosynthesis 0.30893846631129629 -0.54987341543034907 2
ecoli riboflavin, FMN and FAD biosynthesis 0.36462802479645218 -0.27645186608716366 2
bsub riboflavin, FMN and FAD biosynthesis 0.39009849568278238 -0.27498605058543429 2
hin riboflavin, FMN and FAD biosynthesis 0.40956991070460397 -0.32848589577594045 2
agro riboflavin, FMN and FAD biosynthesis 0.58518175768197511 1.1911277059028944 2
mtbrv riboflavin, FMN and FAD biosynthesis 0.53705758659480018 -0.43167767925092193 2
hpy riboflavin, FMN and FAD biosynthesis 0.61784777684323988 1.3120651664060208 2
yeast lysine and diaminopimelate biosynthesis 0.36502964586112618 0.44292287299798588 2
vcho lysine and diaminopimelate biosynthesis 0.30644946987464611 -0.58177284380592975 2
ecoli lysine and diaminopimelate biosynthesis 0.35945783104420959 -0.34250987464016885 2
bsub lysine and diaminopimelate biosynthesis 0.43820732603771634 0.5316817134317714 2
hin lysine and diaminopimelate biosynthesis 0.40770221389613193 -0.35534813212676319 2

agro lysine and diaminopimelate biosynthesis 0.5244704807785681
0.22553661603194311
mtbrv lysine and diaminopimelate biosynthesis 0.56074235807661255
0.058139264453666926
hpy lysine and diaminopimelate biosynthesis 0.57959416826342736 -
0.29239199841367564
yeast glycogen catabolism 0.27838541045482157 -0.27655809624132993
vcho glycogen catabolism 0.34291802528027521 -0.11438524373028422
ecoli glycogen catabolism 0.36387548988910873 -0.28606677797014018
bsub glycogen catabolism 0.38392483804372407 -0.3785032337463039
agro glycogen catabolism 0.55374587364048311 0.69115124220611923
mtbrv glycogen catabolism 0.55569676366799869 -0.046207008606134872
yeast arginine biosynthesis II 0.24736448586012985 -0.53415128509488985

vcho arginine biosynthesis II 0.33389717106235178 -0.22999814247693151

ecoli arginine biosynthesis II 0.36991362914533449 -0.20891929109714102

bsub arginine biosynthesis II 0.37943382347927129 -0.45380659593881839

agro arginine biosynthesis II 0.57689123267540121 1.0592698784116916

vcho pyridoxal 5'-phosphate biosynthesis 0.29196917468482503 -
0.76735492518754456
ecoli pyridoxal 5'-phosphate biosynthesis 0.35352741222625617 -
0.4182810499136963
hin pyridoxal 5'-phosphate biosynthesis 0.3951796777258661 -
0.53545409193327054
agro pyridoxal 5'-phosphate biosynthesis 0.56213299275163953
0.82454536429490266
mtbrv pyridoxal 5'-phosphate biosynthesis 0.58658919770906648
0.5926692261597802
hpy pyridoxal 5'-phosphate biosynthesis 0.583154190685200 69 -
0.14307527527066422
yeast proline utilization 0.20653240998076783 -0.87321482916073101
ecoli proline utilization 0.34967527084663591 -0.46749870023714207
bsub proline utilization 0.39152569392627506 -0.25105541649198954
mtbrv proline utilization 0.61945212932727967 1.2722966711096679
yeast formylTHF biosynthesis 0.2866672062266305 -0.20778728395357349
vcho formylTHF biosynthesis 0.30269119304538517 -0.62993959919589082
ecoli formylTHF biosynthesis 0.39689928579252498 0.13586831707235039
bsub formylTHF biosynthesis 0.42267117059571568 0.27117827405565498
hin formylTHF biosynthesis 0.39393368353156732 -0.55337466147495562
agro formylTHF biosynthesis 0.5319730115305018 0.3448616774546488
mtbrv formylTHF biosynthesis 0.55547443249936923 -0.050804966141506473
hpy formylTHF biosynthesis 0.58058928528069831 -0.25065416798486306
yeast anaerobic respiration, electron acceptors reaction list
0.24173134739194152 -0.58092803724632613
vcho anaerobic respiration, electron acceptors reaction list
0.36170565443411279 0.12640040855710996
ecoli anaerobic respiration, electron acceptors reaction list
0.38960419020166487 0.042661077647908704
bsub anaerobic respiration, electron acceptors reaction list
0.34132815814351503 -1.0927456768934223
hin anaerobic respiration, electron acceptors reaction list
0.37968756475770543 -0.75827012836738095
mtbrv anaerobic respiration, electron acceptors reaction list
0.60323226221221571 0.93685895140458164
hpy anaerobic respiration, electron acceptors reaction list
0.59806514713160408 0.48232953731927014

vcho glucosamine catabolism 0.33893638538442561 -0.16541466056864182
ecoli glucosamine catabolism 0.37203674309199031 -0.18179290358287015
bsub glucosamine catabolism 0.35095983791400631 -0.93124589552542381
hin glucosamine catabolism 0.42114736963698901 -0.16197255336781338
agro glucosamine catabolism 0.50630869984864524 -0.063319997378169901
mtbrv glucosamine catabolism 0.59197169076926326 0.70398278906585665
yeast sulfate assimilation pathway 0.29355928221231081 -0.15055650008208851

vcho sulfate assimilation pathway 0.28401562163428962 -0.86928909919078123

ecoli sulfate assimilation pathway 0.36703815262457912 -0.24565838864442988

bsub sulfate assimilation pathway 0.41405726094532913 0.12674401560748805

agro sulfate assimilation pathway 0.53202361353549654 0.34566648419969981

yeast glutamate degradation V 0.21813134649369936 -0.77689896873059738
vcho glutamate degradation V 0.37913655918191347 0.3497980355430203
ecoli glutamate degradation V 0.45597222074967697 0.89062541702785092
bsub glutamate degradation V 0.34970573740744432 -0.95227410269690527
hin glutamate degradation V 0.47687270997419179 0.63949974988712155
hpy glutamate degradation V 0.55979287921415755 -1.1229102492992356
yeast aspartate biosynthesis and degradation 0.21813134649369936 -
0.77689896873059738
vcho aspartate biosynthesis and degradation 0.37913655918191347
0.3497980355430203
ecoli aspartate biosynthesis and degradation 0.45597222074967697
0.89062541702785092
bsub aspartate biosynthesis and degradation 0.34970573740744432 -
0.95227410269690527
hin aspartate biosynthesis and degradation 0.47687270997419179
0.63949974988712155
hpy aspartate biosynthesis and degradation 0.55979287921415755 -
1.1229102492992356
yeast mannose and GDP-mannose metabolism 0.42187117411450392
0.91492655159249237
vcho mannose and GDP-mannose metabolism 0.28874385969269378 -
0.80869114530630293
ecoli mannose and GDP-mannose metabolism 0.3415316257036759 -
0.57154760174551444
bsub mannose and GDP-mannose metabolism 0.37784417709957807 -
0.48046108912072683
mtbrv mannose and GDP-mannose metabolism 0.52002632381623581 -
0.783895604935032 3
hpy mannose and GDP-mannose metabolism 0.60316166337641741
0.69609086097452455
yeast folic acid biosynthesis 0.31771526343642725 0.050031210139535563
vcho folic acid biosynthesis 0.28756125113325348 -0.82384767043535712
ecoli folic acid biosynthesis 0.35951162618185112 -0.34182255036709047
bsub folic acid biosynthesis 0.42263908157094027 0.27064021936436228
hin folic acid biosynthesis 0.38911829217931032 -0.62263225191430449
agro folic acid biosynthesis 0.52341000720424546 0.20867016408696445
mtbrv folic acid biosynthesis 0.52748824091349178 -0.6295781596701876
hpy folic acid biosynthesis 0.59529330224913624 0.36607105749074731
yeast chorismate biosynthesis 0.30389965716727813 -0.064691549459459055
vcho chorismate biosynthesis 0.30480512781176494 -0.60284702900260567
ecoli chorismate biosynthesis 0.31814342713369048 -0.87037157144787636
bsub chorismate biosynthesis 0.38444446573362723 -0.36979034458140203
hin chorismate biosynthesis 0.36680773147203671 -0.94351493058015201
agro chorismate biosynthesis 0.51252511910579568 0.03554992188175294

mtbrv chorismate biosynthesis 0.62019306528501683 1.2876197231635305
hpy chorismate biosynthesis 0.58624801057811537 -0.013312314908585922
yeast alanine biosynthesis 0.29927715769637842 -0.10307610423145659
vcho alanine biosynthesis 0.30604811553296557 -0.58691667361908029
ecoli alanine biosynthesis 0.35181468959841733 -0.44016399113802251
bsub alanine biosynthesis 0.34048477586325421 -1.1068871410115568
hin alanine biosynthesis 0.46572126628822053 0.479113591605621
agro alanine biosynthesis 0.49649878574054412 -0.21934316372093238
mtbrv alanine biosynthesis 0.53034244801600017 -0.57055124439156024
hpy alanine biosynthesis 0.60652876477042594 0.83731596775157136
yeast anaerobic respiration, electron donors reaction list 0.22136804666030419
-0.75002188727116037
vcho anaerobic respiration, electron donors reaction list 0.37334019176288069
0.27551074264081166
ecoli anaerobic respiration, electron donors reaction list 0.37962893656325369
-0.084789734012436044
bsub anaerobic respiration, electron donors reaction list 0.39323452196656822
-0.22240253750525674
hin anaerobic respiration, electron donors reaction list 0.41563702195879793
-0.24122538553807948
mtbrv anaerobic respiration, electron donors reaction list 0.57525883148848878
0.35834966105530852
hpy anaerobic respiration, electron donors reaction list 0.56584147754113223
-0.86921609381628295
ecoli xylose degradation 0.32494193133048505 -0.78350913071541828
bsub xylose degradation 0.38562672901943912 -0.34996667241541052
hin xylose degradation 0.34880125531985329 -1.2024939126351215
agro xylose degradation 0.60166981682531118 1.453364374444734
vcho asparagine degradation 1 0.34871374746363054 -
0.040106220285184832
agro asparagine degradation 1 0.47420347572617905 -0.57394207505717887

mtbrv asparagine degradation 1 0.602498614582660 85 0.9216866268609134

hpy asparagine degradation 1 0.55746749858821776 -1.2204428415104429

ecoli D-galacturonate degradation 0.45911144795808073 0.93073437768191047

bsub D-galacturonate degradation 0.35213126995897531 -0.91160383685466395

hin D-galacturonate degradation 0.38405742405523952 -0.69542042345931676

agro D-galacturonate degradation 0.49443593563479504 -0.25215205497551385

yeast glutathione biosynthesis 0.17004362635628442 -1.176212314052804

vcho glutathione biosynthesis 0.30388781861183828 -0.61460342957050029

ecoli glutathione biosynthesis 0.39092244273073762 0.059503993216157312

agro glutathione biosynthesis 0.55656171117551234 0.73593612852426 26

mtbrv glutathione biosynthesis 0.54610648068442347 -0.24454048646485776

yeast colanic acid biosynthesis 0.29771093759963696 -0.11608176523084539

vcho colanic acid biosynthesis 0.2923324758431825 -0.76269879185238 11

ecoli colanic acid biosynthesis 0.38303554943836193 -
0.041264467218891154

bsub colanic acid biosynthesis 0.38351465728055306 -0.38538096485364715

hin colanic acid biosynthesis 0.41641661058101881 -0.23001291586338865

agro colanic acid biosynthesis 0.46253165202043972 -0.75957824592437384

mtbrv colanic acid biosynthesis 0.5329993415841332 -0.51560490520941327

hpy colanic acid biosynthesis 0.60202444027163226 0.648392726701425
vcho salvage pathways of pyrimidine ribonucleotides 0.34661700227876174 -
0.066978485693721598
ecoli salvage pathways of pyrimidine ribonucleotides 0.40106436227056269
0.18908424490692996
bsub salvage pathways of pyrimidine ribonucleotides 0.40232052972307009 -
0.070052345103859895
hin salvage pathways of pyrimidine ribonucleotides 0.39689561282685315 -
0.51077457540987059
agro salvage pathways of pyrimidine ribonucleotides 0.45873735390495901 -
0.81992519692742083
mtbrv salvage pathways of pyrimidine ribonucleotides 0.48781050721095714 -
1.4501402778322379
hpy salvage pathways of pyrimidine ribonucleotides 0.60547060273503217
0.7929338631016144
yeast aerobic respiration, electron donors reaction list 0.23114367677927022
-0.66884649458707934
vcho aerobic respiration, electron donors reaction list 0.36225000825057624
0.13337694549527446
ecoli aerobic respiration, electron donors reaction list 0.37536722855369004
-0.13924029382444628
bsub aerobic respiration, electron donors reaction list 0.42128106379448221
0.24786957299551562
hin aerobic respiration, electron donors reaction list 0.39961231891481142
-0.47170142354741373
hpy aerobic respiration, electron donors reaction list 0.56739369536457873
-0.80411198728490962
vcho galactose metabolism 0.29976725904648693 -0.6674132660117057
ecoli galactose metabolism 0.4009123290735111 0.1871417625334563
bsub galactose metabolism 0.38348682455877969 -0.38588765173232674
mtbrv galactose metabolism 0.53783699298996002 -0.41555903277488732
yeast fatty acid oxidation pathway 0.226035474686564 24 -0.7112642523928453

vcho fatty acid oxidation pathway 0.37678707514989163 0.31968662337084419

ecoli fatty acid oxidation pathway 0.41707732759132027 0.39367708045758248

bsub fatty acid oxidation pathway 0.34264432278341767 -1.0706780555590792

hin fatty acid oxidation pathway 0.37108579152968973 -0.8819855325159639

agro fatty acid oxidation pathway 0.50394324233674681 -0.10094175092144378

mtbrv fatty acid oxidation pathway 0.58916014765519298 0.64583819365419726

hpy fatty acid oxidation pathway 0.55599443860917175 -1.2822268594197177

yeast serine biosynthesis 0.27589284197132763 -0.29725601780518157
vcho serine biosynthesis 0.29530470769991307 -0.72460613095769566
ecoli serine biosynthesis 0.3888692286018281 0.033270694622690562
bsub serine biosynthesis 0.39491561444542378 -0.19421471162645411
hin serine biosynthesis 0.37827221720278448 -0.77862643050720692

agro serine biosynthesis 0.47410518290868547 -0.57550538707450161
mtbrv serine biosynthesis 0.56530897124060242 0.15257988444378651
hpy serine biosynthesis 0.57484295909879479 -0.49167023303687002
yeast L-serine degradation 0.17000968576725695 -1.1764941517050787
vcho L-serine degradation 0.34367292457113752 -0.10471031792281776
ecoli L-serine degradation 0.44810812620046836 0.79014824926833815
agro L-serine degradation 0.45879413754826193 -0.8190220734416318
mtbrv L-serine degradation 0.53256250147804785 -0.52463905129837296
hpy L-serine degradation 0.57818451218978484 -0.35151668942337344
vcho peptidoglycan biosynthesis 0.2805194566939621 -0.91409658122228332

ecoli peptidoglycan biosynthesis 0.34203013654837122 -0.56517827881088256

bsub peptidoglycan biosynthesis 0.40217206137553435 -
0.072541797228353244
hin peptidoglycan biosynthesis 0.40249448500924423 -0.43024853543420855

agro peptidoglycan biosynthesis 0.49087196592541021 -0.30883571526859588

mtbrv peptidoglycan biosynthesis 0.55610278145531367 -
0.037810288721164244
hpy peptidoglycan biosynthesis 0.57501996629622265 -0.48424608465763302

yeast histidine biosynthesis 0.23328485574945432 -0.65106645978662459
vcho histidine biosynthesis 0.31739823059183364 -0.44145154677372256
ecoli histidine biosynthesis 0.40789170664632601 0.27631516792076521
bsub histidine biosynthesis 0.36449173448688266 -0.70434898968047122
hin histidine biosynthesis 0.34768457256970003 -1.2185546543076651
agro histidine biosynthesis 0.53346858121125906 0.36864817695980601
mtbrv histidine biosynthesis 0.52792030183038929 -0.62064285041582323
yeast glycerol metabolism 0.20549952823558804 -0.88179172704258912
vcho glycerol metabolism 0.29473719883326849 -0.73187942720572086
ecoli glycerol metabolism 0.36482610991266512 -0.27392099221123939
bsub glycerol metabolism 0.37994057236499979 -0.44530965291294483
hin glycerol metabolism 0.41009818801630155 -0.32088792273169298
agro glycerol metabolism 0.4618616329914853 -0.77023465833078242
mtbrv glycerol metabolism 0.51464442316338152 -0.89519691645136701
hpy glycerol metabolism 0.60730452625338804 0.86985344893933425
yeast tyrosine biosynthesis 0.24264817712469613 -0.57331481818268704
vcho tyrosine biosynthesis 0.2667858131293947 -1.0901094403667513
ecoli tyrosine biosynthesis 0.29686957992465524 -1.1421811105546493
bsub tyrosine biosynthesis 0.40879438606467144 0.038498438216370834
hin tyrosine biosynthesis 0.38951255392791667 -0.61696176394906743
agro tyrosine biosynthesis 0.50549212183081416 -0.076307377950920283
hpy tyrosine biosynthesis 0.59662163471018126 0.42178482185207838
vcho lipid-A-precursor biosynthesis 0.30474198596919183 -
0.60365626627390279
ecoli lipid-A-precursor biosynthesis 0.33977097281781382 -
0.594042933442262 33
hin lipid-A-precursor biosynthesis 0.39304203259987536 -
0.56619887253581613
agro lipid-A-precursor biosynthesis 0.46323249397636818 -
0.74843160591663804
hpy lipid-A-precursor biosynthesis 0.59128015169950288
0.19774894640349827
vcho ppGpp metabolism 0.29199822767476941 -0.76698257681525261
ecoli ppGpp metabolism 0.35336875843386345 -0.42030812164003128
bsub ppGpp metabolism 0.37366122011682118 -0.55059907691561405
hin ppGpp metabolism 0.35476710952581131 -1.1166897366103739
mtbrv ppGpp metabolism 0.57790505175136231 0.4130752691332753

hpy ppGpp metabolism 0.57439336550700815 -0.51052737322258 79
yeast cysteine biosynthesis 0.47115765155190786 1.3241942009723702
vcho cysteine biosynthesis 0.29998347496775352 -0.66464220367005522
ecoli cysteine biosynthesis 0.3512725307002928 -0.44709099210657693
bsub cysteine biosynthesis 0.44138359615833828 0.58494001751469293
agro cysteine biosynthesis 0.48958866724411437 -0.32924612064145453
mtbrv cysteine biosynthesis 0.53337989358318194 -0.50773483488858018
hpy cysteine biosynthesis 0.5051859189403235 -3.4132700849622726
vcho alkanesulfonate monooxygenase two-component system
-1.0769603381604134 0.26781178977547709
ecoli alkanesulfonate monooxygenase two-component system
-0.88586629794462668 0.31693069396354162
agro alkanesulfonate monooxygenase two-component system
-1.7646864909413185 0.39933574474536693
hpy alkanesulfonate monooxygenase two-component system
1.6771845725763748 0.62655298577918794
yeast biosynthesis of proto- and siroheme 0.20742854483475764 -
0.86577345732226696
vcho biosynthesis of proto- and siroheme 0.288178160389435 -0.81594124986278271

ecoli biosynthesis of proto- and siroheme 0.3512361731013332 -
0.44755552219928335
bsub biosynthesis of proto- and siroheme 0.39363463796939691 -
0.21569356788433519
hin biosynthesis of proto- and siroheme 0.40838824983960681 -
0.34548118821210377
agro biosynthesis of proto- and siroheme 0.46266721036036224 -
0.75742223913513884
mtbrv biosynthesis of proto- and siroheme 0.52506783586572092 -
0.67963375779730795
hpy biosynthesis of proto- and siroheme 0.58441500836833526 -
0.090193258636442911
vcho ubiquinone biosynthesis 0.2652486328589434 -1.1098102206553766
ecoli ubiquinone biosynthesis 0.2986382193748422 -1.1195837369307005
agro ubiquinone biosynthesis 0.49981020227955547 -0.166676271044504
hpy ubiquinone biosynthesis 0.5917254970333875 0.21642790345612239
vcho pyridine nucleotide biosynthesis 0.29625203297864527 -
0.71246503889652524
ecoli pyridine nucleotide biosynthesis 0.30034577100662391 -
1.097766863965735
bsub pyridine nucleotide biosynthesis 0.37305146130666333 -
0.56082324516811399
hin pyridine nucleotide biosynthesis 0.35831452759517451 -
1.0656688309782807
agro pyridine nucleotide biosynthesis 0.45874868425062931 -
0.81974499184226335
mtbrv pyridine nucleotide biosynthesis 0.47035992673851779 -
1.8110299743802902
hpy pyridine nucleotide biosynthesis 0.63193830438950915
1.9030590286068199
vcho salvage pathways of pyrimidine deoxyribonucleotides
-0.56843726394201266 0.30748999669447347
ecoli salvage pathways of pyrimidine deoxyribonucleotides
-0.52554141625990092 0.34513241382872772
bsub salvage pathways of pyrimidine deoxyribonucleotides
-0.5498732410413415 0.37370450821695178
hin salvage pathways of pyrimidine deoxyribonucleotides
-1.2562011237553494 0.34506706187850522
agro salvage pathways of pyrimidine deoxyribonucleotides
0.02414668350085606 0.51180814359701099

mtbrv salvage pathways of pyrimidine deoxyribonucleotides
-0.73950013292223282 0.52217303724247555
vcho cyanate degradation 0.25621291635788612 -1.2256135971099649
ecoli cyanate degradation 0.31431688460921503 -0.91926215290830926
bsub cyanate degradation 0.37559956136747941 -0.51809782109552893
agro cyanate degradation 0.52673756216669776 0.2615937326014573
mtbrv cyanate degradation 0.52211468003948669 -0.74070699898100401
hpy cyanate degradation 0.57502293597717513 -0.48412152841166126
yeast tryptophan biosynthesis 0.22239910072184063 -0.74146016620508237
vcho tryptophan biosynthesis 0.29866154047410409 -0.68158435516390481
ecoli tryptophan biosynthesis 0.32752282286373774 -0.75053385683829621
bsub tryptophan biosynthesis 0.36306299607443709 -0.72830544865130864
hin tryptophan biosynthesis 0.3836649750407149 -0.70106483969218081
agro tryptophan biosynthesis 0.54190667575886031 0.50285304508695272
mtbrv tryptophan biosynthesis 0.46656789013141164 -1.8894518321860521
hpy tryptophan biosynthesis 0.58712109287331304 0.023307057642488332
yeast proline biosynthesis 0.24234713215382728 -0.57581465128075 36
vcho proline biosynthesis 0.2899152134106468 -0.79367886426077416
ecoli proline biosynthesis 0.36107005683212939 -0.32191095127456243
bsub proline biosynthesis 0.35220883334322256 -0.91030328805148 73
hin proline biosynthesis 0.34507019415793244 -1.2561560736005764
agro proline biosynthesis 0.48262637369877581 -0.43997890300643372
mtbrv proline biosynthesis 0.54412385910746075 -0.28554242908847055
yeast degradation of short-chain fatty acids 0.39224627351426106
0.66892574037256691
vcho degradation of short-chain fatty acids 0.29141068579026963 -
0.77451261984234454
ecoli degradation of short-chain fatty acids 0.26534257429147801 -
1.5449921670771876
bsub degradation of short-chain fatty acids 0.34675412673584183 -
1.0017654156875715
yeast polyisoprenoid biosynthesis 0.36192218622977 39 0.41711898590782748

vcho polyisoprenoid biosynthesis 0.30759117607959474 -0.56714053064772751

ecoli polyisoprenoid biosynthesis 0.29170475431732124 -1.2081705319367906

bsub polyisoprenoid biosynthesis 0.34918345487987174 -0.96103150701527951

agro polyisoprenoid biosynthesis 0.51181745295363745 0.024294745479938564

mtbrv polyisoprenoid biosynthesis 0.42580122239501689 -2.7325338357846518

hpy polyisoprenoid biosynthesis 0.59262569065415982 0.25418439645624513

yeast mannose catabolism 0.29292258233645052 -0.15584356207357999
ecoli mannose catabolism 0.34083319017616076 -0.58047130214461573
bsub mannose catabolism 0.36630056347728451 -0.6740193386286385
agro mannose catabolism 0.45734941168369808 -0.84199992028132942
mtbrv mannose catabolism 0.49878924785158479 -1.2230925653201263
vcho KDO biosynthesis -- including transfer to lipid IV_A
0.29291877928600302 -0.75518462091777727
ecoli KDO biosynthesis -- including transfer to lipid IV_A
0.33626435568007812 -0.63884592458281386
hin KDO biosynthesis -- including transfer to lipid IV_A
0.35688272686989153 -1.0862617716072771
agro KDO biosynthesis -- including transfer to lipid IV_A
0.46685372583961043 -0.69083721159897726
hpy KDO biosynthesis -- including transfer to lipid IV_A
0.57619890569780263 -0.43479825894972129

vcho menaquinone biosynthesis 0.26356575298849316 -1.13137831336 2003

ecoli menaquinone biosynthesis 0.3281952717278982 -0.74194218021091585

bsub menaquinone biosynthesis 0.37694240641858306 -0.49558158432977134

hin menaquinone biosynthesis 0.38373144141672072 -0.70010888394307191

mtbrv menaquinone biosynthesis 0.53119052434350755 -0.55301245770379892

yeast phenylalanine biosynthesis 0.20475614749307358 -0.88796465123806567

ecoli phenylalanine biosynthesis 0.29226960983946604 -1.2009535430382856

bsub phenylalanine biosynthesis 0.40095690707369258 -
0.092916971523191588
hin phenylalanine biosynthesis 0.37966928792178506 -0.75853299581139599

vcho L-alanine degradation 0.26593370312608 55 -1.1010302362419195
ecoli L-alanine degradation 0.3082499050407122 -0.99677812376592567
bsub L-alanine degradation 0.34048477586325421 -1.1068871410115568
hin L-alanine degradation 0.39246919493528093 -0.57443773693135869
agro L-alanine degradation 0.45531287835247203 -0.87439025267354331
mtbrv L-alanine degradation 0.49544643811915848 -1.2922239924830934
hpy L-alanine degradation 0.60422243819959975 0.74058255283058205
vcho threonine biosynthesis from homoserine 0.27569411256078852 -
0.97593906411566123
ecoli threonine biosynthesis from homoserine 0.32253784696444654 -
0.81422539266305494
bsub threonine biosynthesis from homoserine 0.4049783173799 39 -
0.025487727536118589
hin threonine biosynthesis from homoserine 0.38056266364 14578 -
0.74568397790705621
agro threonine biosynthesis from homoserine 0.49199128954847254 -
0.29103327440030957
mtbrv threonine biosynthesis from homoserine 0.45810362240305574 -
2.0644985601050592
hpy threonine biosynthesis from homoserine 0.57862456185918187 -
0.33305984649658066
yeast trehalose degradation, low osmolarity 0.20629487490178225 -
0.87518728547078395
vcho trehalose degradation, low osmolarity 0.2994621740116935 -
0.67132329098102717
ecoli trehalose degradation, low osmolarity 0.30759053427673017 -
1.0052027054458355
bsub trehalose degradation, low osmolarity 0.3786619953151511 -
0.46674827202536839
yeast thiamin biosynthesis 0.19976889877851101 -0.92937803000659613
vcho thiamin biosynthesis 0.25495493131881619 -1.2417361608310165
ecoli thiamin biosynthesis 0.30239572536026987 -1.0715752145391195
bsub thiamin biosynthesis 0.38329779971414774 -0.38901737040559535
hin thiamin biosynthesis 0.31068576927248609 -1.7506916662461522
agro thiamin biosynthesis 0.45791849665959566 -0.8329488277968079
mtbrv thiamin biosynthesis 0.55173276317473785 -0.1281851947981992
hpy thiamin biosynthesis 0.59374727274369077 0.30122650532623124
vcho pyridine nucleotide cycling 0.26670590350407386 -1.0911335765735801

ecoli pyridine nucleotide cycling 0.31528642008361674 -0.90687469013040267

```
bsub  pyridine nucleotide cycling   0.38802887759031224     -0.30968849890324546
agro  pyridine nucleotide cycling   0.4616820337364374      -0.77309112008331038
vcho  glycogen biosynthesis   0.26259967932026823     -1.1437596881728691
ecoli glycogen biosynthesis   0.35380752949180022     -0.41470207596999692
bsub  glycogen biosynthesis   0.34117751956864517     -1.0952715184378641
hin   glycogen biosynthesis   0.37191197785838775     -0.87010286915720336
agro  glycogen biosynthesis   0.45328036708129077     -0.90671661564293704
mtbrv glycogen biosynthesis   0.54433875713231017     -0.2810981939468849
yeast phospholipid biosynthesis     0.16756589234142572     -1.1967870523740338
vcho  phospholipid biosynthesis     0.27359228672394026     -1.002876444078616
ecoli phospholipid biosynthesis     0.29336464686311403     -1.1869625847608283
bsub  phospholipid biosynthesis     0.33076215547798304     -1.2699117747162596
agro  phospholipid biosynthesis     0.50341509292896924     -0.10934177787330682
mtbrv phospholipid biosynthesis     0.51424662739687088     -0.90342359944608852
hpy   phospholipid biosynthesis     0.58810540070675354     0.0645915224128314 06
yeast pantothenate and coenzyme A biosynthesis  0.1692359165118541      -
1.1829194176357456
vcho  pantothenate and coenzyme A biosynthesis  0.2831088957028699      -
0.88090986267589588
ecoli pantothenate and coenzyme A biosynthesis  0.32472816901625495     -
0.7862403074291723 9
bsub  pantothenate and coenzyme A biosynthesis  0.36972614826095757     -
0.61658063563981169
hin   pantothenate and coenzyme A biosynthesis  0.39426957180041927     -
0.54854373280149971
agro  pantothenate and coenzyme A biosynthesis  0.42880206524723802     -
1.2960352291146744
mtbrv pantothenate and coenzyme A biosynthesis  0.53456364515221411     -
0.48325405929426657
hpy   pantothenate and coenzyme A biosynthesis  0.56921871415696224     -
0.72756588912371356
yeast methylglyoxal metabolism      0.21927273764675614     -0.7674210247077603
vcho  methylglyoxal metabolism      0.31518027019641442     -0.46987732823798661
ecoli methylglyoxal metabolism      0.33862932885700919     -0.60862937451995069
bsub  methylglyoxal metabolism      0.33840121828826608     -1.1418233204575494
agro  methylglyoxal metabolism      0.43438881913369159     -1.2071799117962083
yeast biotin biosynthesis     0.182625965796456 49     -1.0717304205573903
vcho  biotin biosynthesis     0.25690333285138151     -1.2167650944928954
ecoli biotin biosynthesis     0.30370892401380484     -1.0547968708166273
bsub  biotin biosynthesis     0.34635234228990075     -1.008502361030724
hin   biotin biosynthesis     0.3216636122082227      -1.5928023288417503
agro  biotin biosynthesis     0.4489777487390581      -0.97514821758379566
mtbrv biotin biosynthesis     0.61660990252588033     1.2135175164851131
hpy   biotin biosynthesis     0.5610541778604865      -1.0700085598010 18
vcho  pyridoxal 5'-phosphate salvage pathway    0.29945005087055399     -
0.67147866334989548
ecoli pyridoxal 5'-phosphate salvage pathway    0.30857568968209487     -
0.99261567151400398
hin   pyridoxal 5'-phosphate salvage pathway    0.31707844167208821     -
1.6587487576688345
agro  pyridoxal 5'-phosphate salvage pathway    0.49662948055584766     -
0.21726450954684534
mtbrv pyridoxal 5'-phosphate salvage pathway    0.50349006600746804     -
1.1258764961765457
vcho  enterobacterial common antigen biosynthesis     0.29959823675385749     -
0.66957948627551034
ecoli enterobacterial common antigen biosynthesis     0.33133936739921838     -
0.70177101667232555
bsub  enterobacterial common antigen biosynthesis     0.33463664277491423     -
1.20494607130027 53
hin   enterobacterial common antigen biosynthesis     0.3568259939976639      -
1.0870777347848799
agro  enterobacterial common antigen biosynthesis     0.41435471949688613     -
1.5258150828808845
mtbrv enterobacterial common antigen biosynthesis     0.52781264683154894     -
0.62286922792370836
hpy   enterobacterial common antigen biosynthesis     0.55022612650443348     -
1.5241650720213811
yeast methionine biosynthesis from homoserine   0.1549198536833748      -
1.3017978947926 43
vcho  methionine biosynthesis from homoserine   0.27152809748722179     -
1.0293314665691 12
ecoli methionine biosynthesis from homoserine   0.30250196687085623     -
1.0702177987533081
bsub  methionine biosynthesis from homoserine   0.36038466334188646     -
0.7732145570357974 5
hin   methionine biosynthesis from homoserine   0.39089559030602639     -
0.5970701788148814 5
agro  methionine biosynthesis from homoserine   0.48601588436937482     -
0.3860699511693616
mtbrv methionine biosynthesis from homoserine   0.49891967582609154     -
1.2203952274169283
hpy   methionine biosynthesis from homoserine   0.53563056391125796     -
2.1363414351567 82
vcho  cobalamin biosynthesis  0.26117528852268851     -1.1620149381833442
ecoli cobalamin biosynthesis  0.25900787324509139     -1.6259287346325 97
agro  cobalamin biosynthesis  0.51723138061436236     -0.1104013236485 8996
mtbrv cobalamin biosynthesis  0.47447518404691474     -1.7259236959049056
ecoli dTDP-rhamnose biosynthesis    0.29762877087733919     -1.1324811563848451
hin   dTDP-rhamnose biosynthesis    0.3568259939976639      -1.0870777347848799
agro  dTDP-rhamnose biosynthesis    0.39225204484398696     -1.8773501978663889
mtbrv dTDP-rhamnose biosynthesis    0.51875480275012031     -0.8101915125370522 4
vcho  enterobactin biosynthesis     0.23273093686631767     -1.5265621639109466
ecoli enterobactin biosynthesis     0.28701579326090176     -1.2680799752599374
bsub  enterobactin biosynthesis     0.36565126874464915     -0.6849064278864508 4
agro  enterobactin biosynthesis     0.45431638048987844     -0.8902391938632784 3
mtbrv enterobactin biosynthesis     0.43198478130141438     -2.6046536944425771
```

```
state path  mean  rpi
0     sorbitol degradation    2.1630250000000002      3.7031622157309503
1     sorbitol degradation    1.9057250000000001      3.2469106019372029
2     sorbitol degradation    1.77945     2.4501369855284887
3     sorbitol degradation    2.1045750000000001      4.1399698843152128
4     sorbitol degradation    1.9289499999999999      3.8263259723969418
5     sorbitol degradation    1.2572749999999999      2.3592046054477342
6     sorbitol degradation    0.7971249999999997      1.6409391378423903
EPI012      sorbitol degradation    2.1630250000000002      3.7031622157309503

EPI456      sorbitol degradation    1.9289499999999999      3.8263259723969418

EPI   sorbitol degradation    2.1045750000000001      4.1399698843152128
CAI   sorbitol degradation    0.69044563032330708     3.1451292784085365
0     mannitol degradation    2.1630250000000002      3.7031622157309503
1     mannitol degradation    1.9057250000000001      3.2469106019372029
2     mannitol degradation    1.77945     2.4501369855284887
3     mannitol degradation    2.1045750000000001      4.1399698843152128
4     mannitol degradation    1.9289499999999999      3.8263259723969418
5     mannitol degradation    1.2572749999999999      2.3592046054477342
6     mannitol degradation    0.7971249999999997      1.6409391378423903
EPI012      mannitol degradation    2.1630250000000002      3.7031622157309503

EPI456      mannitol degradation    1.9289499999999999      3.8263259723969418

EPI   mannitol degradation    2.1045750000000001      4.1399698843152128
CAI   mannitol degradation    0.69044563032330708     3.1451292784085365
0     glycolysis  2.0908125000000002      3.5324560447449
1     glycolysis  1.8669312499999999      3.1508816618528082
2     glycolysis  1.7679125000000002      2.4240525772813246
3     glycolysis  2.0054249999999998      3.8807161311070684
4     glycolysis  1.7046124999999999      3.2386631349802442
5     glycolysis  1.47961875  3.0346316634098125
6     glycolysis  0.90865625000000005     2.0865734758770302
EPI012      glycolysis  2.0908125000000002      3.5324560447449
EPI456      glycolysis  1.7046124999999999      3.2386631349802442
EPI   glycolysis  2.0054249999999998      3.8807161311070684
CAI   glycolysis  0.73216433931120328     3.4915552932180622
0     gluconeogenesis   1.4417705882352942      1.9981585260768202
1     gluconeogenesis   1.4030999999999998      2.0027270411853069
2     gluconeogenesis   1.3892705882352294 1.5680048887909686
3     gluconeogenesis   1.4324882352941177      2.3826222672550172
4     gluconeogenesis   1.1873588235294119      1.8836923290341847
5     gluconeogenesis   1.2368294117647056      2.2970958054024488
6     gluconeogenesis   1.1611      3.0952378943447876
EPI012      gluconeogenesis   1.4030999999999998      2.0027270411853069
EPI456      gluconeogenesis   1.1611      3.0952378943447876
EPI   gluconeogenesis   1.1611      3.0952378943447876
CAI   gluconeogenesis   0.60472923305046022     2.4333529403709035
0     glycine cleavage  1.1002000000000001      1.1907054225407312
1     glycine cleavage  1.1404000000000001      1.3524469687465652
2     glycine cleavage  1.6208500000000001      2.0915682186378879
3     glycine cleavage  1.1103499999999999      1.5403071230104579
4     glycine cleavage  1.6384000000000001      3.0652163165818358
5     glycine cleavage  0.48739999999999994     0.020508751624296 44
6     glycine cleavage  0.41794999999999999     0.12590725104578002
EPI012      glycine cleavage  1.6208500000000001      2.0915682186378879
EPI456      glycine cleavage  1.6384000000000001      3.0652163165818358
EPI   glycine cleavage  1.6384000000000001      3.0652163165818358
CAI   glycine cleavage  0.4507795480917719      1.1549774312703325
0     pyruvate dehydrogenase  1.0300666666666667      1.0249142812311012
1     pyruvate dehydrogenase  0.89216666666666666     0.7379772695394448 7
2     pyruvate dehydrogenase  0.91246666666666654     0.4900288849734048 5
3     pyruvate dehydrogenase  1.0442833333333335      1.3675584463056205
4     pyruvate dehydrogenase  0.9893833333333335      1.3650860402612912
5     pyruvate dehydrogenase  0.93806666666666672     1.3895261437850535
6     pyruvate dehydrogenase  0.72283333333333344     1.3440993041949594
EPI012      pyruvate dehydrogenase  1.0300666666666667      1.0249142812311012

EPI456      pyruvate dehydrogenase  0.93806666666666672     1.3895261437850535

EPI   pyruvate dehydrogenase  0.93806666666666672     1.3895261437850535
CAI   pyruvate dehydrogenase  0.31644122380609985     0.0394517726988459 77
0     glutamine biosynthesis  0.82709999999999995     0.545112827127329
1     glutamine biosynthesis  1.6095999999999999      2.5138912397334625
2     glutamine biosynthesis  1.0054000000000001      0.7001360144586923 4
3     glutamine biosynthesis  0.76600000000000001     0.6399134778543896 8
4     glutamine biosynthesis  1.1821999999999999      1.8701785434520761
5     glutamine biosynthesis  0.51419999999999999     0.1019207326374066 7
6     glutamine biosynthesis  0.56379999999999997     0.7086656098228238 9
EPI012      glutamine biosynthesis  1.6095999999999999      2.5138912397334625

EPI456      glutamine biosynthesis  1.1821999999999999      1.8701785434520761

EPI   glutamine biosynthesis  1.6095999999999999      2.5138912397334625
CAI   glutamine biosynthesis  0.54953273363146293     1.9750093389256329
0     thioredoxin pathway     1.5944      2.3589656226626761
1     thioredoxin pathway     1.0103      1.0304011468041196
2     thioredoxin pathway     0.53390000000000004     -0.3658486866036688
3     thioredoxin pathway     0.55130000000000001     0.0785238579472954 67
4     thioredoxin pathway     0.52890000000000004     0.1588278700946197 9
5     thioredoxin pathway     1.6830000000000001      3.6524551881643874
6     thioredoxin pathway     0.3967      0.0410007366541984
EPI012      thioredoxin pathway     1.5944      2.3589656226626761
EPI456      thioredoxin pathway     1.6830000000000001      3.6524551881643874

EPI   thioredoxin pathway     1.6830000000000001      3.6524551881643874
CAI   thioredoxin pathway     0.33934484224977524     0.2296400468485186 9
0     non-oxidative branch of the pentose phosphate pathway 1.2160466666666667
      1.4645602383712859
1     non-oxidative branch of the pentose phosphate pathway 1.0838266666666669
      1.2124069561919364
2     non-oxidative branch of the pentose phosphate pathway 1.0551799999999998
      0.81268048618513633
3     non-oxidative branch of the pentose phosphate pathway 0.76809999999999989
      0.64540448019162688
4     non-oxidative branch of the pentose phosphate pathway 0.77500000000000002
      0.80349861969399228
5     non-oxidative branch of the pentose phosphate pathway 0.67811333333333346
      0.59985017969445631
6     non-oxidative branch of the pentose phosphate pathway 0.60205999999999903
      0.86153729173444316
EPI012      non-oxidative branch of the pentose phosphate pathway
      1.2160466666666667      1.4645602383712859
EPI456      non-oxidative branch of the pentose phosphate pathway
      0.60205999999999903     0.86153729173444316
EPI   non-oxidative branch of the pentose phosphate pathway 1.2160466666666667
      1.4645602383712859
CAI   non-oxidative branch of the pentose phosphate pathway 0.42565117193895424
      0.94631509678196291
```

```
0     asparagine biosynthesis and degradation   1.2035499999999999     1.4350188415666372
1     asparagine biosynthesis and degradation   1.0783499999999999     1.1988501720399645
2     asparagine biosynthesis and degradation   1.26085     1.2776668562128159
3     asparagine biosynthesis and degradation   1.0198      1.3035403317548113
4     asparagine biosynthesis and degradation   0.62660000000000005     0.41475770445406185
5     asparagine biosynthesis and degradation   0.27879999999999999     -0.61316808566431402
6     asparagine biosynthesis and degradation   0.31945000000000001     -0.26765941566343365
EPI012      asparagine biosynthesis and degradation   1.2035499999999999     1.4350188415666372
EPI456      asparagine biosynthesis and degradation   0.62660000000000005     0.41475770445406185
EPI   asparagine biosynthesis and degradation   1.2035499999999999     1.4350188415666372
CAI   asparagine biosynthesis and degradation   0.37372077889859756     0.51509276164971984
0     anaerobic respiration   0.68720555555555551     0.21441045630050798
1     anaerobic respiration   0.57644999999999991     -0.04353874443131912
2     anaerobic respiration   0.67763333333333353     -0.040891031534430508
3     anaerobic respiration   0.70052777777777786     0.46871913249898167
4     anaerobic respiration   0.57400000000000007     0.27696948247548819
5     anaerobic respiration   0.98688888888888904     1.5378363612691357
6     anaerobic respiration   0.88097222222222227     1.9759591557391085
EPI012      anaerobic respiration   0.68720555555555551     0.21441045630050798
EPI456      anaerobic respiration   0.88097222222222227     1.9759591557391085
EPI   anaerobic respiration   0.88097222222222227     1.9759591557391085
CAI   anaerobic respiration   0.36642374387224902     0.45449925754975212
0     sulfate assimilation pathway  0.88693333333333335     0.68655536450888133
1     sulfate assimilation pathway  1.0448333333333335      1.1158839732279924
2     sulfate assimilation pathway  0.52756666666666663     -0.38016732168606743
3     sulfate assimilation pathway  0.75013333333333332     0.59842590463970602
4     sulfate assimilation pathway  0.54900000000000004     0.21148078381647023
5     sulfate assimilation pathway  0.83706666666666674     1.0827123347431089
6     sulfate assimilation pathway  0.60496666666666665     0.87315117103631934
EPI012      sulfate assimilation pathway  1.0448333333333335      1.1158839732279924
EPI456      sulfate assimilation pathway  0.83706666666666674     1.0827123347431089
EPI   sulfate assimilation pathway  1.0448333333333335      1.1158839732279924
CAI   sulfate assimilation pathway  0.29355928221231081     -0.15055650008208993
0     glycine biosynthesis    0.81603333333333328     0.51895186756706424
1     glycine biosynthesis    0.84586666666666677     0.62336757272211063
2     glycine biosynthesis    1.1867333333333334      1.1101011451616916
3     glycine biosynthesis    0.79859999999999998     0.72515475223245796
4     glycine biosynthesis    1.1485333333333334      1.7819870959245989
5     glycine biosynthesis    0.37319999999999998     -0.3264034958270905
6     glycine biosynthesis    0.3246      -0.24708207217559155
EPI012      glycine biosynthesis    1.1867333333333334      1.1101011451616916
EPI456      glycine biosynthesis    1.1485333333333334      1.7819870959245989
EPI   glycine biosynthesis    1.1485333333333334      1.7819870959245989
CAI   glycine biosynthesis    0.37859998542652501     0.55560897401364817
0     TCA cycle, aerobic respiration      0.36978461538461538     -0.53595427677719021
1     TCA cycle, aerobic respiration      0.30456153846153844     -0.7165636719702897
2     TCA cycle, aerobic respiration      0.51077692307692302     -0.41812619719290056
3     TCA cycle, aerobic respiration      0.48849230769230767     -0.085703373127958976
4     TCA cycle, aerobic respiration      0.53179999999999994     0.16642455913906562
5     TCA cycle, aerobic respiration      1.0865307692307695      1.8405245280789777
6     TCA cycle, aerobic respiration      1.1963461538461539      3.2360674505229694
EPI012      TCA cycle, aerobic respiration      0.51077692307692302     -0.41812619719290056
EPI456      TCA cycle, aerobic respiration      1.1963461538461539      3.2360674505229694
EPI   TCA cycle, aerobic respiration      1.1963461538461539      3.2360674505229694
CAI   TCA cycle, aerobic respiration      0.26888666616141943     -0.35543426981162879
0     ribose catabolism 0.91478333333333328     0.75239115279984869
1     ribose catabolism 0.81603333333333339     0.54951899197947962
2     ribose catabolism 0.83256666666666668     0.30938799925739624
3     ribose catabolism 0.6005166666666667      0.20721377780334654
4     ribose catabolism 0.48015000000000002     0.031124907709534792
5     ribose catabolism 0.66353333333333331     0.55555963181493551
6     ribose catabolism 0.63748333333333329     1.0030747863915943
EPI012      ribose catabolism 0.91478333333333328     0.75239115279984869
EPI456      ribose catabolism 0.63748333333333329     1.0030747863915943
EPI   ribose catabolism 0.63748333333333329     1.0030747863915943
CAI   ribose catabolism 0.31473803493381353     0.025308743161060788
0     valine biosynthesis     1.2159666666666666      1.4643711230009706
1     valine biosynthesis     1.3556333333333335      1.8852294110428425
2     valine biosynthesis     0.80003333333333337     0.23583543169009352
3     valine biosynthesis     0.51200000000000001     -0.024236328649578327
4     valine biosynthesis     0.62443333333333328     0.40908201723694676
5     valine biosynthesis     0.29360000000000003     -0.56820923047796956
6     valine biosynthesis     0.27783333333333332     -0.4339429971816921
EPI012      valine biosynthesis     1.3556333333333335      1.8852294110428425
EPI456      valine biosynthesis     0.62443333333333328     0.40908201723694676
EPI   valine biosynthesis     1.3556333333333335      1.8852294110428425
CAI   valine biosynthesis     0.50448644104551632     1.6009515600278992
0     degradation of short-chain fatty acids    0.60840000000000005     0.028118683528241144
1     degradation of short-chain fatty acids    1.3125      1.7784583903937199
2     degradation of short-chain fatty acids    0.9022      0.46681762389683834
3     degradation of short-chain fatty acids    0.62090000000000001     0.26051136398145364
4     degradation of short-chain fatty acids    1.0183      1.4408346350435548
5     degradation of short-chain fatty acids    0.2893      -0.581271600565894
6     degradation of short-chain fatty acids    0.2268      -0.63785181841072969
EPI012      degradation of short-chain fatty acids    1.3125      1.7784583903937199
EPI456      degradation of short-chain fatty acids    1.0183      1.4408346350435548
EPI   degradation of short-chain fatty acids    1.3125      1.7784583903937199
CAI   degradation of short-chain fatty acids    0.39224627351426106     0.66892574037256558
0     UDP-N-acetylglucosamine biosynthesis      0.77249999999999996     0.41604158688722753
1     UDP-N-acetylglucosamine biosynthesis      0.76449999999999996     0.42195485138941519
2     UDP-N-acetylglucosamine biosynthesis      1.0469999999999999      0.7941868385611448
3     UDP-N-acetylglucosamine biosynthesis      0.53069999999999995     0.024659739782012861
4     UDP-N-acetylglucosamine biosynthesis      0.58199999999999996     0.29792586604637367
5     UDP-N-acetylglucosamine biosynthesis      0.4325      -0.14626429903315655
6     UDP-N-acetylglucosamine biosynthesis      0.52590000000000003     0.55723234415501499
EPI012      UDP-N-acetylglucosamine biosynthesis      1.0469999999999999      0.7941868385611448
EPI456      UDP-N-acetylglucosamine biosynthesis      0.52590000000000003     0.55723234415501499
EPI   UDP-N-acetylglucosamine biosynthesis      1.0469999999999999      0.7941868385611448
CAI   UDP-N-acetylglucosamine biosynthesis      0.29647433209423935     -0.12635035521168017
0     trehalose biosynthesis  0.44127142857142854     -0.36696358742124841
1     trehalose biosynthesis  0.31695714285714283     -0.68587994709668632
2     trehalose biosynthesis  0.47577142857142857     -0.4972679184995264
3     trehalose biosynthesis  0.80674285714285709     0.74644639394827683
4     trehalose biosynthesis  0.51038571428571433     0.11032881097342712
5     trehalose biosynthesis  1.0128571428571427      1.6167216970529823
6     trehalose biosynthesis  0.74698571428571425     1.4406025738855139
EPI012      trehalose biosynthesis  0.44127142857142854     -0.36696358742124841
EPI456      trehalose biosynthesis  1.0128571428571427      1.6167216970529823
EPI   trehalose biosynthesis  1.0128571428571427      1.6167216970529823
CAI   trehalose biosynthesis  0.2240587114615448      -0.72767900306176592
0     removal of superoxide radicals      0.58023999999999987     -0.038449926822698127
1     removal of superoxide radicals      0.38302000000000003     -0.52234983849993155
2     removal of superoxide radicals      0.69485999999999992     -0.0019443441176462204
3     removal of superoxide radicals      0.75873000000000013     0.62090415071547722
4     removal of superoxide radicals      0.48224999999999996     0.03662595839689213
5     removal of superoxide radicals      1.0305699999999998      1.6705291145679901
6     removal of superoxide radicals      0.47434000000000004     0.35121917323595853
EPI012      removal of superoxide radicals      0.69485999999999992     -0.0019443441176462204
EPI456      removal of superoxide radicals      1.0305699999999998      1.6705291145679901
EPI   removal of superoxide radicals      1.0305699999999998      1.6705291145679901
CAI   removal of superoxide radicals      0.30551868706056601     -0.051247363687749764
0     fatty acid elongation, saturated    0.92170000000000007     0.76874175252501442
1     fatty acid elongation, saturated    0.84889999999999988     0.63087619936745021
2     fatty acid elongation, saturated    0.60940000000000005     -0.19515548420888656
3     fatty acid elongation, saturated    0.50598571428571426     -0.039962260513367535
4     fatty acid elongation, saturated    0.48107142857142859     0.033538634031538603
5     fatty acid elongation, saturated    0.56379999999999997     0.25259365272137158
6     fatty acid elongation, saturated    0.43981428571428571     0.21326820585338727
EPI012      fatty acid elongation, saturated    0.92170000000000007     0.76874175252501442
EPI456      fatty acid elongation, saturated    0.56379999999999997     0.25259365272137158
EPI   fatty acid elongation, saturated    0.92170000000000007     0.76874175252501442
CAI   fatty acid elongation, saturated    0.3728481881237119      0.50784689637639846
0     glyoxylate cycle  0.25394166666666662     -0.80980030359213762
1     glyoxylate cycle  0.27290833333333331     -0.79491711134481424
2     glyoxylate cycle  0.40857499999999997     -0.64918809840059521
3     glyoxylate cycle  0.38221666666666665     -0.36358898896758357
4     glyoxylate cycle  0.46840833333333332     0.00036704890601593846
5     glyoxylate cycle  0.94264166666666682     1.4034238980065084
6     glyoxylate cycle  1.0629166666666667      2.7029365011833701
EPI012      glyoxylate cycle  0.40857499999999997     -0.64918809840059521
EPI456      glyoxylate cycle  1.0629166666666667      2.7029365011833701
EPI   glyoxylate cycle  1.0629166666666667      2.7029365011833701
CAI   glyoxylate cycle  0.26073471732764425     -0.42312685225072666
0     methyl-donor molecule biosynthesis  0.78416666666666668     0.44362091172485618
1     methyl-donor molecule biosynthesis  0.76783333333333326     0.43020608946121747
2     methyl-donor molecule biosynthesis  1.5000666666666664      1.8184967754205494
3     methyl-donor molecule biosynthesis  0.63490000000000002     0.29711804622970384
4     methyl-donor molecule biosynthesis  0.42426666666666674     -0.1152641633958982
```

```
5     methyl-donor molecule biosynthesis  0.24929999999999999     -
0.70278201998844647
6     methyl-donor molecule biosynthesis  0.20929999999999996     -
0.70777483026262067
EPI012      methyl-donor molecule biosynthesis  1.5000666666666664
      1.8184967754205494
EPI456      methyl-donor molecule biosynthesis  0.42426666666666674     -
0.11526416335958982
EPI   methyl-donor molecule biosynthesis  1.5000666666666664
      1.8184967754205494
CAI   methyl-donor molecule biosynthesis  0.5710148939327877
      2.1533940340236155
0     purine biosynthesis     0.73285555555555548     0.32232441448660015
1     purine biosynthesis     0.71910555555555555     0.30958674091492044
2     purine biosynthesis     1.1255166666666669      0.97170023293079888
3     purine biosynthesis     0.67495555555555553     0.40185383155108628
4     purine biosynthesis     0.57246666666666657     0.27295284229106803
5     purine biosynthesis     0.30848888888888887     -0.52298035213735294
6     purine biosynthesis     0.21505555555555553     -0.68477792858688757
EPI012      purine biosynthesis     1.1255166666666669      0.97170023293079888

EPI456      purine biosynthesis     0.57246666666666657     0.27295284229106803

EPI   purine biosynthesis     1.1255166666666669      0.97170023293079888
CAI   purine biosynthesis     0.27806586786805376     -0.27921153081736327
0     folic acid biosynthesis 0.68287500000000001     0.20417327358101695
1     folic acid biosynthesis 0.76643333333333319     0.42674056947106032
2     folic acid biosynthesis 0.97545833333333321     0.63244278308847701
3     folic acid biosynthesis 0.52004166666666662     -0.0032092760486490306
4     folic acid biosynthesis 0.78318333333333323     0.82493525372171039
5     folic acid biosynthesis 0.31709999999999999     -0.49682185906722015
6     folic acid biosynthesis 0.24982499999999999     -0.54585311281702775
EPI012      folic acid biosynthesis 0.97545833333333321     0.63244278308847701

EPI456      folic acid biosynthesis 0.78318333333333323     0.82493525372171039

EPI   folic acid biosynthesis 0.78318333333333323     0.82493525372171039
CAI   folic acid biosynthesis 0.31771526343642725     0.050031210139534182
0     fatty acid elongation, unsaturated  0.86306000000000016
      0.63012018608399711
1     fatty acid elongation, unsaturated  0.79967999999999995
      0.50903841799921701
2     fatty acid elongation, unsaturated  0.57630000000000003     -
0.26998919280963624
3     fatty acid elongation, unsaturated  0.47689999999999999     -
0.11601451057197711
4     fatty acid elongation, unsaturated  0.45464000000000004     -
0.035699760402127037
5     fatty acid elongation, unsaturated  0.53502000000000005
      0.16516690594684535
6     fatty acid elongation, unsaturated  0.41936000000000001
      0.13154104800070388
EPI012      fatty acid elongation, unsaturated  0.86306000000000016
      0.63012018608399711
EPI456      fatty acid elongation, unsaturated  0.53502000000000005
      0.16516690594684535
EPI   fatty acid elongation, unsaturated  0.86306000000000016
      0.63012018608399711
CAI   fatty acid elongation, unsaturated  0.35722866423138122
      0.3781446705282262

0     glucose 1-phosphate metabolism      0.40494999999999992     -
0.45282534260451857
1     glucose 1-phosphate metabolism      0.37185000000000007     -
0.54999973727854112
2     glucose 1-phosphate metabolism      0.9229666666666666
      0.51376767471080298
3     glucose 1-phosphate metabolism      0.67366666666666664
      0.39848369255045368
4     glucose 1-phosphate metabolism      0.25546666666666668     -
0.55744385670527907
5     glucose 1-phosphate metabolism      0.72698333333333343
      0.74830553462395955
6     glucose 1-phosphate metabolism      0.58561666666666679
      0.795836297931515
EPI012      glucose 1-phosphate metabolism      0.9229666666666666
      0.51376767471080298
EPI456      glucose 1-phosphate metabolism      0.58561666666666679
      0.795836297931515
EPI   glucose 1-phosphate metabolism      0.58561666666666679
      0.795836297931515
CAI   glucose 1-phosphate metabolism      0.262160815564925526     -
0.4112847425341607
0     (deoxy)ribose phosphate metabolism  0.70837499999999998
      0.26445379786897638
1     (deoxy)ribose phosphate metabolism  0.68799999999999994
      0.23258893764155147
2     (deoxy)ribose phosphate metabolism  0.62785000000000002     -
0.15344303938460171
3     (deoxy)ribose phosphate metabolism  0.45772499999999999     -
0.16615259143699124
4     (deoxy)ribose phosphate metabolism  0.44130000000000003     -
0.070644530006579054
5     (deoxy)ribose phosphate metabolism  0.54847500000000005
      0.2060399732801064
6     (deoxy)ribose phosphate metabolism  0.50612499999999994
      0.47821934076237799
EPI012      (deoxy)ribose phosphate metabolism  0.70837499999999998
      0.26445379786897638
EPI456      (deoxy)ribose phosphate metabolism  0.50612499999999994
      0.47821934076237799
EPI   (deoxy)ribose phosphate metabolism  0.50612499999999994
      0.47821934076237799
CAI   (deoxy)ribose phosphate metabolism  0.25736013770239113     -
0.45114886442691915
0     isoleucine biosynthesis 0.84132857142857131     0.57874834656195506
1     isoleucine biosynthesis 0.87965714285714292     0.70701155180426678
2     isoleucine biosynthesis 0.74032857142857134     0.10085268986356478
3     isoleucine biosynthesis 0.47750000000000004     -0.11444456527613377
4     isoleucine biosynthesis 0.53228571428571425     0.16769691099872661
5     isoleucine biosynthesis 0.35818571428571427     -0.37201329968891278
6     isoleucine biosynthesis 0.28735714285714281     -0.3958896573983503
EPI012      isoleucine biosynthesis 0.87965714285714292     0.70701155180426678

EPI456      isoleucine biosynthesis 0.53228571428571425     0.16769691099872661

EPI   isoleucine biosynthesis 0.87965714285714292     0.70701155180426678
CAI   isoleucine biosynthesis 0.37733907991205851     0.54513860033658357
0     fatty acid biosynthesis, initial steps    0.82396666666666663
      0.53770580845665172

1     fatty acid biosynthesis, initial steps    0.76101666666666656
      0.41333230760438161
2     fatty acid biosynthesis, initial steps    0.55814999999999992     -
0.3110223864985672
3     fatty acid biosynthesis, initial steps    0.47241666666666671     -
0.12773736476814282
4     fatty acid biosynthesis, initial steps    0.42141666666666672     -
0.12272987500671791
5     fatty acid biosynthesis, initial steps    0.47778333333333345     -
0.0087043783785416724
6     fatty acid biosynthesis, initial steps    0.38955000000000001
      0.012432191811854497
EPI012      fatty acid biosynthesis, initial steps    0.82396666666666663
      0.53770580845665172
EPI456      fatty acid biosynthesis, initial steps    0.38955000000000001
      0.012432191811854497
EPI   fatty acid biosynthesis, initial steps    0.82396666666666663
      0.53770580845665172
CAI   fatty acid biosynthesis, initial steps    0.35722304482209549
      0.3780980077811838
0     nucleotide metabolism   0.80694166666666656     0.49745969371145499
1     nucleotide metabolism   0.7458083333333333      0.37568603390178357
2     nucleotide metabolism   0.91103333333333347     0.48678835177115753
3     nucleotide metabolism   0.61494166666666672     0.24493173433413298
4     nucleotide metabolism   0.46300000000000008     -0.013800339570551354
5     nucleotide metabolism   0.33060000000000006     -0.45581209251210852
6     nucleotide metabolism   0.18964166666666671     -0.78632168024291094
EPI012      nucleotide metabolism   0.80694166666666656     0.49745969371145499

EPI456      nucleotide metabolism   0.46300000000000008     -
0.013800339570551354
EPI   nucleotide metabolism   0.80694166666666656     0.49745969371145499
CAI   nucleotide metabolism   0.32370807810046348     0.099794660445642266
0     glyoxylate degradation  0.40664999999999996     -0.44880664098532119
1     glyoxylate degradation  0.34068333333333328     -0.62714881324989324
2     glyoxylate degradation  0.49871666666666653     -0.44539247253596576
3     glyoxylate degradation  0.41775000000000001     -0.2706777430708342
4     glyoxylate degradation  0.35191666666666666     -0.30478845727878789
5     glyoxylate degradation  0.74575000000000002     0.80531417306970687
6     glyoxylate degradation  0.77789999999999992     1.5641237148222416
EPI012      glyoxylate degradation  0.49871666666666653     -0.44539247253596576

EPI456      glyoxylate degradation  0.77789999999999992     1.5641237148222416

EPI   glyoxylate degradation  0.77789999999999992     1.5641237148222416
CAI   glyoxylate degradation  0.25011367135211532     -0.51132245368889051
0     threonine catabolism    0.61670000000000003     0.047739403198439667
1     threonine catabolism    0.48740000000000006     -0.26397056951951303
2     threonine catabolism    1.1579666666666666      1.0450643974049469
3     threonine catabolism    0.61019999999999996     0.23253339969171943
4     threonine catabolism    0.25763333333333333     -0.55176816948816421
5     threonine catabolism    0.47066666666666662     -0.030323107167471268
6     threonine catabolism    0.30969999999999998     -0.30661652226663011
EPI012      threonine catabolism    1.1579666666666666      1.0450643974049469

EPI456      threonine catabolism    0.47066666666666662     -
0.030323107167471268
EPI   threonine catabolism    1.1579666666666666      1.0450643974049469
CAI   threonine catabolism    0.32242686499780132     0.089155655547245916

0     mannose and GDP-mannose metabolism  0.45079999999999998     -
0.34443859599263826
1     mannose and GDP-mannose metabolism  0.47359999999999997     -
0.29813069513677493
2     mannose and GDP-mannose metabolism  1.81765     2.5365009634302602
3     mannose and GDP-mannose metabolism  0.61010000000000009
      0.23227192338994654
4     mannose and GDP-mannose metabolism  0.14974999999999999     -
0.83437373376804624
5     mannose and GDP-mannose metabolism  0.22994999999999999     -
0.7615626853841061
6     mannose and GDP-mannose metabolism  0.27405000000000002     -
0.44905968641062455
EPI012      mannose and GDP-mannose metabolism  1.81765     2.5365009634302602

EPI456      mannose and GDP-mannose metabolism  0.27405000000000002     -
0.44905968641062455
EPI   mannose and GDP-mannose metabolism  1.81765     2.5365009634302602
CAI   mannose and GDP-mannose metabolism  0.42187117411450392
      0.91492655159249114
0     phosphatidic acid synthesis   0.51900000000000002     -0.18321774279895819

1     phosphatidic acid synthesis   0.70479999999999998     0.27417517752343534

2     phosphatidic acid synthesis   1.0699000000000001      0.8459600085598511

3     phosphatidic acid synthesis   0.79369999999999996     0.71234241344557037

4     phosphatidic acid synthesis   0.2447      -0.58564765626109605
5     phosphatidic acid synthesis   0.21260000000000001     -0.81426782980863821

6     phosphatidic acid synthesis   0.32940000000000003     -0.22790318892478714

EPI012      phosphatidic acid synthesis   1.0699000000000001
      0.8459600085598511
EPI456      phosphatidic acid synthesis   0.32940000000000003     -
0.22790318892478714
EPI   phosphatidic acid synthesis   1.0699000000000001      0.8459600085598511

CAI   phosphatidic acid synthesis   0.24426581104065304     -0.55988222440112489

0     fermentation      0.46705454545454544     -0.30601379120587474
1     fermentation      0.38059090909090904     -0.52836274071661971
2     fermentation      0.47498181818181817     -0.49905309897699557
3     fermentation      0.43960000000000005     -0.21354517113338645
4     fermentation      0.33997272727272726     -0.33607617918963872
5     fermentation      0.73515454545454528     0.77312771992493701
6     fermentation      0.63062727272727272     0.97568070599074552
EPI012      fermentation      0.46705454545454544     -0.30601379120587474
EPI456      fermentation      0.63062727272727272     0.97568070599074552
EPI   fermentation      0.63062727272727272     0.97568070599074552
CAI   fermentation      0.29791630966303417     -0.11437638586504360
0     threonine biosynthesis  0.68012000000000006     0.19766061301578849
1     threonine biosynthesis  0.66680000000000006     0.18011106350488887
2     threonine biosynthesis  0.98795999999999995     0.66070701512343311
3     threonine biosynthesis  0.61015999999999992     0.23242880917101003
4     threonine biosynthesis  0.34009999999999996     -0.33574278217828379
5     threonine biosynthesis  0.32016     -0.48752631198139484
6     threonine biosynthesis  0.22911999999999999     0.62858202483950765
```

EPI012 threonine biosynthesis 0.98795999999999995 0.66070701512343311

EPI456 threonine biosynthesis 0.34009999999999996 -0.33574278217828379

EPI threonine biosynthesis 0.98795999999999995 0.66070701512343311
CAI threonine biosynthesis 0.3832589101272823 0.59429599852941817
0 homoserine biosynthesis 0.61940000000000006 0.054122046946576644
1 homoserine biosynthesis 0.74403333333333332 0.3712922496285489
2 homoserine biosynthesis 0.86359999999999992 0.37954931114792767
3 homoserine biosynthesis 0.56963333333333332 0.12646117993905165
4 homoserine biosynthesis 0.35243333333333332 -0.3034350241731682
5 homoserine biosynthesis 0.35626666666666668 -0.37784290671597087
6 homoserine biosynthesis 0.25193333333333334 -0.53742905472249036
EPI012 homoserine biosynthesis 0.86359999999999992 0.37954931114792767

EPI456 homoserine biosynthesis 0.35243333333333332 -0.3034350241731682

EPI homoserine biosynthesis 0.86359999999999992 0.37954931114792767
CAI homoserine biosynthesis 0.40274729569188206 0.75612468187085435
0 trehalose degradation, low osmolarity 0.23550000000000001 -0.85339533635333165
1 trehalose degradation, low osmolarity 0.17123333333333335 -1.046600500629965
2 trehalose degradation, low osmolarity 0.36026666666666668 -0.75840537150194087
3 trehalose degradation, low osmolarity 0.53286666666666671 0.030325059653766116
4 trehalose degradation, low osmolarity 0.69563333333333333 0.59559383101782992
5 trehalose degradation, low osmolarity 0.79789999999999994 0.96373338239185924
6 trehalose degradation, low osmolarity 0.57973333333333332 0.772328847280355
EPI012 trehalose degradation, low osmolarity 0.36026666666666668 -0.75840537150194087
EPI456 trehalose degradation, low osmolarity 0.79789999999999994 0.96373338239185924
EPI trehalose degradation, low osmolarity 0.79789999999999994 0.96373338239185924
CAI trehalose degradation, low osmolarity 0.20629487490178225 -0.87518728547078539
0 proline utilization 0.81689999999999996 0.52100061741214521
1 proline utilization 0.83509999999999995 0.59671607375018876
2 proline utilization 0.32929999999999998 -0.82841596091794945
3 proline utilization 0.47023000000000001 -0.13353342279078254
4 proline utilization 0.37733000000000002 -0.23829559857366495
5 proline utilization 0.44490000000000002 -0.10859606901216523
6 proline utilization 0.32669999999999999 -0.23869131075336469
EPI012 proline utilization 0.83509999999999995 0.59671607375018876

EPI456 proline utilization 0.44490000000000002 -0.10859606901216523

EPI proline utilization 0.83509999999999995 0.59671607375018876
CAI proline utilization 0.20653240998076783 -0.87321482916073245
0 mannose catabolism 0.29749999999999999 -0.70683092435907724
1 mannose catabolism 0.32679999999999998 -0.6615152198189499
2 mannose catabolism 1.9286000000000001 2.7873408416554319
3 mannose catabolism 0.58630000000000004 0.17004056356792108
4 mannose catabolism 0.11119999999999999 -0.93535730710025178
5 mannose catabolism 0.23269999999999999 -0.75320884404880561
6 mannose catabolism 0.28370000000000001 -0.41050213987515338
EPI012 mannose catabolism 1.9286000000000001 2.7873408416554319

EPI456 mannose catabolism 0.28370000000000001 -0.41050213987515338

EPI mannose catabolism 1.9286000000000001 2.7873408416554319
CAI mannose catabolism 0.29292258233645052 -0.15584356207358141
0 colanic acid biosynthesis 0.43233333333333334 -0.38809272730570558

1 colanic acid biosynthesis 0.35696666666666665 -0.58684151526913875

2 colanic acid biosynthesis 1.0998833333333333 0.91374744147664266

3 colanic acid biosynthesis 0.60086666666666666 0.20812894485955269

4 colanic acid biosynthesis 0.23974999999999999 -0.59861441859558162

5 colanic acid biosynthesis 0.48196666666666665
0.0040035863193998746
6 colanic acid biosynthesis 0.35699999999999998 -0.11762461023266242

EPI012 colanic acid biosynthesis 1.0998833333333333
0.91374744147664266
EPI456 colanic acid biosynthesis 0.48196666666666665
0.0040035863193998746
EPI colanic acid biosynthesis 1.0998833333333333 0.91374744147664266

CAI colanic acid biosynthesis 0.29771093759963696 -0.11608176523084678

0 glycogen catabolism 0.30745 -0.68330970017612835
1 glycogen catabolism 0.49365000000000003 -0.2484994981348837
2 glycogen catabolism 0.38750000000000001 -0.69683524065922942
3 glycogen catabolism 0.43790000000000001 -0.21799026826353121
4 glycogen catabolism 0.35320000000000001 -0.30142670408059829
5 glycogen catabolism 0.55345 0.2211528316957862
6 glycogen catabolism 0.72225000000000006 1.3417685371332295
EPI012 glycogen catabolism 0.49365000000000003 -0.2484994981348837

EPI456 glycogen catabolism 0.72225000000000006 1.3417685371332295

EPI glycogen catabolism 0.72225000000000006 1.3417685371332295
CAI glycogen catabolism 0.27838541045482157 -0.27655809624133137
0 anaerobic respiration, electron acceptors reaction list 0.25040000000000001 -0.81817259863213188
1 anaerobic respiration, electron acceptors reaction list 0.20899999999999999 -0.95311397327644465
2 anaerobic respiration, electron acceptors reaction list 0.315 -0.86074593170316749
3 anaerobic respiration, electron acceptors reaction list 0.31 -0.55241845823147417
4 anaerobic respiration, electron acceptors reaction list 0.32605000000000001 -0.37254743082465175
5 anaerobic respiration, electron acceptors reaction list 0.82045000000000001 1.0322348813413234
6 anaerobic respiration, electron acceptors reaction list 0.86470000000000002 1.9109418536076201
EPI012 anaerobic respiration, electron acceptors reaction list 0.25040000000000001 -0.81817259863213188
EPI456 anaerobic respiration, electron acceptors reaction list 0.86470000000000002 1.9109418536076201
EPI anaerobic respiration, electron acceptors reaction list 0.86470000000000002 1.9109418536076201
CAI anaerobic respiration, electron acceptors reaction list 0.24173134739194152 -0.58092803724632758
0 formylTHF biosynthesis 0.56134166666666674 -0.083124493156107634
1 formylTHF biosynthesis 0.66680833333333334 0.18013169160006823
2 formylTHF biosynthesis 0.8222583333333332 0.28608253663425209
3 formylTHF biosynthesis 0.36316666666666664 -0.41340022445538122
4 formylTHF biosynthesis 0.56635000000000002 0.25692994068582858
5 formylTHF biosynthesis 0.26704166666666668 -0.64888708604040179
6 formylTHF biosynthesis 0.19371666666666665 -0.77003960748311373
EPI012 formylTHF biosynthesis 0.8222583333333332 0.28608253663425209

EPI456 formylTHF biosynthesis 0.56635000000000002 0.25692994068582858

EPI formylTHF biosynthesis 0.8222583333333332 0.28608253663425209
CAI formylTHF biosynthesis 0.2866672062266305 -0.20778728395357488
0 alanine biosynthesis 0.55895000000000006 -0.088778254747821528
1 alanine biosynthesis 0.65654999999999997 0.15473850643409645
2 alanine biosynthesis 0.61010000000000009 -0.19357289822639329
3 alanine biosynthesis 0.33555000000000001 -0.48561126312841751
4 alanine biosynthesis 0.65949999999999998 0.50094083188932925
5 alanine biosynthesis 0.30454999999999999 -0.53494575316104598
6 alanine biosynthesis 0.23714999999999997 -0.59649735140118298
EPI012 alanine biosynthesis 0.65654999999999997 0.15473850643409645

EPI456 alanine biosynthesis 0.65949999999999998 0.50094083188932925

EPI alanine biosynthesis 0.65949999999999998 0.50094083188932925
CAI alanine biosynthesis 0.29927715769637842 -0.10307610423145799
0 glutamate degradation V 0.62875000000000003 0.076224905852161726
1 glutamate degradation V 0.47015000000000001 -0.30667072654109023
2 glutamate degradation V 1.05965 0.82278642810191482
3 glutamate degradation V 0.41470000000000001 -0.27865277027491725
4 glutamate degradation V 0.22520000000000001 -0.63672884121513007
5 glutamate degradation V 0.21949999999999997 -0.80712909266756339
6 glutamate degradation V 0.35120000000000001 -0.14079909416071754
EPI012 glutamate degradation V 1.05965 0.82278642810191482
EPI456 glutamate degradation V 0.35120000000000001 -0.14079909416071754

EPI glutamate degradation V 1.05965 0.82278642810191482
CAI glutamate degradation V 0.21813134649369936 -0.77689896873059894
0 aspartate biosynthesis and degradation 0.62875000000000003 0.076224905852161726
1 aspartate biosynthesis and degradation 0.47015000000000001 -0.30667072654109023
2 aspartate biosynthesis and degradation 1.05965 0.82278642810191482
3 aspartate biosynthesis and degradation 0.41470000000000001 -0.27865277027491725
4 aspartate biosynthesis and degradation 0.22520000000000001 -0.63672884121513007
5 aspartate biosynthesis and degradation 0.21949999999999997 -0.80712909266756339
6 aspartate biosynthesis and degradation 0.35120000000000001 -0.14079909416071754
EPI012 aspartate biosynthesis and degradation 1.05965 0.82278642810191482
EPI456 aspartate biosynthesis and degradation 0.35120000000000001 -0.14079909416071754
EPI aspartate biosynthesis and degradation 1.05965 0.82278642810191482

CAI aspartate biosynthesis and degradation 0.21813134649369936 -0.77689896873059894
0 cysteine biosynthesis 0.58919999999999995 -0.017269005347399217
1 cysteine biosynthesis 0.93630000000000002 0.84722366161010787
2 cysteine biosynthesis 0.65080000000000005 -0.10155682753000334
3 cysteine biosynthesis 0.503 -0.047769195809167768
4 cysteine biosynthesis 0.31280000000000002 -0.40725644111393122
5 cysteine biosynthesis 0.23699999999999999 -0.74014647396088129
6 cysteine biosynthesis 0.15490000000000001 -0.92513550710506942
EPI012 cysteine biosynthesis 0.93630000000000002 0.84722366161010787

EPI456 cysteine biosynthesis 0.31280000000000002 -0.40725644111393122

EPI cysteine biosynthesis 0.93630000000000002 0.84722366161010787
CAI cysteine biosynthesis 0.47115765155190786 1.3241942009723688
0 pyrimidine biosynthesis 0.58833999999999997 -0.019301995578287198
1 pyrimidine biosynthesis 0.53539999999999999 -0.14515274128555952
2 pyrimidine biosynthesis 0.65405999999999997 -0.094186498525820894
3 pyrimidine biosynthesis 0.4546466666666667 -0.17420170359324327
4 pyrimidine biosynthesis 0.34355999999999998 -0.32667914628387568
5 pyrimidine biosynthesis 0.34905333333333327 -0.39975528568517138
6 pyrimidine biosynthesis 0.27877333333333337 -0.43018713254507601
EPI012 pyrimidine biosynthesis 0.58833999999999997 -0.019301995578287198
EPI456 pyrimidine biosynthesis 0.34355999999999998 -0.32667914628387568

EPI pyrimidine biosynthesis 0.58833999999999997 -0.019301995578287198
CAI pyrimidine biosynthesis 0.23324451545152713 -0.65140143967900943
0 galactose, galactoside and glucose catabolism 0.30227999999999999 -0.69553128098274597
1 galactose, galactoside and glucose catabolism 0.34585999999999995 -0.61433464052438425
2 galactose, galactoside and glucose catabolism 0.32816000000000006 -0.83099331523229536
3 galactose, galactoside and glucose catabolism 0.39648 -0.32629375245799719
4 galactose, galactoside and glucose catabolism 0.53766000000000003 0.18177511010473965
5 galactose, galactoside and glucose catabolism 0.58499999999999996 0.31699417501532429
6 galactose, galactoside and glucose catabolism 0.45038 0.25548458100902677
EPI012 galactose, galactoside and glucose catabolism 0.34585999999999995 -0.61433464052438425
EPI456 galactose, galactoside and glucose catabolism 0.58499999999999996 0.31699417501532429
EPI galactose, galactoside and glucose catabolism 0.58499999999999996 0.31699417501532429
CAI galactose, galactoside and glucose catabolism 0.22360686391827458 -0.73143107850978584
0 thiamin biosynthesis 0.52769999999999995 -0.16265144627718395
1 thiamin biosynthesis 0.31180000000000002 -0.69864579114206038
2 thiamin biosynthesis 0.42159999999999997 -0.61974069494063244
3 thiamin biosynthesis 0.65739999999999998 0.35595021412867733
4 thiamin biosynthesis 0.36109999999999998 -0.28073227530470868
5 thiamin biosynthesis 0.51990000000000003 0.1192359674051205
6 thiamin biosynthesis 0.25430000000000003 -0.52797279978632983

```
mtbrv salvage pathways of pyrimidine deoxyribonucleotides   0.5221730372424755
      -0.7395001329223282
vcho  cyanate degradation     0.25621291635788612     -1.2256135971099649
ecoli cyanate degradation     0.31431688460921503     -0.9192621529080926
bsub  cyanate degradation     0.37559956136747941     -0.5180978210955289 3
agro  cyanate degradation     0.52673756216669776     0.2615937326014573
mtbrv cyanate degradation     0.52211468003948669     -0.74070699898100401
hpy   cyanate degradation     0.57502293597717513     -0.4841215284116126
yeast tryptophan biosynthesis 0.22239910072184063     -0.74146016620508237
vcho  tryptophan biosynthesis 0.29866154047410409     -0.68158435516390481
ecoli tryptophan biosynthesis 0.32752282286373774     -0.75053385683829621
bsub  tryptophan biosynthesis 0.36306299607443709     -0.72830544865130864
hin   tryptophan biosynthesis 0.3836649750407149      -0.70106483969218081
agro  tryptophan biosynthesis 0.54190667575886031     0.50285304508695272
mtbrv tryptophan biosynthesis 0.46656789013141164     -1.8894518321860521
hpy   tryptophan biosynthesis 0.58712109287331304     0.023307057642488332
yeast proline biosynthesis    0.24234713215382728     -0.5758146512807536
vcho  proline biosynthesis    0.2899152134106468      -0.79367886426077416
ecoli proline biosynthesis    0.36107005683212939     -0.32191095127456243
bsub  proline biosynthesis    0.35220883334322256     -0.9103032880514873
hin   proline biosynthesis    0.34507019415793244     -1.2561560736005764
agro  proline biosynthesis    0.48262637369877581     -0.4399789030064372
mtbrv proline biosynthesis    0.54412385910746075     -0.28554242908847055
yeast degradation of short-chain fatty acids    0.39224627351426106
      0.66892574037256691
vcho  degradation of short-chain fatty acids    0.29141068579026963     -
0.77451261984234454
ecoli degradation of short-chain fatty acids    0.26534257429147801     -
1.5449921670771876
bsub  degradation of short-chain fatty acids    0.34675412673584183     -
1.0017654156875715
yeast polyisoprenoid biosynthesis   0.3619221862297739      0.41711898590782748

vcho  polyisoprenoid biosynthesis   0.30759117607959474     -0.56714053064772751

ecoli polyisoprenoid biosynthesis   0.29170475431732124     -1.2081705319367906

bsub  polyisoprenoid biosynthesis   0.34918345487987174     -0.96103150701527951

agro  polyisoprenoid biosynthesis   0.51181745295363745     0.024294745479938564

mtbrv polyisoprenoid biosynthesis   0.42580122239501689     -2.7325338357846518

hpy   polyisoprenoid biosynthesis   0.59262569065415982     0.25418439645624513

yeast mannose catabolism      0.29292258233645052     -0.15584356207357999
ecoli mannose catabolism      0.34083319017616076     -0.5804713021461573
bsub  mannose catabolism      0.36630056347728451     -0.6740193386286385
agro  mannose catabolism      0.45734941168369808     -0.84199992028132942
mtbrv mannose catabolism      0.49878924785158479     -1.2230925653201263
vcho  KDO biosynthesis -- including transfer to lipid IV<SUB>A</SUB>
      0.29291877928600302     -0.7551846209177727
ecoli KDO biosynthesis -- including transfer to lipid IV<SUB>A</SUB>
      0.33626435568007812     -0.63884592458281386
hin   KDO biosynthesis -- including transfer to lipid IV<SUB>A</SUB>
      0.35688272686989153     -1.0862617716072771
agro  KDO biosynthesis -- including transfer to lipid IV<SUB>A</SUB>
      0.46685372583961043     -0.69083721159897726
hpy   KDO biosynthesis -- including transfer to lipid IV<SUB>A</SUB>
```

```
vcho  menaquinone biosynthesis      0.26356575298849316     -1.1313788313362003

ecoli menaquinone biosynthesis      0.3281952717278982      -0.74194218021091585

bsub  menaquinone biosynthesis      0.37694240641858306     -0.49558158432977134

hin   menaquinone biosynthesis      0.38373144141672072     -0.70010888394307191

mtbrv menaquinone biosynthesis      0.53119052434350755     -0.55301245770379892

yeast phenylalanine biosynthesis    0.20475614749307358     -0.8879646512380656 7

ecoli phenylalanine biosynthesis    0.29226960983946604     -1.2009535430382856

bsub  phenylalanine biosynthesis    0.40095690707369258     -
0.09291697152319158 8
hin   phenylalanine biosynthesis    0.37966928792178506     -0.7585329958113959 9

vcho  L-alanine degradation   0.2659337031260855      -1.1010302362419195
ecoli L-alanine degradation   0.3082499050407122      -0.9967781237692567
bsub  L-alanine degradation   0.34048477586325421     -1.1068871410115568
hin   L-alanine degradation   0.39246919493528093     -0.5744377369313586 9
agro  L-alanine degradation   0.45531287835247203     -0.8743902526735433 1
mtbrv L-alanine degradation   0.49544644381915848     -1.2922239924830934
hpy   L-alanine degradation   0.60422243819959975     0.7405825528305820 5
vcho  threonine biosynthesis from homoserine    0.27569411256078852     -
0.9759390641156612 3
ecoli threonine biosynthesis from homoserine    0.32253784696444654     -
0.8142253926630549 4
bsub  threonine biosynthesis from homoserine    0.404978317379939 -
0.025487727536118589
hin   threonine biosynthesis from homoserine    0.3805626636414578      -
0.7456839779070562 1
agro  threonine biosynthesis from homoserine    0.49199128954847254     -
0.2910332744003095 7
mtbrv threonine biosynthesis from homoserine    0.45810362240305574     -
2.0644985601050592
hpy   threonine biosynthesis from homoserine    0.57862456185918187     -
0.3330598464968606 6
yeast trehalose degradation, low osmolarity     0.20629487490178225     -
0.8751872854707839 5
vcho  trehalose degradation, low osmolarity     0.2994621740116935      -
0.6713232909810271 7
ecoli trehalose degradation, low osmolarity     0.30759053427673017     -
1.0052027054458355
bsub  trehalose degradation, low osmolarity     0.3786619953151511      -
0.4667482720253683 9
yeast thiamin biosynthesis    0.19976889877851101     -0.9293780300065961 3
vcho  thiamin biosynthesis    0.25495493131881619     -1.2417361608310165
ecoli thiamin biosynthesis    0.30239572536026987     -1.0715752145391195
bsub  thiamin biosynthesis    0.38329779971414774     -0.3890171374005953 5
hin   thiamin biosynthesis    0.31068576927248609     -1.7506916662461522
agro  thiamin biosynthesis    0.45791849665959566     -0.8329488277968079
mtbrv thiamin biosynthesis    0.55173276317473785     -0.1281851947981992
hpy   thiamin biosynthesis    0.59374727274369077     0.3012265053226312 4
vcho  pyridine nucleotide cycling   0.26670590350407386     -1.0911335765735801

ecoli pyridine nucleotide cycling   0.31528642008361674     -0.9068746901304026 7
```

```
5     superpathway for gluconate utilization    0.343449999999999998     -
0.41677687027261384
6     superpathway for gluconate utilization    0.28499999999999998     -
0.40530785899472732
EPI012      superpathway for gluconate utilization    0.59650000000000003
      0.0060924525705774628
EPI456      superpathway for gluconate utilization    0.31999999999999995     -
0.38839569590013423
EPI   superpathway for gluconate utilization    0.59650000000000003
      0.0060924525705774628
CAI   superpathway for gluconate utilization    0.4544360853673704
      1.1853407782462799
0     proline biosynthesis    0.32766666666666672     -0.63551867013606622
1     proline biosynthesis    0.40526666666666666     -0.46728107560872284
2     proline biosynthesis    0.44550000000000001     -0.56570668782407907
3     proline biosynthesis    0.28449999999999998     -0.61909491518364423
4     proline biosynthesis    0.36769999999999997     -0.26344325885872799
5     proline biosynthesis    0.71576666666666677     0.71423198784421882
6     proline biosynthesis    0.17466666666666666     -0.84615580038474336
EPI012      proline biosynthesis    0.40526666666666666     -0.4672810756087228 4

EPI456      proline biosynthesis    0.71576666666666677     0.7142319878442188 2

EPI   proline biosynthesis    0.71576666666666677     0.7142319878442188 2
CAI   proline biosynthesis    0.24234713215382728     -0.5758146512807550 4
0     D-arabinose catabolism  0.40510000000000002     -0.4524707512851773 9
1     D-arabinose catabolism  0.33360000000000001     -0.6446826941524731 5
2     D-arabinose catabolism  1.2248000000000001      1.1961636781144167
3     D-arabinose catabolism  0.377 -0.37722933604341963
4     D-arabinose catabolism  0.155 -0.82062110704965252
5     D-arabinose catabolism  0.18759999999999999     -0.8902118419477335 1
6     D-arabinose catabolism  0.21210000000000001     -0.6965871483663178 5
EPI012      D-arabinose catabolism  1.2248000000000001      1.1961636781144167

EPI456      D-arabinose catabolism  0.21210000000000001     -0.6965871483663178 5

EPI   D-arabinose catabolism  1.2248000000000001      1.1961636781144167
CAI   D-arabinose catabolism  0.33186885399733107     0.1675605415165473 4
0     riboflavin, FMN and FAD biosynthesis      0.37553999999999998     -
0.52234888061663176
1     riboflavin, FMN and FAD biosynthesis      0.33339999999999997     -
0.64517776843678132
2     riboflavin, FMN and FAD biosynthesis      0.37494     -0.7252313548593931 6

3     riboflavin, FMN and FAD biosynthesis      0.28736000000000006     -
0.61161669295293009
4     riboflavin, FMN and FAD biosynthesis      0.3256      -0.3737262274005140 9

5     riboflavin, FMN and FAD biosynthesis      0.54752000000000001
      0.20313891201639284
6     riboflavin, FMN and FAD biosynthesis      0.34560000000000002     -
0.16317445795332255
EPI012      riboflavin, FMN and FAD biosynthesis      0.37553999999999998     -
0.52234888061663176
EPI456      riboflavin, FMN and FAD biosynthesis      0.54752000000000001
      0.20313891201639284
EPI   riboflavin, FMN and FAD biosynthesis      0.54752000000000001
      0.20313891201639284
CAI   riboflavin, FMN and FAD biosynthesis      0.20650060389073052     -
0.8734789422477678
```

```
0     lysine and diaminopimelate biosynthesis   0.47435000000000005     -
0.28876775885611078
1     lysine and diaminopimelate biosynthesis   0.45974999999999999     -
0.33241458932511359
2     lysine and diaminopimelate biosynthesis   0.90470000000000006
      0.47246971669145699
3     lysine and diaminopimelate biosynthesis   0.39019999999999999     -
0.34271446420935514
4     lysine and diaminopimelate biosynthesis   0.19849999999999998     -
0.7066707713829613
5     lysine and diaminopimelate biosynthesis   0.21245     -0.8147234938814726 9

6     lysine and diaminopimelate biosynthesis   0.17845     -0.8310391111558107 5

EPI012      lysine and diaminopimelate biosynthesis   0.90470000000000006
      0.47246971669145699
EPI456      lysine and diaminopimelate biosynthesis   0.19849999999999998     -
0.7066707713829613
EPI   lysine and diaminopimelate biosynthesis   0.90470000000000006
      0.47246971669145699
CAI   lysine and diaminopimelate biosynthesis   0.36502964586112618
      0.44292287299798455
0     oxidative branch of the pentose phosphate pathway     0.35294999999999999
      -0.57575033330937708
1     oxidative branch of the pentose phosphate pathway     0.51715     -
0.19032826972867731
2     oxidative branch of the pentose phosphate pathway     0.29575000000000001
      -0.90426704622173038
3     oxidative branch of the pentose phosphate pathway     0.27394999999999997
      -0.64668066502071853
4     oxidative branch of the pentose phosphate pathway     0.35544999999999999
      -0.2955327212016467
5     oxidative branch of the pentose phosphate pathway     0.39400000000000002
      -0.26321807772736311
6     oxidative branch of the pentose phosphate pathway     0.36465000000000003
      -0.087058265051692854
EPI012      oxidative branch of the pentose phosphate pathway     0.51715     -
0.19032826972867731
EPI456      oxidative branch of the pentose phosphate pathway
      0.36465000000000003     -0.087058265051692854
EPI   oxidative branch of the pentose phosphate pathway     0.36465000000000003
      -0.087058265051692854
CAI   oxidative branch of the pentose phosphate pathway     0.42205103830715995
      0.91642011735663886
0     chorismate biosynthesis 0.52242500000000003     -0.17512124100734008
1     chorismate biosynthesis 0.40928750000000008     -0.4573280196846110 6
2     chorismate biosynthesis 0.42275000000000007     -0.6171407322551076 8
3     chorismate biosynthesis 0.31353750000000002     -0.5431687340562466 6
4     chorismate biosynthesis 0.33332500000000004     -0.3534902195148774 7
5     chorismate biosynthesis 0.26648749999999999     -0.6505705116428184 3
6     chorismate biosynthesis 0.17458750000000001     -0.8464721187716923 7
EPI012      chorismate biosynthesis 0.52242500000000003     -0.1751212410073400 8

EPI456      chorismate biosynthesis 0.33332500000000004     -0.3534902195148774 7

EPI   chorismate biosynthesis 0.52242500000000003     -0.17512124100734008
CAI   chorismate biosynthesis 0.30389965716727813     -0.0646915494594604 43
0     tryptophan biosynthesis 0.40523333333333328     -0.4521555590013189 9
1     tryptophan biosynthesis 0.35241666666666677     -0.5981044552371487 2
2     tryptophan biosynthesis 0.58086666666666664     -0.2596647033047998 5
```

5 polyisoprenoid biosynthesis 0.15440000000000001 -0.9910654900684520 2

6 polyisoprenoid biosynthesis 0.21376666666666666 -0.68992781390423308

EPI012 polyisoprenoid biosynthesis 0.63293333333333335 -0.14195045070221066
EPI456 polyisoprenoid biosynthesis 0.21376666666666666 -0.68992781390423308
EPI polyisoprenoid biosynthesis 0.63293333333333335 -0.14195045070221066

CAI polyisoprenoid biosynthesis 0.3619221862297739 0.41711898590782615

0 phospholipid biosynthesis 0.25961666666666666 -0.79638493201040539

1 phospholipid biosynthesis 0.33353333333333329 -0.64484771891390924

2 phospholipid biosynthesis 0.46983333333333333 -0.51069298462312518

3 phospholipid biosynthesis 0.24809999999999999 -0.71427228902909479

4 phospholipid biosynthesis 0.17759999999999998 -0.76141932346190022

5 phospholipid biosynthesis 0.27663333333333334 -0.61974990004970221

6 phospholipid biosynthesis 0.22776666666666665 -0.63398940422720562

EPI012 phospholipid biosynthesis 0.46983333333333333 -0.51069298462312518
EPI456 phospholipid biosynthesis 0.27663333333333334 -0.61974990004970221
EPI phospholipid biosynthesis 0.46983333333333333 -0.51069298462312518

CAI phospholipid biosynthesis 0.16756589234142572 -1.1967870523740354

0 4-aminobutyrate degradation 0.25840000000000002 -0.79926106160061516

1 4-aminobutyrate degradation 0.15625 -1.0836898157627166
2 4-aminobutyrate degradation 0.36780000000000002 -0.74137373188082367

3 4-aminobutyrate degradation 0.2792 -0.63295315917762462
4 4-aminobutyrate degradation 0.13275000000000001 -0.8789060488561784

5 4-aminobutyrate degradation 0.26584999999999998 -0.65250708395236545

6 4-aminobutyrate degradation 0.3246 -0.24708207217559155
EPI012 4-aminobutyrate degradation 0.36780000000000002 -0.74137373188082367
EPI456 4-aminobutyrate degradation 0.3246 -0.24708207217559155
EPI 4-aminobutyrate degradation 0.3246 -0.24708207217559155
CAI 4-aminobutyrate degradation 0.25791611381479673 -0.44653212067758968

0 L-serine degradation 0.2555 -0.80611649377453998
1 L-serine degradation 0.14904999999999999 -1.1015124899978097
2 L-serine degradation 0.29364999999999997 -0.9090148041692101
3 L-serine degradation 0.22894999999999999 -0.76434500081866563
4 L-serine degradation 0.093299999999999994 -0.98224721534010873
5 L-serine degradation 0.39629999999999999 -0.25623122861056646
6 L-serine degradation 0.30354999999999999 -0.33118946643172309
EPI012 L-serine degradation 0.2555 -0.80611649377453998
EPI456 L-serine degradation 0.39629999999999999 -0.25623122861056646

EPI L-serine degradation 0.39629999999999999 -0.25623122861056646
CAI L-serine degradation 0.17000968576725695 -1.17649415170508
0 methionine biosynthesis from homoserine 0.316 -0.66309799497369482
1 methionine biosynthesis from homoserine 0.3493 -0.60581936283428406

2 methionine biosynthesis from homoserine 0.52034999999999998 -0.39648302955319958
3 methionine biosynthesis from homoserine 0.20074999999999998 -0.83808131791871243
4 methionine biosynthesis from homoserine 0.16494999999999999 -0.79455660498336333
5 methionine biosynthesis from homoserine 0.1729 -0.9348669210855215

6 methionine biosynthesis from homoserine 0.11549999999999999 -1.0825621737887755
EPI012 methionine biosynthesis from homoserine 0.52034999999999998 -0.39648302955319958
EPI456 methionine biosynthesis from homoserine 0.16494999999999999 -0.79455660498336333
EPI methionine biosynthesis from homoserine 0.52034999999999998 -0.39648302955319958
CAI methionine biosynthesis from homoserine 0.1549198536833748 -1.3017978947926445
0 glutamate biosynthesis 0.3196 -0.65458780330951227
1 glutamate biosynthesis 0.49880000000000002 -0.23575133531394912
2 glutamate biosynthesis 0.25040000000000001 -1.006796009516111
3 glutamate biosynthesis 0.17610000000000001 -0.90253522630580996
4 glutamate biosynthesis 0.16389999999999999 -0.79730713032704204
5 glutamate biosynthesis 0.1401 -1.0345054650120145
6 glutamate biosynthesis 0.15010000000000001 -0.94431439035587372
EPI012 glutamate biosynthesis 0.49880000000000002 -0.23575133531394912

EPI456 glutamate biosynthesis 0.16389999999999999 -0.79730713032704204

EPI glutamate biosynthesis 0.49880000000000002 -0.23575133531394912
CAI glutamate biosynthesis 0.31416589667552036 0.020557791332755922
0 anaerobic respiration, electron donors reaction list 0.154525 -1.0448155502442149
1 anaerobic respiration, electron donors reaction list 0.1953 -0.98702656175155212
2 anaerobic respiration, electron donors reaction list 0.16044999999999998 -1.2101583082664866
3 anaerobic respiration, electron donors reaction list 0.20627499999999999 -0.82363475224574223
4 anaerobic respiration, electron donors reaction list 0.13475000000000001 -0.87366695296345698
5 anaerobic respiration, electron donors reaction list 0.41389999999999999 -0.2027666440646434
6 anaerobic respiration, electron donors reaction list 0.27144999999999997 -0.4594482817147706
EPI012 anaerobic respiration, electron donors reaction list 0.1953 -0.98702656175155212
EPI456 anaerobic respiration, electron donors reaction list 0.41389999999999999 -0.2027666440646434
EPI anaerobic respiration, electron donors reaction list 0.41389999999999999 -0.2027666440646434
CAI anaerobic respiration, electron donors reaction list 0.22136804666030419 -0.75002188727116181

5 polyisoprenoid biosynthesis 0.15440000000000001 -0.9910654900684520 2

6 polyisoprenoid biosynthesis 0.21376666666666666 -0.68992781390423308

EPI012 polyisoprenoid biosynthesis 0.63293333333333335 -0.14195045070221066
EPI456 polyisoprenoid biosynthesis 0.21376666666666666 -0.68992781390423308
EPI polyisoprenoid biosynthesis 0.63293333333333335 -0.14195045070221066

CAI polyisoprenoid biosynthesis 0.3619221862297739 0.41711898590782615

0 phospholipid biosynthesis 0.25961666666666666 -0.79638493201040539

1 phospholipid biosynthesis 0.33353333333333329 -0.64484771891390924

2 phospholipid biosynthesis 0.46983333333333333 -0.51069298462312518

3 phospholipid biosynthesis 0.24809999999999999 -0.71427228902909479

4 phospholipid biosynthesis 0.17759999999999998 -0.76141932346190022

5 phospholipid biosynthesis 0.27663333333333334 -0.61974990004970221

6 phospholipid biosynthesis 0.22776666666666665 -0.63398940422720562

EPI012 phospholipid biosynthesis 0.46983333333333333 -0.51069298462312518
EPI456 phospholipid biosynthesis 0.27663333333333334 -0.61974990004970221
EPI phospholipid biosynthesis 0.46983333333333333 -0.51069298462312518

CAI phospholipid biosynthesis 0.16756589234142572 -1.1967870523740354

0 4-aminobutyrate degradation 0.25840000000000002 -0.79926106160061516

1 4-aminobutyrate degradation 0.15625 -1.0836898157627166
2 4-aminobutyrate degradation 0.36780000000000002 -0.74137373188082367

3 4-aminobutyrate degradation 0.2792 -0.63295315917762462
4 4-aminobutyrate degradation 0.13275000000000001 -0.8789060488561784

5 4-aminobutyrate degradation 0.26584999999999998 -0.65250708395236545

6 4-aminobutyrate degradation 0.3246 -0.24708207217559155
EPI012 4-aminobutyrate degradation 0.36780000000000002 -0.74137373188082367
EPI456 4-aminobutyrate degradation 0.3246 -0.24708207217559155
EPI 4-aminobutyrate degradation 0.3246 -0.24708207217559155
CAI 4-aminobutyrate degradation 0.25791611381479673 -0.44653212067758968

0 L-serine degradation 0.2555 -0.80611649377453998
1 L-serine degradation 0.14904999999999999 -1.1015124899978097
2 L-serine degradation 0.29364999999999997 -0.9090148041692101
3 L-serine degradation 0.22894999999999999 -0.76434500081866563
4 L-serine degradation 0.093299999999999994 -0.98224721534010873
5 L-serine degradation 0.39629999999999999 -0.25623122861056646
6 L-serine degradation 0.30354999999999999 -0.33118946643172309
EPI012 L-serine degradation 0.2555 -0.80611649377453998
EPI456 L-serine degradation 0.39629999999999999 -0.25623122861056646

EPI L-serine degradation 0.39629999999999999 -0.25623122861056646
CAI L-serine degradation 0.17000968576725695 -1.17649415170508
0 methionine biosynthesis from homoserine 0.316 -0.66309799497369482
1 methionine biosynthesis from homoserine 0.3493 -0.60581936283428406

2 methionine biosynthesis from homoserine 0.52034999999999998 -0.39648302955319958
3 methionine biosynthesis from homoserine 0.20074999999999998 -0.83808131791871243
4 methionine biosynthesis from homoserine 0.16494999999999999 -0.79455660498336333
5 methionine biosynthesis from homoserine 0.1729 -0.9348669210855215

6 methionine biosynthesis from homoserine 0.11549999999999999 -1.0825621737887755
EPI012 methionine biosynthesis from homoserine 0.52034999999999998 -0.39648302955319958
EPI456 methionine biosynthesis from homoserine 0.16494999999999999 -0.79455660498336333
EPI methionine biosynthesis from homoserine 0.52034999999999998 -0.39648302955319958
CAI methionine biosynthesis from homoserine 0.1549198536833748 -1.3017978947926445
0 glutamate biosynthesis 0.3196 -0.65458780330951227
1 glutamate biosynthesis 0.49880000000000002 -0.23575133531394912
2 glutamate biosynthesis 0.25040000000000001 -1.006796009516111
3 glutamate biosynthesis 0.17610000000000001 -0.90253522630580996
4 glutamate biosynthesis 0.16389999999999999 -0.79730713032704204
5 glutamate biosynthesis 0.1401 -1.0345054650120145
6 glutamate biosynthesis 0.15010000000000001 -0.94431439035587372
EPI012 glutamate biosynthesis 0.49880000000000002 -0.23575133531394912

EPI456 glutamate biosynthesis 0.16389999999999999 -0.79730713032704204

EPI glutamate biosynthesis 0.49880000000000002 -0.23575133531394912
CAI glutamate biosynthesis 0.31416589667552036 0.020557791332755922
0 anaerobic respiration, electron donors reaction list 0.154525 -1.0448155502442149
1 anaerobic respiration, electron donors reaction list 0.1953 -0.98702656175155212
2 anaerobic respiration, electron donors reaction list 0.16044999999999998 -1.2101583082664866
3 anaerobic respiration, electron donors reaction list 0.20627499999999999 -0.82363475224574223
4 anaerobic respiration, electron donors reaction list 0.13475000000000001 -0.87366695296345698
5 anaerobic respiration, electron donors reaction list 0.41389999999999999 -0.2027666440646434
6 anaerobic respiration, electron donors reaction list 0.27144999999999997 -0.4594482817147706
EPI012 anaerobic respiration, electron donors reaction list 0.1953 -0.98702656175155212
EPI456 anaerobic respiration, electron donors reaction list 0.41389999999999999 -0.2027666440646434
EPI anaerobic respiration, electron donors reaction list 0.41389999999999999 -0.2027666440646434
CAI anaerobic respiration, electron donors reaction list 0.22136804666030419 -0.75002188727116181

0 biosynthesis of proto- and siroheme 0.21655454545454544 -0.89818129450524187
1 biosynthesis of proto- and siroheme 0.19857272727272732 -0.97892534619014604
2 biosynthesis of proto- and siroheme 0.30891818181818181 -0.87449593199262143
3 biosynthesis of proto- and siroheme 0.24970909090909091 -0.71006489762783487
4 biosynthesis of proto- and siroheme 0.25841818181818182 -0.54971222125147501
5 biosynthesis of proto- and siroheme 0.26659090909090905 -0.65025637959260685
6 biosynthesis of proto- and siroheme 0.13808181818181819 -0.9923342457679255
EPI012 biosynthesis of proto- and siroheme 0.30891818181818181 -0.87449593199262143
EPI456 biosynthesis of proto- and siroheme 0.25841818181818182 -0.54971222125147501
EPI biosynthesis of proto- and siroheme 0.25841818181818182 -0.54971222125147501
CAI biosynthesis of proto- and siroheme 0.20742854483475764 -0.8657734573222684
0 tyrosine biosynthesis 0.25209999999999999 -0.81415389701293461
1 tyrosine biosynthesis 0.22420000000000001 -0.91548832766902588
2 tyrosine biosynthesis 0.11799999999999999 -1.3061308439191095
3 tyrosine biosynthesis 0.1113 -1.0719718698548539
4 tyrosine biosynthesis 0.4118 -0.14792119442422028
5 tyrosine biosynthesis 0.30199999999999999 -0.54269204239923363
6 tyrosine biosynthesis 0.13089999999999999 -1.0210299233590914
EPI012 tyrosine biosynthesis 0.25209999999999999 -0.81415389701293461

EPI456 tyrosine biosynthesis 0.4118 -0.14792119442422028
EPI tyrosine biosynthesis 0.4118 -0.14792119442422028
CAI tyrosine biosynthesis 0.24264817712469613 -0.57331481818268848
0 phenylalanine biosynthesis 0.23075000000000001 -0.86462406146579474

1 phenylalanine biosynthesis 0.23925000000000002 -0.8782339877748383

2 phenylalanine biosynthesis 0.1171 -1.3081655973251722
3 phenylalanine biosynthesis 0.1047 -1.089229305771886
4 phenylalanine biosynthesis 0.28249999999999997 -0.48662874388866106

5 phenylalanine biosynthesis 0.21704999999999999 -0.8007497956478794

6 phenylalanine biosynthesis 0.11199999999999999 -1.0965467761591332

EPI012 phenylalanine biosynthesis 0.23075000000000001 -0.86462406146579474
EPI456 phenylalanine biosynthesis 0.28249999999999997 -0.48662874388866106
EPI phenylalanine biosynthesis 0.28249999999999997 -0.48662874388866106

CAI phenylalanine biosynthesis 0.20475614749307358 -0.887964651238067l2

0 deoxypyrimidine nucleotide/side metabolism 0.21744285714285713 -0.89608137708161228
1 deoxypyrimidine nucleotide/side metabolism 0.20897142857142856 -0.95318469817420282
2 deoxypyrimidine nucleotide/side metabolism 0.17228571428571429 -1.1833996860931066
3 deoxypyrimidine nucleotide/side metabolism 0.16599999999999998 -0.92894433278490496
4 deoxypyrimidine nucleotide/side metabolism 0.23884285714285713 -0.60099072280406607
5 deoxypyrimidine nucleotide/side metabolism 0.17782857142857145 -0.91989510154952836
6 deoxypyrimidine nucleotide/side metabolism 0.12461428571428572 -1.0461451276160967
EPI012 deoxypyrimidine nucleotide/side metabolism 0.21744285714285713 -0.89608137708161228
EPI456 deoxypyrimidine nucleotide/side metabolism 0.23884285714285713 -0.60099072280406607
EPI deoxypyrimidine nucleotide/side metabolism 0.23884285714285713 -0.60099072280406607
CAI deoxypyrimidine nucleotide/side metabolism 0.18332369468094525 -1.0659365826670326
0 pantothenate and coenzyme A biosynthesis 0.22170000000000001 -0.8860177377326981
1 pantothenate and coenzyme A biosynthesis 0.20046666666666665 -0.97423714274025852
2 pantothenate and coenzyme A biosynthesis 0.26433333333333336 -0.97529501234077021
3 pantothenate and coenzyme A biosynthesis 0.13066666666666668 -1.0213326260781077
4 pantothenate and coenzyme A biosynthesis 0.20820000000000002 -0.68126115630326223
5 pantothenate and coenzyme A biosynthesis 0.16883333333333336 -0.94722048039348072
6 pantothenate and coenzyme A biosynthesis 0.10963333333333332 -1.1060030310952937
EPI012 pantothenate and coenzyme A biosynthesis 0.22170000000000001 -0.8860177377326981
EPI456 pantothenate and coenzyme A biosynthesis 0.20820000000000002 -0.68126115630326223
EPI pantothenate and coenzyme A biosynthesis 0.20820000000000002 -0.68126115630326223
CAI pantothenate and coenzyme A biosynthesis 0.1692359165118541 -1.1829194176357472
0 glycerol metabolism 0.070300000000000001 -1.2439185760541518
1 glycerol metabolism 0.18554999999999999 -1.0111614331115741
2 glycerol metabolism 0.12740000000000001 -1.2848789750113438
3 glycerol metabolism 0.16955000000000001 -0.91966192407195579
4 glycerol metabolism 0.076049999999999993 -1.0274344174148311
5 glycerol metabolism 0.21995000000000001 -0.79194029023974433
6 glycerol metabolism 0.17699999999999999 -0.83683273213782461
EPI012 glycerol metabolism 0.18554999999999999 -1.0111614331115741

EPI456 glycerol metabolism 0.21995000000000001 -0.79194029023974433

EPI glycerol metabolism 0.21995000000000001 -0.79194029023974433
CAI glycerol metabolism 0.20549952823558804 -0.88179172704259057
0 lactose degradation 0.068500000000000005 -1.2481736718862431
1 lactose degradation 0.085300000000000001 -1.2593174181210294
2 lactose degradation 0.1709 -1.1865325603849808
3 lactose degradation 0.051700000000000003 -1.2278117457116904
4 lactose degradation 0.049099999999999998 -1.0980312345692524
5 lactose degradation 0.1128 -1.1174363262679063
6 lactose degradation 0.16109999999999999 -0.90036278290611393
EPI012 lactose degradation 0.1709 -1.1865325603849808
EPI456 lactose degradation 0.16109999999999999 -0.90036278290611393

EPI lactose degradation 0.16109999999999999 -0.90036278290611393
CAI lactose degradation 0.21164978398535764 -0.83072090914958707
0 biotin biosynthesis 0.098275000000000001 -1.1777872949970669
1 biotin biosynthesis 0.08514999999999999 -1.2596887238342607
2 biotin biosynthesis 0.071124999999999994 -1.4121075838182076
3 biotin biosynthesis 0.068925 -1.182772452731254
4 biotin biosynthesis 0.074300000000000005 -1.0320186263209623
5 biotin biosynthesis 0.085175000000000001 -1.2013544596816066
6 biotin biosynthesis 0.059249999999999997 -1.3073147118841182
EPI012 biotin biosynthesis 0.098275000000000001 -1.1777872949970669

EPI456 biotin biosynthesis 0.074300000000000005 -1.0320186263209623

EPI biotin biosynthesis 0.074300000000000005 -1.0320186263209623
CAI biotin biosynthesis 0.18262596579645649 -1.0717304205573919